Assessing impacts of mineral and hydrocarbon resources exploitation and consumption

Submitted in partial fulfillment of the requirements for
the degree of
Doctor of Philosophy
in
Engineering & Public Policy

Yu Gan

B.S in Environmental Engineering, Tsinghua University
LL.B., Law, Tsinghua University
M.S., Environmental Science and Engineering, Tsinghua University

Carnegie Mellon University

Pittsburgh, Pennsylvania 15213

December 2017

DOCTORAL THESIS COMMITTEE

W. Michael Griffin (Chair)
Research Professor, Engineering & Public Policy
Carnegie Mellon University

H. Scott Matthews
Professor, Civil & Environmental Engineering and Engineering & Public Policy
Carnegie Mellon University

Paulina Jaramillo
Associate Professor, Engineering & Public Policy
Carnegie Mellon University

Austin Mitchell
Quantitative Risk Analyst
IGS Energy

Acknowledgments

Support for this research was provided by Carnegie Mellon College of Engineering (CIT) Dean's Fellowship, Carnegie Mellon Department of Engineering and Public Policy, and the Fundação para a Ciência e a Tecnologia (Portuguese Foundation for Science and Technology) through the Carnegie Mellon Portugal Program.

First, I would like to express my sincere gratitude to my advisor W. Michael Griffin for his support and encouragement of my study, for his patience and dedication. I want to thank my co-advisor, H. Scott Matthews for his invaluable help, insightful guidance and contributions. I would like to thank the rest of my thesis committee members, Paulina Jaramillo and Austin Mitchell for their comments and suggestions.

Finally, I want to thank my family for their love and giving. I want to thank my parents for their support for my every decision. I would like to thank my husband for his help and encouragement. I also want to thank my baby for staying with me and fighting together for the thesis over the past seven months.

Thank you to everyone that has helped me along the way.

Abstract

The exploitation of natural resources lays the foundation for the economic and social development, but also is the root cause of various environmental issues. The study aims to analyze the process of natural resource exploitation, to optimize the extraction and utilization processes, maximizing their economic and social values while reducing the accompanied negative environmental impacts. This dissertation focuses on the impacts of exploitation of mineral and hydrocarbon resources in emerging countries on global warming effect, economy and society.

Chapter 2 of the dissertation analyzes the life cycle GHG emissions associated with iron ore mining and processing in China. With rapid economic development and nationwide urbanization, the iron ore demand grows while the ore grade declines significantly, leading to the increasing GHG emissions from iron ore production. Results of the research show that the mean life-cycle GHG emissions for Chinese iron ore production are 270 kg CO_2e/tonne, with a 90% confidence interval of 210 to 380 kg CO_2e/tonne. The two largest contributors to overall GHG emissions are agglomeration (60%) and ore processing (23%). Iron content (ore grade) varies from 15% to 60% and is the largest contributor (40%) to the uncertainty of the results.

Chapter 3 explores the impact of China's outsourcing of iron resources on the global warming effect. This chapter applies the same life cycle assessment framework of Chinese iron ore in Chapter 2 to Australian and Brazilian ore production, and compares the LCA results of Australian and Brazilian ore to Chinese iron ore. Results show that among the three iron ore sources, Australian iron ore is the optimal choice for reducing GHG emissions. The mean life cycle GHG emissions of Australian iron ore fines is 60% less than that of Chinese iron ore fines (42 kg CO_2e/tonne versus 110 kg CO_2e/tonne). There is no significant difference between the imported iron ores sourced from Brazil versus the China's domestic supplied iron ores, but if Chinese ore grade falls below 20% in the future, Brazilian iron ores would be preferred. The largest source of GHG

emissions for Australian and Brazilian iron ores comes from ocean shipping (accounts for 58% and 75% of the overall GHG emissions respectively).

Chapter 4 studies the impacts of the exploitation of pre-salt natural gas in Brazil. Natural gas production and its associated downstream industries are currently underdeveloped in Brazil, while the on-going exploitation of deep-sea pre-salt reservoir would potentially change the current situation. This study analyzes the impacts of the increasing pre-salt gas production and potential natural gas use pathways in downstream industries.

Results reveal that GHG emissions associated with pre-salt gas production vary according to the stage of reservoir exploitation. At the early stage, the estimate of GHG emissions is 5.4 (90%CI: 4.5~6.4) gCO_2e/MJ, and the value becomes 7.1 (90% CI: 6.3~8.0) gCO_2e/MJ for the intermediate stage. All six natural gas use pathways analyzed in the study emit less GHG on average than their current corresponding incumbent pathways. The mean GHG emissions reduction from natural gas use for power generation, nitrogen fertilizer production, methanol production, as the reducing agent for steel making, ethylene-based polymer production, heavy-duty vehicle fueling are estimated to be 0.83, 2.3, 0.38, 35, 2.6 and 0.078 million tonnes CO_2 equivalent per year, respectively. The specific economic profits of the six pathways are affected by the prices of natural gas and traditional fuel. Under current fuel prices, the net annual profits for the six pathways are -270, 87, 92, 1700, 190 and -1500 million dollars, respectively. The job creation potential from the pathways of power generation, nitrogen fertilizer production, methanol production and as reducing agent for steel production are estimated to be 28, 17, 5 and 36 thousand, respectively.

Contents

List of Tables

List of Figures

1. Introduction and Background

1.1 Motivation

The past two centuries have witnessed tremendous development in economy, technology, politics, society and culture, at the cost of huge consumption of natural resources, especially the depletion of non-renewable minerals and fossil fuels[1-3]. The recent accelerating development of emerging countries (e.g. China, Brazil, etc.) who have vast territory area and large population is unprecedented, attracting global attention[2, 4]. As the per capita consumption level of material goods and service increases, the demand for resources has become enormously huge, turning into a new challenge for the environmental carrying capacity locally and globally[2, 4].

Over-exploitation of natural resources is the root cause of various environmental issues. Associated with the extraction and manufacturing of natural resources, waste and toxic pollutants are produced, the disposal of which change the original mass cycle and balance of the ecosystem, leading to environmental degradation such as air and water pollution, biodiversity loss, desertification, etc[2, 5, 6]. For example, climate change could result from over-exploitation of fossil fuels[7-9]. Through the extraction and combustion of fossil fuels, the underground carbon storage is emitted into the atmosphere in form of greenhouse gas (GHG), which cannot be completely absorbed by the marine and forest, and consequently aggregating the global warming effects[7-9].

Therefore, the motivation of the present study is to analyze the process of natural resource exploitation, in order to optimize the extraction and utilization, maximize their economic and social values, while reducing the accompanied negative environmental impacts. The study focuses on the impacts of exploitation of mineral and hydrocarbon resources in emerging countries on global warming effect, economy and society, and provides information for future energy policies with strategies of optimizing resource extraction and consumption.

1.2 Research topics and background

Within the frame of analyzing natural resource exploitation in emerging countries, this dissertation focuses on the following three sub-topics:

1. Analysis of life cycle GHG emissions for iron ore mining and processing in China

2. Life cycle GHG emissions of iron ore mining in China, Australia and Brazil—a comparison of different iron ore sources for China.

3. Integration of pre-salt natural gas into Brazilian Fossil-derived feedstock: accessing the global warming effect, economic and employment impacts of pre-salt gas production and utilization.

The following sections introduce the backgrounds of the three sub-topics.

1.2.1 Iron ore production and consumption in China

China is currently both the largest iron ore producer and consumer worldwide, accounts for 45% of global production and 55% of global consumption[10]. The rapid nationwide economic growth and urbanization drive the infrastructure construction and upgrade, which consumes more than half (54%) of the iron ore[11].

In the past century, the scale of China's urbanization is unprecedented in human history. In 1980, there was less than 200 million urban population national wide, which increased to 670 million in the year 2010[12]. In only three decades, half billion people were transferred from rural to urban areas. From 2000 to 2010, the city of Shanghai alone, witnessed a population growth by 7 million, corresponding to a 44% increase[13]. China has the largest population of 1.34 billion in the world, and now roughly half live in urban areas[14]. Therefore, the urbanization process is still on-going and will continue to drive iron ore consumption and production in the foreseeable future.

On the other hand, the iron ore reserves of China have not increased since 1997[15, 16], which necessitated the industries to exploit lower quality iron ores. China's iron ore grade has dropped from 30% Fe to 27% Fe from 2006 to 2012[17]. Exploiting lower grade ore would result in increased production cost, energy input and GHG emissions for obtaining an equivalent mass of ore concentrate[16].

1.2.2 China's outsourcing of iron ores

Another option to alleviate the relative deficiency of iron ore domestically is to source it overseas. China has been the largest importer of iron ore globally. In 2013, 73% of the iron ore consumption in China was imported. From 1995 to 2011, China's iron ore import has increased by 1570 percent, from 41 tonnes to 686 tonnes[16].

The high dependence on imports results in vulnerability to the fluctuating iron ore price. Figure 1.1 demonstrates the historical prices of imported iron ore from 2011 to 2017[18]. The price of iron ore ranged from 40 to 180 dollar per tonne in the past seven years, which could be one major unfavorable factor of outsourcing iron ores.

Figure 1.1 Historical iron ore price 2011~2017[18]

In comparison the domestic iron ore, the imported iron ore is of significantly higher quality: in 2011, imported iron ore grade was 62% on average, while the domestic iron ore grade was only 28%[17]. China mainly imports iron ores from Australia and Brazil, which are also the top two largest net exporters of iron ores globally. In 2013, 57% of China's imported iron ores were from Australia, and 18% from Brazil[19].

1.2.3 Iron ore mining in Australia

Australia processes the largest quantity of iron ores among all nations worldwide, which accounts for 28% of the total global iron reserve[20]. Ninety percent of the proven iron ore reserves in Australia are located in Western Australia, mainly in the Pilbara region. While the regions of Midwest, Kimberley and Wheatbell also represent a minor part of the reserves[21].

In 2015, 94% of Australia's total iron ore production took place in Pilbara region, where the iron ores are of high-grade (with 58% to 65% Fe content) hematite[22]. With a shallow depth of burial (less than 100 meter depth), iron ore reserves in this area can be accessed by open pit mining with low cost[22].

Nearly all the iron ore production in Australia is for export, with a great portion to China eventually (82% of Western Australia iron ores were exported to China in 2016)[22, 23]. BHP Billiton, Rio Tinto and Fortescue Metals Group are the three largest iron ore producers in Australia, and operate private rail networks to transport ores from mining sites to ports. Port Hedland, Cape Lambert and Dampier are the three largest iron ore export ports, representing 57%, 22% and 16% of the total quantity of iron ore exports from Western Australia respectively[22, 23]. With the operation capacity of 490 million tonnes, Port Hedland is the world's largest bulk export port[22, 23].

1.2.4 Iron ore mining in Brazil

Brazil has the second largest iron ore deposits in the world. As of 2015, Brazil has reserves of 23 billion tonnes of crude ore and 12 billion tonnes of iron content, accounting for 12% and 14% of the world's total crude ore and iron content reserves, respectively[20]. In Brazil, iron ore is generally extracted through open pit mining with relatively high productivity.

The Iron Quadrangle region in Minas Gerais state and Carajas region in Para state are the two major iron ore mining regions. They account for 70% and 7.3% of Brazil's iron ore reserves respectively[24, 25].

The Iron Quadrangle is named because of rich iron ore resource and its quadrangular shape. Located in Southeastern Brazil, it is approximately 7000 km^2 in size[25]. Two main types of iron ores are found in the area: high-grade (with Fe content greater than 64%) hematite and intermediate-grade (with Fe content between 45% and 64%) itabirite ore[25].

The Carajas mine, the largest iron ore mining site worldwide, is located on the edge of Amazon area. The Carajas mine holds 1.5 billion tonnes of crude iron ore which is high quality with the Fe content being 65% to 67%[26, 27]. The mine has implemented a serial of operations (e.g. a complete truckless conveyer transport system) to reduce fuel use and GHG emissions[26, 27].

Vale is Brazil's largest iron ore producer, and is also the largest iron ore producer and exporter globally, yielding approximately 80% of Brazil's total iron ore production[28].

1.2.5 Brazil's energy matrix

Brazil has a unique energy matrix of high diversity. Oil takes the largest share of approximately 40% in the total energy supply, followed by biofuels (about 30%), and hydropower (14%)[29]. Of note, more than 40% of Brazil's energy supply comes from renewable sources, which is 4 times of the world average[30].

Oil in Brazil is mainly used as transportation fuels. Brazil has transitioned from importing majority (80%) of its oil in the 1970s to being self-sufficient currently through obtaining 90% of its supply from deep-sea offshore, which are mostly of heavy grade[29, 31]. With the limited capability of refining heavier crudes, Brazil has to export heavy crude oil and import light crude oil as well as refinery products (e.g. gasoline) to satisfy the demand from transportation sector[29].

Biofuel accounts for a significant share in Brazil's energy mix, owing to policy supports from the government since 1970s[32, 33]. The ethanol blend requirement set by the government has been gradually increased and reached 27% since the last adjustment in 2015[33]. Currently, Brazil ranks in second place globally after the U.S regarding the quantity of ethanol production and consumption[33, 34].

Hydropower is the primary source for power generation in Brazil, accounting for approximately two-thirds of the installed generation capacity[29]. However, further exploitation of hydropower is limited by the remoteness and ecological sensitivity of the remaining hydro resources[35]. On the other hand, with the growth of economy and population, the demand for electricity will keep increasing, outpacing the increment of hydropower capacity[36]. Brazil's Ministry of Mines and Energy(MME) projected that the total electricity supply will increase by 87% from 2014 to 2024, and the share of hydro will decline from 66% in 2014 to 55% in 2024[36].

The share of natural gas is currently relatively small in Brazil's energy mix, accounting for 12% in the total energy supply and 7.2% in the final consumption in 2016[37, 38]. Approximately half of the natural gas is used for power generation while the rest served various purposes in downstream industrial demands[37, 38]. Natural gas consumption grew by 60% from 2011 to 2015, which is

mainly driven by the increasing demand for power generation[37, 38]. According to MME's "Electricity in the 2024 Brazilian Energy Plan", the natural gas installed generation capacity will be increased by 10.4% and the percentage in power generation mix will increase from 8.8% to 10.6% from 2014 to 2024[36]. The gas sources for power generation are imported liquefied natural gas (LNG) and pipeline gas, accounting for 47% and 53%, respectively in 2015[37, 38]. For Brazil, LNG power is a flexible backup source for hydropower during the drought seasons[37, 38].

Brazil has three different natural gas sources: pipeline natural gas from Bolivia, domestically produced gas, and regasification LNG imported from other markets, representing 35%, 44%, and 21% of the total supply, respectively[37, 38]. Brazil imports LNG primarily from Nigeria, Qatar, Spain, and Trinidad and Tobago[36, 37]. U.S. targets Brazil as an important LNG market in Southern America and has started to export LNG to Brazil since early 2017[39].

Due to the limited quantity and low quality of the coal reserves, coal mining and utilization is not in large scale in Brazil[40]. Coal represents a low percentage, around 5% in the energy mix[29]. Most of the domestic coal production is used for power generation, while imported metallurgical coal is for steel production[29].

1.2.6 Deep-sea pre-salt reservoir

Brazil's pre-salt reservoirs are located in the Santos and Campos basin, positioned 5000 to 6000 meters below the sea surface, under a water depth of 1900 to 2400 meters and a thick salt layer (up to 2500 meters)[30, 41]. The deposits are formed about 160 million years ago when the South American and African continents began to separate[30, 41, 42].

The pre-salt oil reserves are estimated to be 50 billion barrels of oil equivalent, which is four times greater than the current national oil reserves[30, 42]. Currently, most of the exploration and production are in Santo Basin Pre-Salt Cluster (SBPSC), 300 km offshore the Rio de Janeiro Coast, Southeastern Brazil[30, 41]. The best estimate of contingent resources in SBPSC is 15 billion barrels of oil equivalent[42].

The petroleum reveres in SBPSC are generally of good quality, with an intermediate API gravities from 28 to 32, high gas to oil ratio (GOR) between 200 and 350 m^3 of gas /m^3 of oil, while has a high CO_2 content (8% to 15%, some part can reach up to 20%)[30, 41]. Considering the high GOR

and CO_2 content, the GHG emissions from pre-salt oil extraction will be enormous if the produced gas is directly vented to the air. The Lula reservoir alone can emit up to 3.1 billion tonnes of CO_2, which is more than double of the Brazil's annual GHG emissions[43].

Petrobras has promised not to vent the produced CO_2 for environmental reasons[30, 44]. Gas processing facilities are installed in the production platform to separate and reinject CO_2 back to the reservoir. After CO_2 separation, the produced gas will be transported through the pipeline for sale[30, 43]. Thus the exploitation of oil reserves will also increase gas supply significantly.

Since reservoir production began in 2008, the supply of pre-salt natural gas has risen by more than 90% per year on average, and accounted for 30% of the total domestic production in 2015[37, 38]. With the on-going exploration, it is expected that pre-salt natural gas will replace imported gas as the primary source of Brazil's natural gas supply, and Brazil has the potential of gradually achieving self-sufficiency in the future.

1.3 Research question

After reviewing the background of the three topics, the study raises specific research questions corresponding to each topic.

1.3.1 Topic 1: Analysis of life cycle GHG emissions for iron ore mining and processing in China —uncertainty and trends.

The project will answer the following research questions:

1. What is the life cycle GHG emissions for iron ore mining and processing in China? How certain are the estimates?

2. What parameters/factors contribute most to the uncertainty of the LCA results?

3. What are the emissions from different iron ore mining and processing steps? Which stage contributes most to the overall life cycle emissions?

4. What is the future trend of GHG emissions of iron ore mining and processing as the iron ore grade decreases?

5. What are viable ways to reduce GHG emissions associated with China's increasing iron ore consumption?

1.3.2 Topic 2: Life cycle GHG emissions of iron ore mining in China, Australia and Brazil—a comparison of different iron ore sources for China.

The project will answer the following research questions:

1. What are the life cycle GHG emissions of iron ore mining and processing in Brazil and Australia? How certain are the estimates? How are the GHG emissions associated with iron ore production from the two countries compared to that of China? Which iron ore source leads to the lowest GHG emissions?
2. What are the emissions associated with different iron ore mining and processing stages for Australia and Brazil? Which stage contributes most to the overall life cycle emissions?
3. What are the viable ways to reduce the embedded GHG emissions of Brazilian and Australian iron ores?
4. Considering the future trends of iron ore grade, how will the comparison LCA results of Chinese, Brazilian and Australian iron ore change over time?
5. What parameters/factors contribute most to the uncertainty of the LCA results?

1.3.3 Topic 3: Integration of pre-salt natural gas into Brazilian Fossil-derived feedstock: accessing the global warming effect, economic and employment impacts of pre-salt gas production and utilization.

The project will answer the following research questions:

1. What are the global warming effects of pre-salt natural gas exploration and downstream industry developments? How certain are the estimates?
2. With the exploration of pre-salt natural gas resources, what are the possible use (e.g.: fertilizer, power generation, etc.) of the increasing gas supply in Brazil?
3. What are the break-even gas prices for alternative natural gas uses? What are the economic benefits and cost of these uses under different gas price?
4. What are the social impacts in terms of jobs of natural gas exploration and associated downstream industry development? How many jobs will be created by the different gas uses?

5. What are the policy implications for the future development of the natural gas sector and associated downstream industry?

1.4 Thesis Outline

Chapter 1 introduces the motivation, background information and research questions of the dissertation.

Chapter 2 of the dissertation focuses on the increasing GHG emissions associated with iron ore mining and processing in China. With rapid economic development and nationwide urbanization, the iron ore demand grows while the ore grade declines significantly, leading to the increasing GHG emissions from iron ore production. The chapter will analyze the life cycle GHG emissions of China's iron ore mining and processing with uncertainty analysis, estimates the trend of emissions as the ore grade decline, and discuss the viable ways for emission reduction.

Chapter 3 explores the impact of China's outsourcing of iron resources on the global warming effect. The chapter compares the embedded GHG emissions of iron ore soured form Australia, Brazil and domestically, analyzes the future trends, uncertainty and potential ways for emissions reduction.

Chapter 4 focus on the impacts of the exploitation of pre-salt natural gas in Brazil. The chapter discusses the possible use pathways of the increasing amount of gas supply; compares the economic, social and global warming effects of different gas use pathways; provides information for future policies regarding the development of the natural gas sector and associated downstream industries.

Chapter 5 summarizes the main findings of the three projects, concludes the answers to each research question, and puts forward the plan for future work.

2. Analysis of Life-cycle GHG emissions for iron ore mining and processing in China —uncertainty and trends.

2.1 Abstract

Total iron ore demand in China grew to 1.1 billion tonnes in 2013 as a result of ongoing urbanization and massive infrastructure development. Iron ore and steel production are major sources for greenhouse gas (GHG) emissions. Because China has committed to lowering carbon intensity to meet climate change mitigation goals, detailed studies of the energy use and GHG emissions associated with iron ore mining and processing can aid in quantifying the impact and effectiveness of emissions reduction strategies. In this study, a life-cycle model for mining and processing of Chinese iron ores is developed and used to estimate GHG emissions. Results show that the mean life-cycle GHG emissions for Chinese iron ore production are 270 kg CO_2e/tonne, with a 90% confidence interval ranging from 210 to 380 kg CO_2e/tonne. The two largest contributors to overall GHG emissions are agglomeration (60%) and ore processing (23%). Iron content (ore grade) varies from 15% to 60% and is the largest contributor (40%) to the uncertainty of the results. Iron ore demand growth and the depletion of rich ore deposits will result in increased exploitation of lower grade ores with the concomitant increase in energy consumption and GHG emissions.

2.2 Introduction

China's urbanization and its associated massive infrastructure development are creating rising demand for iron ore and steel production[45]. Total iron ore demand grew from 200 million tonnes in 2001 to 1.1 billion tonnes in 2013 (all grades converted to 62% Fe iron ore): an average yearly increase of 15%[17]. China is the world's largest iron ore producer and consumer, responsible for 45% of total global production and 55% of total consumption[10]. The consumptive growth leads to the depletion of iron-ore resources and increased exploitation of lower quality ores[17]. Produced crude ore grade dropped from 30% Fe to 27% Fe between 2006 and 2012[17]. Processing lower grade ores for an equivalent mass of ore concentrate requires higher energy intensity, potentially resulting in increased GHG emissions[46].

As the largest GHG emitter[47], China committed to lowering the carbon intensity of its economy by 60% to 65% from the 2005 level by 2030[48]. To meet this commitment, China will need to develop a range of GHG emissions reduction strategies. The iron and steel sector could be a major focus, as it contributes about 12% of the country's total GHG emissions[49]. Iron ore mining and processing accounts for about 4% of these emissions and will increase as iron ore grade declines.[46]

Life-cycle assessment (LCA) is a widely used tool for estimating environmental effects of products and services over their entire life-cycle. Some studies have investigated the emissions of the iron and steel sector[11, 48-50], but don't provide a detailed breakout of the iron ore mining and processing steps[51, 52]. Stewart *et al.* suggest that data deficiencies are the primary reason for this "black-box modeling" approach[53].

Two LCA studies reported GHG emissions of iron ore mining and production in Australia and Brazil. Norgate and Haque estimated the life-cycle GHG emissions of Australian iron ore mining at 12 kg CO_2e/tonne[46] and Ferreira *et al.* reported Brazilian mining emissions of 13 kg CO_2e/tonne[54]. The GHG estimates vary slightly due to geological and operating conditions[54]. There are, however, substantial differences in Chinese ore mining compared to these studies, such as greater average mine depth and lower grade ore extraction. These attributes are expected to change the emissions estimate[17].

This study develops a life-cycle model to determine the GHG emissions of iron ore mining and processing in China. By using data from varied sources and at different levels of aggregation, the study provides average sectoral estimates, and uncertainty ranges for the life-cycle inventory (LCI) results. Sensitivity analysis is used to determine the parameters that drive model results and highlight future data needs and areas requiring further study. Based on the results, the study further discusses viable ways of GHG emissions reduction and provide utility for policymakers.

2.3 Methods

The following presents data and methods used for estimating GHG emissions from Chinese iron ore production. The emissions embodied in three forms of iron products (lumps, sinters and pellets; defined below) are analyzed. This analysis includes GHG emissions throughout the mining and ore processing stages, as well as indirect emissions associated with the consumption of energy and explosives during the mining and concentrating processes.

2.3.1 Goal, scope, system boundary, and functional unit

The goal of the study is to determine the GHG emissions of Chinese iron ore mining. The iron ore production system and the system boundary used are shown in Figure 2.1 and include mining, ore processing, and agglomeration stages.

Open pit and underground mining are modeled. The functional unit is one metric ton of processed iron-ore delivered to the blast furnace, the entry point to the steel making process. The blast furnace requires ore with the Fe content of 60% or higher. Lumps, sinters or pellets are all used as feedstock. These three forms of iron ore are treated as equivalent in this study as they all are sized to between 10 – 30mm, and have an iron content of 60% or higher.

The final results are presented in terms of 100-year global warming potentials (GWPs), using GWP factors reported by the Intergovernmental Panel on Climate Change (IPCC) assessment report (IPCC 2007). This approach was made necessary as some data sources are aggregated making updating to more recent values impossible. However, as the majority of emissions in the system are CO_2 the differences should be small.

Figure 2.1 shows the detailed mining steps for both open pit and underground mining. Crude ore is delivered by diesel truck to the processing facilities, i.e., "loading and hauling" as depicted. The ore is sized, and Fe content increased if needed. High-grade ore (>60% Fe content) requires only simple crushing and screening. The generated iron ore lumps are suitable for direct use in the blast furnaces and are shipped by rail to the steel mill. Low-grade ore (<60% Fe content) undergoes multiple processing steps to increase the overall iron content. These include crushing, screening, milling, flotation or magnetic separation, followed by filtering and drying. These processes produce fines with an iron content greater than 60% and smaller than 0.1mm.

After ore processing, fines require agglomeration, by sintering or pelleting, to form aggregates for use in the blast furnace. Pelletizing plants are usually located at or near the iron ore mines and assumed so located for this study. After pelleting, the pellets are transported to steel mills, where the blast furnaces are located. Sintering plants, co-located at the steel mills, receive fines for processing directly from the mines and transfer the sinters to the blast furnace[55]. All three ore forms ship to the steel mill by rail[17].

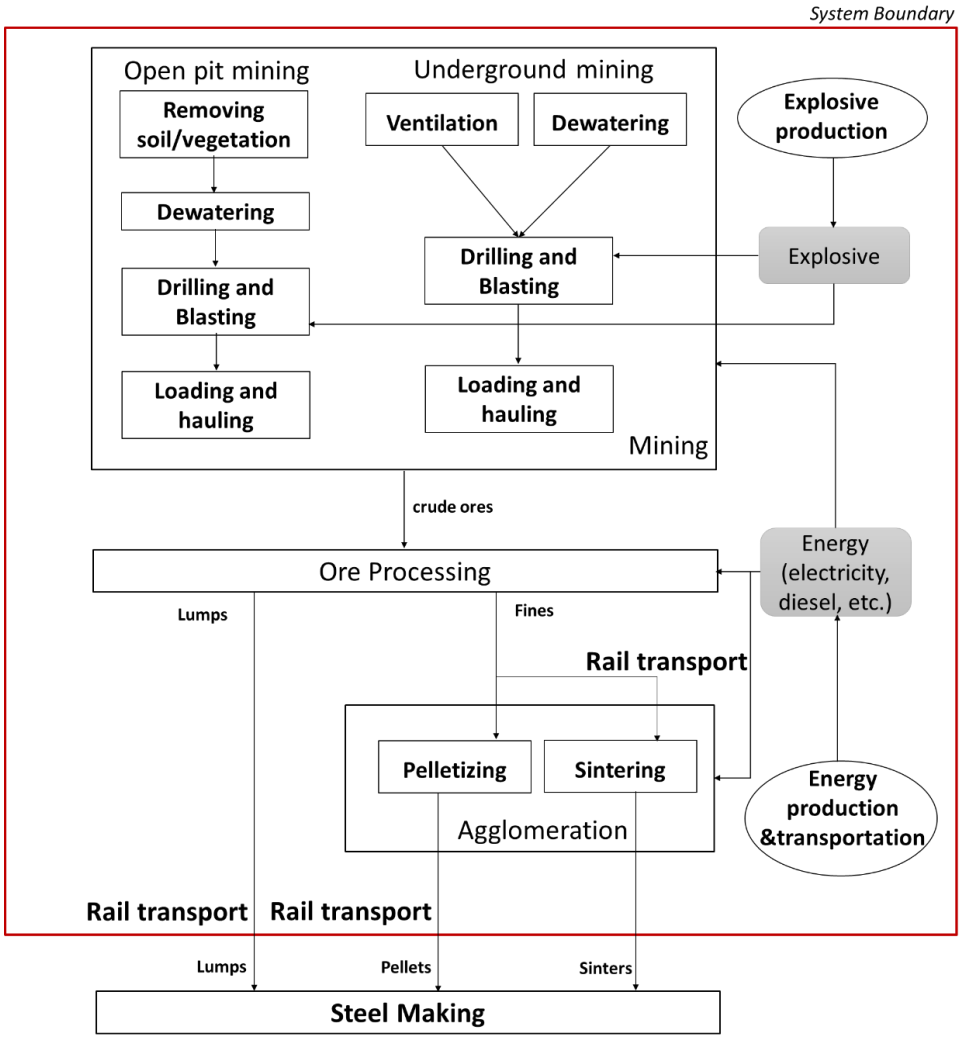

Figure 2.1 Chinese iron ore mining flowsheet and the associated LCA system boundary. Rectangular boxes indicate unit operations of iron mining and processing; Shaded boxes indicate energy and explosives input; Rounded boxes indicate upstream processes of energy and explosives production.

2.3.2 Estimation Approaches

Three estimation approaches were applied to calculate GHG emissions using data with different aggregation levels and from a variety of sources.

2.3.2.1 Approach I (Bottom-up modeling)

In this study, a bottom-up approach is used to estimate GHG emissions associated with each individual mining process of open pit mining, which accounts for 87% of the Chinese iron ore

extraction[17]. Because of the lack of disaggregated data related to underground mining, the bottom-up assessment was not applied to underground mining. The assumptions and parameters used in the assessment are shown in Table 2.1. Detailed calculations, and a discussion of the data and its representativeness are reported in the appendix section Approach I: bottom up model. The bottom-up analysis of open pit mining includes the following stages:

Vegetation and soil removal. Vegetation and soil are removed to expose the ore seam. GHG emissions arise from microbial decomposition of the removed biomass and soil (soil organic carbon degradation). Additionally, a debt accrues due to reduced photosynthetic productivity during the life of the mine due to the removed biomass. The CO_2 emissions estimates account for changes in the soil carbon stock, vegetation carbon stock, net primary production of the mining area, and ground disturbance area over the mine lifetime. Emissions associated with heavy truck and tractor diesel use from removal and transport of the soil and vegetation were estimated using bulldozer load factors, fuel consumption and estimated distances to dumping sites (Table 2.1).

Drilling and blasting. Greenhouse gas emissions can arise through diesel use from drilling blasting boreholes and production of the explosives used for blasting. The drilling diesel use for extracting one tonne of crude ore was calculated as unit diesel use for drilling one tonne of rocks adjusted using the stripping ratio, defined as the ratio of overburden to the extracted crude ores. The explosives used for blasting were adjusted in the same way and coupled with the explosives emissions factor (Table 2.1) to determine GHG emissions associated with explosive use. The emissions factor represents emissions from its production, transportation, and detonation.

Dewatering. Ground and rainwater accumulate continuously during mining and require removal. The electricity consumption for dewatering was calculated based on the water volume, pumping efficiency, and pumping water head.

Loading and hauling. After blasting, the ore is removed from the mine via truck and sent to the ore treatment processes. Emissions rise from loading ores on trucks and hauling ore to the processing plant and hauling waste rock to the disposal area. Diesel consumption is based on a tonne of crude ore produced. Conversion from this basis to the per tonne function unit basis is by comparing the ore grade before and after processing and accounting for the Fe loss rate.

Table 2.1 Parameters used for bottom up modeling of open pit mining

Processes	Details and Assumptions	Emissions Source	Parameter (units)	Value Distributions (cardinal parameters)	Data sources
Vegetation and soil removal	Soil/vegetation carbon stock loss	Soil/vegetation carbon	Soil carbon stock (kg CO_2e/m^2) [a]	Uniform[b] (10, 33)	56
			Vegetation carbon stock (kg CO_2e/m^2)	Uniform (0, 24)	57
			Ground disturbance[c] (m^2/tonne)	Uniform (0.85, 1)	17, 58-60
			Mine lifetime (years)	Triangular[d] (2, 10, 30)	17, 51, 57, 59, 60
	Loss of photosynthetic productivity during project life time	Net primary production (NPP)	NPP ($gC/m^2/yr$)	Uniform (0.34, 0.36)	61-63
	Vegetation and soil clearance with bulldozer CAT D11R[e]	Diesel fuel	Bulldozer load factor for soil clearance (%)[f]	Uniform (50,65)	63
		Diesel fuel	Bulldozer load factor for vegetation clearance (%)	Uniform (35,50)	63
	Heavy trucks for soil transport	Diesel fuel	Distance of dumping soil (km)	Uniform (5,10)	17, 57, 59, 60, 64
			Fuel consumption factor (MJ/tonne.km)	Uniform (1.0,1.5)	49, 54, 64
Drilling	Electric-diesel engine powered rotary drills	Diesel fuel	Diesel use in drilling holes for blasting out one tonne of rocks (MJ/tonne)	Uniform (0.3,1.0)	17, 46, 57, 59, 60, 65
			Stripping ratio (tonne of waste rock/tonne of iron ore) [g]	Triangular (2, 3, 5)	17, 57, 59, 60
Blasting	Ammonium nitrate/fuel oil mixture explosive for blasting	Explosives	Explosive for blasting one tonne of rocks (kg/tonne)	Triangular (0.07 ,0.14 ,0.2)	17, 46, 57, 59, 60, 65, 66
Dewatering	Pumping water from groundwater intrusion	Electricity	Ratio of water and mining ores (m^3/tonne)	Triangular (0, 0.4, 4)	17, 57, 59, 60, 67
			Pumping efficiency (%)	Uniform (50, 85)	67-69
			Pumping water head (m)	Uniform (100, 300)	17, 57, 59, 60
Ore Loading	Front-end loader	Diesel	Diesel use for loading one tonne of rocks (MJ/tonne)	Triangular (2.5, 8.5, 18.5)	69, 70
Ore Hauling	Ore carriers (heavy trucks)	Diesel	Diesel use for hauling per unit (MJ/tonne.km)	Uniform (1.5, 4.8)	69-71
			Hauling distance (km)	Triangular (2, 4.5, 6)	17, 57, 59, 60, 64

[a] Carbon stock in top 1 meter soil is calculated. Soil carbon stock and vegetation carbon stock are correlated with net primary production, detail in SI; [b] Uniform (x, y) means the value for the parameter in the model is a uniform distribution, with a lower bound of x, and a upper bound of y; [c] Ground disturbance is the quotient of the mining area and the annual iron ore production, in unit of m^2/tonne; [d] Triangular (a, b, c) means the value for the parameter in the model is a triangular distribution, with a lower bound of a, a upper bound of c, and most likely value of b; [e] Caterpillar D11R is a type of large bulldozer, mainly used in mining industry for push-loading scrapers; [f] Bulldozer load factor is the percentage of bulldozer working load compared with the full capacity; [g] The parameter of stripping ratio is also used in modeling the processes of blasting, loading and hauling, but is not listed repeatedly in the table.

Ore Processing. The estimation of energy use and GHG emissions of ore processing were based on the data from 53 iron ore processing plants reported in the Ferrous Metal Mining Statistical Yearbook of China[71]. Electricity use for one tonne of crude ore treatment, ore grade before processing, ore grade after processing and Fe loss rate are reported for 53 processing plants. The Akaike Information Criterion (AIC) method was used to determine the best-fit distributions for modeling parameters related to ore processing energy use. The Ore Processing section of the appendix provides more detail.

*Rail Transportation***.** The database from Department of Metallurgy of China included 53 ore processing plants. These facilities represent 18% of total iron ore production and 83% of pig iron production in China, respectively. The database also provided latitudes and longitudes for these facilities in addition to 66 steel mills[72]. Assuming that steel mills acquire raw material from the nearest processing plants, the distance for the closest processing plants to a mill was identified using the great-circle distance calculated by Haversine's Formula[72] and a circuity factor of 1.5 for rail[73]. The model uses a discrete distribution of 66 distances, weighted by the percentage of total pig iron production from each steel mill, as shown in Table 2.2. Fuel consumption associated with rail transportation was then calculated using the distance distribution and fuel consumption factor. The fuel consumption factor is based on public LCI databases and existing literature[11, 49, 54]. The Approach II and Approach III described below also use these data for rail transportation.

Table 2.2 Rail distance for steel mills to acquire iron ores and percentage of ores shipped in the distance

	Steel mills	Distance (km)	Production (% of Total)
1	Shougang Jingtang company	116	1.11
2	Shougang Changzhi Iron & Steel Group Co., Ltd	160	0.71
3	Tianjin Steel Pipe Group Co., Ltd	137	0.23
4	Tianjin Tian Gang Group Co., Ltd	154	1.29
5	Tianjin Tiantie Metallurgical Group Co., Ltd	159	1.65
6	Tianjin Rongcheng United Steel Group Co., Ltd	144	0.90
7	Handan Iron and Steel	43	2.65
8	Xuanhua Steel	1	1.42
9	Chengde Steel	116	1.80
10	Xingtai Iron and Steel Co., Ltd	58	0.66
11	Beijing Jianlong Heavy Industry Group	21	2.12
12	Tangshan Guofeng Iron & Steel Co., Ltd	23	2.02
13	De Long Steel Co., Ltd	57	0.66
14	Hebei Zongheng Steel & Iron Group Co., Ltd.	34	1.23
15	Hebei Xinwuan Steel Group Co.,Ltd	5	4.26
16	Hebei Wenfeng Iron & Steel Co., Ltd	12	0.75
17	Hebei Xinjin Iron and Steel Co., Ltd.	2	0.71

18	Wuan Wenan Iron & Steel Co., Ltd	5	0.46
19	Tangshan Ganglu Iron & Steel Co., Ltd	67	0.77
20	Hebei Qianjin Steel Group Co., Ltd	140	0.64
21	Taiyuan Iron and Steel Group Co., Ltd.	1	1.94
22	Shanxi Zhongyang Iron & Steel Co., Ltd	204	0.59
23	Shanxi Jiexiu Xintai Iron & Steel Co., Ltd	161	0.14
24	Jincheng Fusheng Iron & Steel Co., Ltd	246	0.62
25	Baotou Iron & Steel Group Co., Ltd.	239	2.30
26	Benxi Iron and Steel Group Co., Ltd.	1	2.32
27	Beitai Iron and Steel Company	20	1.93
28	Tonghua Iron & Steel Group Co., Ltd	76	1.30
29	Baosteel Group Co., Ltd	24	9.53
30	Ningbo Iron and Steel Co., Ltd	159	1.04
31	CITIC Pacific Special Steel Group	3	1.33
32	Hubei New Metallurgical Steel Co., Ltd	38	0.37
33	Nanjing Iron and Steel Group Co., Ltd	96	1.49
34	Jiangsu Shagang Group	166	5.72
35	Jiangsu Shagang Group Huai Special Steel Co., Ltd	325	0.72
36	Jiangsu Yonggang Group Co., Ltd	142	0.97
37	Jiangsu Xixing Group Company	184	0.28
38	Jiangsu Su Steel Group Co., Ltd	139	0.14
39	Changzhou Zhongtian Iron & Steel Co., Ltd	209	1.12
40	Saint-Gobain (Xuzhou) Pipeline Co., Ltd.	334	0.16
41	Jiangsu Shente Iron & Steel Co., Ltd	144	0.27
42	Jiangyin Huaxi Iron & Steel Co., Ltd	174	0.64
43	Hangzhou Iron and Steel Group Company	181	0.70
44	Magang Group Co., Ltd	5	3.47
45	Xinyu Iron & Steel Co., Ltd.	4	2.12
46	Jiangxi Ping Steel Industry Co., Ltd	170	1.65
47	Fujian three Steel Group Co., Ltd	480	1.12
48	Laiwu Iron & Steel Group Co., Ltd	43	3.15
49	Zhangdian Iron and Steel Plant	106	0.25
50	Qingdao Iron & Steel Group Co., Ltd	200	0.81
51	Jinan Gengchen Iron and Steel Co., Ltd	96	0.20
52	Shandong Weifang Iron and Steel Group Company	15	0.60
53	Rizhao Iron & Steel Group Co., Ltd	254	3.38
54	Shandong Linyi Jiangxin Steel Co., Ltd	236	0.34
55	Anyang Iron & Steel Group Co., Ltd	105	2.15
56	Nanyang Han Ye Special Steel Co., Ltd	602	0.49
57	Wuhan Iron and Steel Group Company	15	7.91
58	Wuhan Iron and Steel Co., Ltd	301	1.46
59	Guangxi Iron and Steel Group Liu Steel Company	626	2.03
60	Hunan Valin Iron and Steel Group Co., Ltd	291	3.07
61	Lianyuan Iron & Steel Group Co., Ltd	433	1.45
62	Hunan Hengyang Steel Pipe Group Co., Ltd	380	0.21
63	Lengshuijiang Iron and Steel Co., Ltd	514	0.64
64	Chongqing Iron & Steel Group Co., Ltd	857	1.09
65	Shaanxi Hanzhong Iron & Steel Group Co., Ltd	1130	0.25
66	Yingkou Medium Plate Plant	95	0.46

Agglomeration. In the process of Agglomeration, iron fines are mixed with other materials (e.g., coke, limestone, etc.) that help the high-temperature process form larger iron particles compatible

with the blast furnace. The thermal process requires fuel for heating, a major source of GHG emissions. About 75% of the Chinese iron ore fines are transported to steel mills for sintering, while the remaining 25% undergoes pelletizing at the mining site, and then are transported to the mill[17]. The GHG emissions associated with sintering were modeled using a uniform distribution ranging from 200 to 280 kg CO_2e/tonne iron fines[52, 74, 75]. GHG emissions associated with pelletizing processes were modeled as a uniform distribution ranging from 25 to 30 kg CO_2e/tonne iron fines[52, 74, 75]. The emissions of the agglomeration stage were calculated as a weighted average of the pelletizing and sintering processes emissions (using the fraction of iron ore produced by the two agglomeration techniques).

Diesel and electricity emissions factors. The GHG emissions associated with energy consumption were calculated by multiplying the appropriate emissions factor the fuel used. Various studies have estimated the emissions factor of diesel fuel, which includes the emissions from oil production, refining, transportation and combustion[11, 49, 50, 76, 77]. Using the lowest and highest estimates from the previous studies, the emissions factor was assumed to be a uniform distribution of 90 to 100 gCO_2e/MJ. Table 2.3 presented the estimates and their applicability of previous studies.

Table 2.3 Emissions factors reported for diesel fuel

	Emissions factor estimate (CO_2e/MJ)	**Applicability**	**Data source**
1	96	Global Average	SimaPro[78]
2	92	United States	NETL[79]
3	93 (90%CI: 90~100)	United States	Venkatesh,2010[76]
4	100	China	Lixue, J.,2013[77]

Electricity is assumed to be the Chinese grid mix. The Chinese government reported the emissions factors of different regional grids[55], as shown in Table 2.4. These data were used to develop a uniform distribution of 760 to 830 gCO_2e/kWh. The 10% range is relatively low compared to the range of 260 to 810 g CO_2e/kWh reported for the U. S. different sub-region emissions factors[80]. It should be noted that the range used here might underestimation of the actual uncertainty of the Chinese grid. Approach II and Approach III will also use the estimates listed here for diesel and electricity emissions factors.

Table 2.4 Baseline Emission Factors for Regional Power Grids in China (gCO_2e/kWh)

Regional Grid	Covered Region	Installed capacity		
		600 MW	660 MW	1000 MW
North China	Beijing, Tianjin, Hebei, Shanxi, Shandong, Inner-Mongolia	810	810	780
Northeast China	Liaoning, Jilin, Heilongjiang	800	800	790
East China	Shanghai, Jiangsu, Zhejiang, Anhui, Fujian	780	780	760
Central China	Henan, Hubei, Hunan, Jiangxi, Sichuan, Chongqing	800	800	800
Northwest China	Shaanxi, Gansu, Qinghai, Ningxia, Xinjiang Uyghur	830	830	820
Southern China	Guangdong, Jiangxi, Yunnan, Guizhou, Hainan	810	800	800

2.3.2.2 Approach II: Estimation based on aggregate mining level observations.

Approach II uses data for electricity use, diesel use, stripping ratio and explosive use for extracting a ton of rocks reported for 55 Chinese mines (24 underground and 31 open pit) by the Chinese government's Department of Metallurgy[72]. Total iron ore production for the 55 mines accounted for 18% of Chinese production in 2011[72]. As above, the AIC method was used to develop the most likely probability distribution for the aggregated data for each parameter for each category of mine (open pit and underground). The parameters were then used to estimate the energy use and associated GHG emissions of underground and open pit mining. Table 2.5 shows the parameters and their fitted probability distributions. Approach II used the same methods and data sources as Approach I to estimate the emissions associated with ore processing, rail transportation and agglomeration.

Table 2.5 Parameters estimation based on mining site data.

Parameters(units)	Estimates	
	Open pit	Underground
Electricity use (kWh/tonne rock)	Invgauss (110, 2.18)[a]	Pearson5 (5.6, 73)[b]
Diesel use(MJ/tonne rock)	Triangular(0, 15, 63)[c]	--
Stipping ratio (tonne of waste rock/tonne of iron ore)	Loglogistic (0, 2.94, 2.67)[d]	--
Explosive use (kg/tonne rock)	Triangular (0, 0.22, 0.41)	Invgauss (3.3, 4.2)

[a] InvGauss(υ,β) means the value input for the parameter in the model is an inverse Gaussian distribution with mean of υ and shape parameter of β; [b]Pearson5(α,β) means the value input in the model is a Pearson type 5 distribution with parameters of α and β; [c] Triangular(a,b,c) means the value input in the model is a triangular distribution, with the lower bound of a, upper bound of c, and most likely value of b;[d] Loglogistic(γ,β,α) means the value input in the model is log-logistic distribution, with the scale parameter of α, the shape parameter of β, and a shift of γ.

2.3.2.3 Approach III

The estimation is based on statistical energy use data from the Chinese Energy Statistics Yearbook, which reports total energy consumption of the iron ore mining and processing sector yearly[73]. The total energy consumption is 1.8 kg coal, 1.2 kg coke, 25 MJ diesel and 34 kWh electricity for

producing per tonne of iron ore in China for 2013[81]. The GHG emissions were calculated using the sum of the products for each energy consumption and its corresponding GHG emissions factor. Same as modeled in Approach I, the emissions factor of electricity was a uniform distribution of 760 to 830 g CO_2e/kWh, and emissions factor of diesel was a uniform distribution of 90 to 100 g CO_2e/MJ. The emissions factor of coal was modeled as a triangular distribution with the lower bound of 89 g CO_2/MJ, upper bound of 96 CO_2/MJ, and most likely value of 106 CO_2/MJ[79]. The emissions factor of coke was modeled as a triangular distribution with the lower bound of 108 g CO_2/MJ, upper bound of 119 CO_2/MJ, and most likely value of 131 CO_2/MJ[79].

2.3.3 Monte Carlo simulation

Monte Carlo simulation was used to generate the probability distribution of the life cycle GHG emissions for each approach and to understand parameter uncertainty associated with each estimate. Spearman's rank correlation coefficient for each parameter was calculated to determine that parameter's corresponding influence on the variance of the final result[82]. The study used Palisade's @Risk™ software for Monte Carlo simulation and sensitivity analysis.

2.4 Results and discussion

This study developed multiple estimates for the GHG emissions for iron ore mining and processing in China. Using data at different levels of aggregation, three approaches were applied to calculate GHG emissions for different mining and ore processing scenarios. Figure 2.2 shows multiple GHG emissions estimates for the mining phase of the analysis. The bottom up (Approach I) provided an estimate for open pit mining. Approach II used more aggregate government sourced data, and estimated emissions for both open pit (surface mining) and underground mining (shaft mining), as well as a combined value based on the weighted average of the two mining processes. Approach I and Approach II estimated the mean for open pit mining as 39 and 35 kg CO_2e/tonne of ore, respectively. The two estimates vary by approximately 10%.

The bottom up approach (Approach I in Figure 2.2) estimated the GHG emissions of each individual mining process. The largest contributor to the total GHG emissions for open pit mining was iron ore loading and hauling (67% in total mining emissions), where diesel-powered loaders and trucks are used to move ore from mine for further processing. The second largest contributor was related to vegetation and soil removal, which included the GHG emissions from microbial

decomposition of the removed biomass and soil and lost photosynthetic productivity during the life of the mine. These GHG emissions, which accounts for 24% of total mining emissions, were neglected in prior iron ore mining LCA studies[46,54].

The mean emissions of underground mining were estimated as 34 kg CO_2e/tonne of ore by Approach II. Using this estimation approach, the values for open pit and underground mining techniques were essentially the same. When the ore is near the surface, open pit mining should result in reduced energy use and emissions as it avoids the energy used for ventilation. This accounts for more than 30% of energy use in underground mining. However, many deposits in China are deeply buried (more than 200 meters from the surface), and the energy consumption for overburden removal in open pit mining offsets the energy use in ventilation for underground mining.

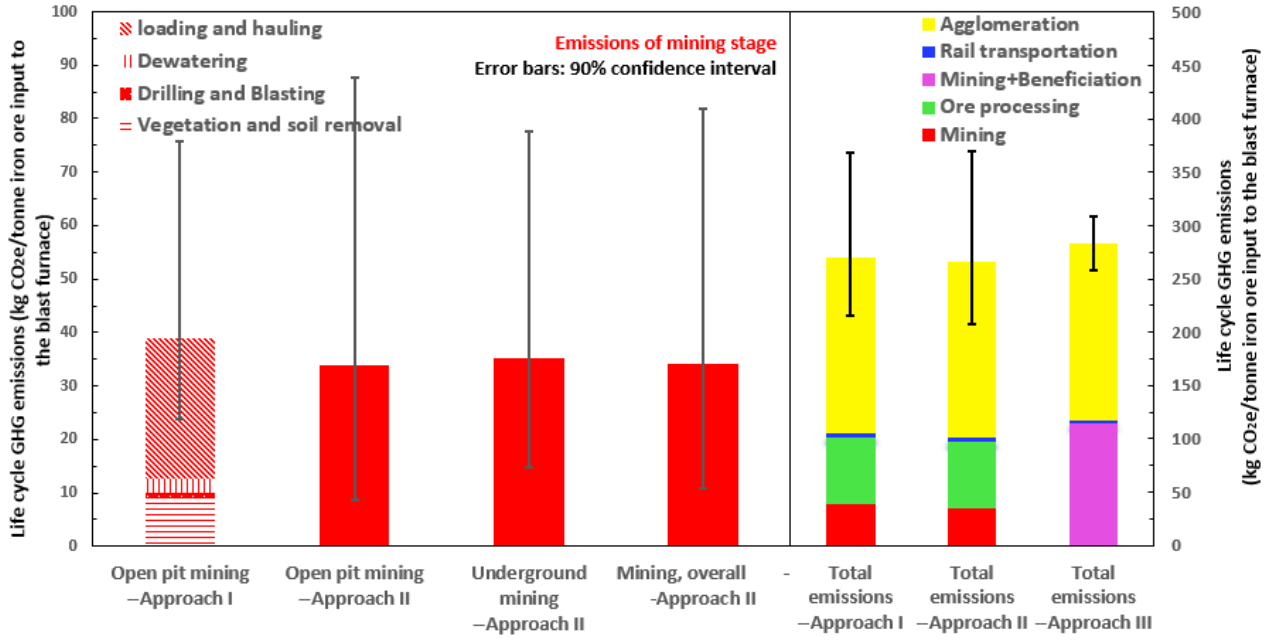

Figure 2.2 GHG emissions for the iron ore mine phase and life cycle emissions for Chinese iron ore mining for a 1 kg of iron ore to the blast furnace. The error bars represent the 90% confidence interval from the Monte Carlo simulation. Three approaches were used to estimate associated emissions of mining stage: Approach I is a bottom up assessment; Approach II used mining plants data reported by Department of Metallurgy of China; Approach III used statistical energy data of iron mining and processing sector, LCA results using this approach aggregates emissions for mining and ore processing stages.

Although most of the iron ores (87%) in China are currently extracted through open pit mining, there is a trend toward greater use of underground mining techniques as shallow ore deposits are depleted[17].

The right panel of Figure 2.2 shows the total iron ore life-cycle GHG emissions estimated by the three approaches. The mining stages use the combined mining values shown in the bar "Mining, overall approach II". The mean estimates for the totals range from 270 to 280 kg CO_2e/tonne, a less than 4% difference between the estimates and should be considered the same as LCA cannot model reliably differences this small[83].

In the overall emissions values, the agglomeration process is responsible for the majority of the GHG emissions arising from the process heat requirements. Sintering GHG emissions are significantly higher than pelletizing associated emissions. The sintering emissions range from 200 to 280 kg CO_2e/tonne, while pelletizing emissions are lower at 25 to 30 kg CO_2e/tonne. Thus, the fraction of sinters in the mixture feed to the steel mills blast furnace impacts the overall GHG emissions estimates for the agglomeration stage and the overall process.

Currently in China 70%-80% of the blast furnace feed are sinters. If the current mix was replaced with 100% pellets, life-cycle GHG emissions would be 130 kg CO_2e/tonne iron ore, which is 140 kg CO_2e/tonne iron ore (52%) lower than current emissions calculated with Approach II. Increasing the fraction of pellets would significantly reduce GHG emissions, however, the additional investment would be required to develop techniques and to install new facilities that were adapted to the feedstock change. Additionally, the production cost of pelletizing is higher than sintering. In 2013, the market price of pellets was $15-40 per tonne higher than sinters[17]. Thus, replacing sinters with pellets would reduce GHG emissions by 170 to 260 kg CO_2e/tonne but raise the iron ore feedstock cost for steel mill by $15-40 per tonne. The cost of GHG emissions mitigation is then estimated to be $60-240 per tonne of CO_2 equivalent.

The pelletizing technique was developing fast in China from 2001 to 2011. During the period, the annual pellets production increased from 18 million tonnes to 204 million tonnes, and the proportion of pellets in total iron ore feed to the blast furnace grew from 7% to 19%. However, the growth of pellet production has stagnated since 2012, and the proportion of pellets in total iron ore feed to the blast furnace declined to 11% in 2015. The higher market price of pellets compared with sinters is claimed to be the primary reason for the growth stagnation[84]. Establishing financial

aids for pelletizing (e.g. subsidy and tax reduction) might be a viable way to promote the further development of pelletizing. A detailed economic analysis should be conducted before taking further actions.

The second largest source of GHG emissions is ore processing, where the iron content is increased to produce concentrated fines. Compared with the high-grade ore of other major producing areas, such as Australia or Brazil that have ores over 50% Fe content, 94% of Chinese crude ores are low grade, averaging around 27% Fe in 2012[17].

High-grade ores (over 60% Fe content), require only simple processing while the low-grade ores require more complicated treatment processes and involve additional steps of milling, floatation/magnetic separation, concentration, filtration, and drying. This complexity comes at the cost of increased energy consumption in the form of electricity. As over 70% of Chinese grid electricity is sourced from coal and peat, the GHG emissions are high.

Increasing iron mining and high-grade ore depletion in China necessitate the use of lower grade ore in the future. By varying the value of iron ore grade in the original model used for estimating life-cycle GHG emissions (Approach II) and maintaining other parameters constant, the study further discusses the change of GHG emissions as the iron ore grade decreases. The analysis results are shown in Figure 2.3.

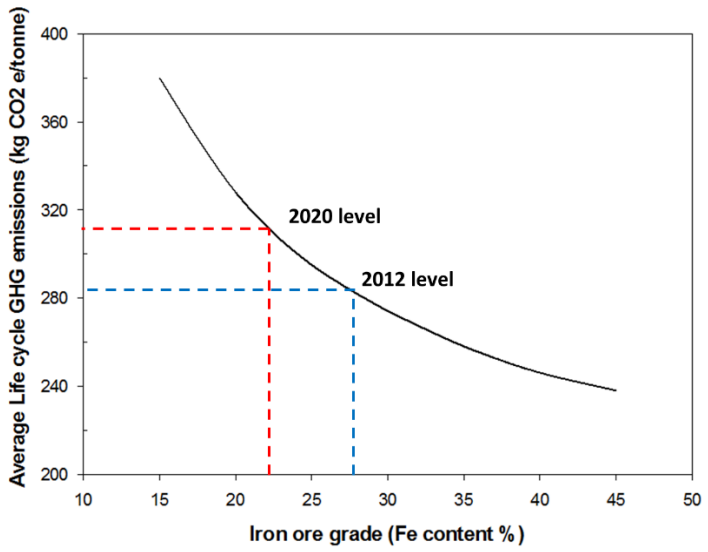

Figure 2.3 Mean life-cycle GHG emissions per tonne of iron ore (total emissions--approach II, Figure 2.2), as a function of iron ore grade

According to Figure 2.3, the relationship between iron ore grade and GHG emissions is non-linear. As the iron ore grade declines, the rate of increase in GHG emissions from mining accelerates. For example, when iron ore grade decreases from 40% to 35%, the average GHG emissions for mining increases by 12 kg CO_2e/tonne. In contrast, the same 5% iron ore grade decrease from 20% to 15% would lead to 52 kg CO_2e/tonne. Thus, China will face accelerating energy consumption and increased GHG emissions for every tonne of iron ore extracted and processed in the future. From 2006 to 2012, average iron ore grade dropped from 30% to 27%[17]. If this trend continued, in 2020, the average iron ore grade could be 23%, and life-cycle mean GHG emissions would increase by 9%, from 2012 level of 285 kg CO_2e/tonne to 310 kg CO_2e/tonne.

From 2001 to 2013, the total iron ore demand in China increased with an average yearly growth rate of 15%. If the increase continues, the total GHG emissions for the iron ore mining/processing sector will increase three times that of the 2013 level by 2020, representative for 2.3% of the total projected GHG emissions for China in 2020[85], if the fraction of ore provided by the domestic supply remains unchanged.

It is possible that importing high-grade iron ores from other countries might be a viable GHG emissions reduction strategy for this important sector of the Chinese economy. For example, in Australia, iron ore has the Fe content of 56 to 62%[77] and most of the deposits are near the surface.

Mining this ore can lead to lower GHG emissions and energy cost. However, detailed analysis of GHG emissions from long distance shipping is required, as shipping could offset some of the savings due to the iron ore grade. The downside though to importation is that shifting can have undesirable socioeconomic impacts making an assessment tradeoffs necessary. Potential impacts include decreased production in the Chinese mining sector leading to unemployment, as well as stability and security issues for the country's economic system.

Results shown here suggest that increasing the fraction of pelletized iron ore used in the blast furnaces can reduce overall GHG emissions. Using 100% pellets to the current sinter-pellet mix would reduce 52% of current life-cycle GHG emissions. However, there are front-end costs of new pelletizing facilities, demolition of existing sintering plants, and potential unemployment among sintering operators.

The present study analyzes the mean value and uncertain range of life-cycle GHG emissions associated with iron ore production in China. In contrast to prior studies which treated ore mining with "black-box modeling," this study applies a bottom-up approach to determine the GHG emissions of each process using technical parameters. The results suggested that iron ore grade is the key parameter driving the LCA results, and that rapidly declining iron ore grade can accelerate increased GHG emissions in China. Importing high-grade iron ore from abroad, and increasing the fraction of pellets fed to the blast furnaces can reduce GHG emissions from iron ore production in China, which can aid in future policymaking.

2.4.1 Importance analysis and sensitivity

Spearman's rank correlation coefficients between each parameter used in Monte Carlo simulation and the total GHG emissions were calculated to determine the influence of each parameter on the uncertainty of the final result. For the result calculated by approach II, iron ore grade was the largest contributor to the variance, contributing 42% of the total variance followed by electricity use for beneficiation (28%). The Fe content in the crude ores extracted from different mines in China varied from 10% to 60%[17]. The crude ore grade determines the quantity of crude ores in weight needed to fulfill the functional unit; this has a direct impact on the amount of GHG emissions from mining and beneficiation.

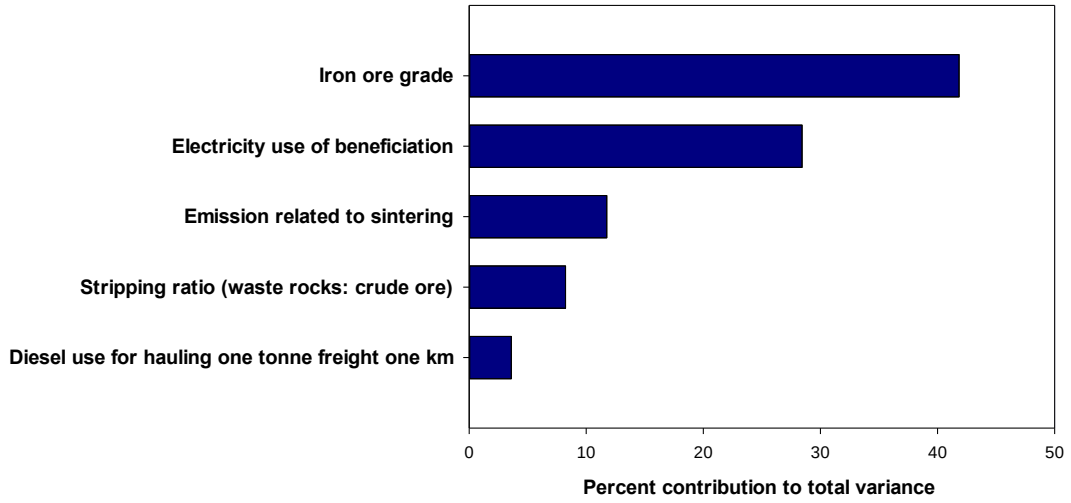

Figure 2.4 Top five parameters with the largest contributions to the uncertainty of LCA result for Chinese iron ore (Approach II)

2.5 Appendix to Chapter 2

This section contains details of data, methods, and modeling parameters used in chapter 2.

2.5.1 Approach I: bottom up modelling

2.5.1.1 Mining

Vegetation and soil removal. Vegetation and soil are removed to expose the ore seam. GHG emissions arise from microbial decomposition of the removed biomass and soil (soil organic carbon degradation). Additionally, a debt accrues due to reduced photosynthetic productivity during the lifecycle of the mine due to the removed biomass.

Equations 1, 2, and 3 describe the calculation of these emissions, and Table 2.6 lists the values and data sources for the parameters used in the estimation. Total emissions due to the biomass and soil loss are the sum of the Equations 1, 2, and 3.

For one tonne of iron ore, CO_2 emissions due to the loss of soil carbon stock:

$$C_1 = SOC \times A/T \quad [1]$$

CO_2 emissions due to the loss of vegetation carbon stock:

$$C_2 = VOC \times A/T \quad [2]$$

CO_2 emissions due to the loss of potential net carbon assimilation by vegetation:

$$C_3 = \frac{44}{12} \times NPP \times A \quad [3]$$

In Equation 1, 2, and 3, SOC is the soil carbon stock (kg CO_{2e}/m^2), VOC is the vegetation carbon stock (kg CO_{2e}/m^2), NPP is the net primary production ($gC/m^2/yr$), A is ground disturbance (mining area/annual crude ore production:m^2/tonne), T is mine lifetime.

Bulldozers were used for clearing and grubbing mining areas by removing vegetation and soil. Heavy trucks were used to transport removed vegetation and soil to dumping site. The greenhouse gas emission associated with these processes were estimated as below:

Table 2.6 Parameters for estimating emissions due to biomass and soil loss.

Parameter(units)	**Estimate**	**Sources**
Net Primary Production (gC/m2/yr)	Uniform (0.34, 0.36)	61, 62, 70
Soil Carbon stock (kg CO_2 e/m^2) [a]	Uniform (10, 33)	56, 61
Vegetation Carbon stock (kg CO_2 e/m^2)	Uniform (0, 24)	57, 63
Ground disturbance (mining area/annual crude ore production:m^2/tonne)	Uniform (0.85, 1)	59, 60, 64, 82, 86
Mine lifetime	Triangular(2, 10, 30)	59, 60, 64, 82, 86

a Carbon storage in top 1 meter soil is accounted. The parameter of soil carbon stock is correlated with net primary production, and the correlation coefficient between the two parameters is 0.43, 12. The correlation coefficient between the parameter of vegetation carbon stock and net primary production is 0.83, 12.

In this study, we use the following empirical model for calculating diesel use of bulldozer[63]:

Fuel consumption (FC):

$$\text{FC (diesel, L/h; for bulldozer D11R[1]; P = 634 kW)} = 1.74 \times LF - 0.117 \quad [4]$$

Where LF is the load factor of the bulldozer, which means the percentage of working load

[1] Caterpillar D11R is a type of large bulldozer, mainly used in mining industry, for push-loading scrapers. Here we assume that D11R is used for the site preparation.

compared with the full capacity.

For mining site vegetation clearance, the bulldozer works in low load, with the load factor of 35%~50%, the diesel consumption for one D11R bulldozer is 61~87 L diesel per hour. The working capacity for the D11R bulldozer is 6000 m^2 per hour. The following equation is used to calculate the diesel use for vegetation clearance for per tonne iron ore production:

$$\mathrm{D}_{\mathrm{clearance}} = (\mathrm{A} \times \mathrm{F})/(\mathrm{W} \times \mathrm{T}) \quad [5]$$

Where, A is ground disturbance (mining area/annual crude ore production: m^2/tonne), T is mine lifetime, in years, F is bulldozer diesel consumption per hour, W is bulldozer working capability.

The similar method (Equation [5]) is used to calculate the diesel use to remove top-soil and sub-soil in the pit area. For soil removal, load factor for bulldozer is 50%-65%, and then the diesel consumption would be 87~113 L diesel per hour.

Heavy trucks are used to transport soil for dumping. Assuming on average one meter deep soil would be removed. The following equation is used to calculate diesel use for soil dumping for per tonne iron ore production:

$$D_{dumping} = \mathrm{E} \times \mathrm{L} \times \rho \times \mathrm{A}/\mathrm{T} \quad [6]$$

Where E is the unit diesel use for transporting one tonne of soil in one km, L is the dumping distance; ρ is soil density, 2.5 tonne/m^3, A is ground disturbance (mining area/annual crude ore production: m^2/tonne), T is mine lifetime.

Drilling and blasting. The mining operation starts with drilling and blasting, and its purpose is to fracture rocks and ores in the pit for further removal. For the majority of large open pit iron mining projects an electric-diesel engine rotary drill is used for drilling, and blasting is accomplished using ammonium nitrate/fuel oil (ANFO) explosive. I calculate energy and explosive use per these presumptions. Figure 2.5 shows the plan view of the drilling design and the parameters used. Based on these parameters, I build models for calculating energy use for drilling and explosive use in blasting.

Equation 7 is used to calculate the weight powder factor (PF), which is the kg of ANFO required for blasting one tonne of rocks:

$$PF=\frac{\frac{\pi}{4}\times D^2\times d_{ANFO}\times(L-T)}{d_{rock}\times B\times S\times H}=\frac{\frac{\pi}{4}\times d_{ANFO}\times(H+K_J\times K_B\times D-K_T\times K_B\times D)}{d_{rock}\times K_S\times K_B^2\times H} \quad [7]$$

Where, H is the bench height, the height of the working bench of the mining pit, and usually it ranges from 10 meter to 15 meters for open pit iron ore mining; D is the blast hole diameter, which depends on the bench height, for different production requirements and environment, D equals to (0.005~0.01) H; d_{rock} is rock density, which is 5150 kg/m^3 for iron ore deposits; B is the burden distance, use burden factor K_B as multiply factor to calculate burden distance based on blast hole diameter, B= K_B×D. K_B varied as the rock density and explosive type, in the model KB=30; S is the spacing, and Ks is the spacing factor, which specifies the blast hole spacing as a function of the burden, S= KS×B. KS varied from 1 to 2, depending on initiation; Sub-drilling factor KJ represent the distance of sub-drilling as a function of the burden, KJ varied from 0.2 to 0.5, sub-drilling distance J= KJ×B,; T is stemming distance, can be calculated with stemming factor KT and burden distance B, T= KT×B, KT varied from 0.5 to 1.3; d_{ANFO} is the density of explosive ANFO, which is 800 kg/m3.

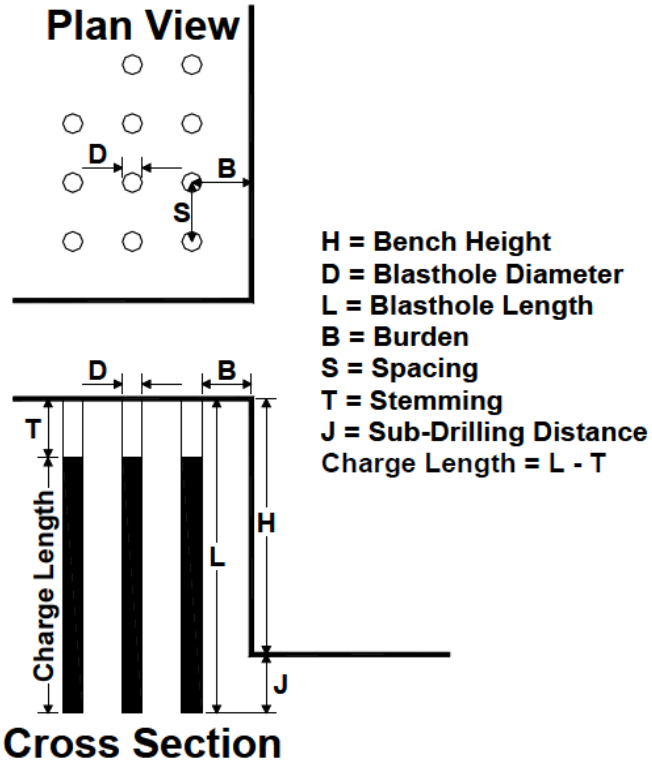

Figure 2.5 View of the drilling and blasting design (from Heasley, 2011).

According to Equation 6, I calculate the typical powder factor for open pit iron ore mining to be 0.07~0.12 kg ANFO per tonne of rocks. Besides of using the model to calculate the unit powder use, I also gathered the data from other published literature for calibration. The comparison of the calculated results and data from different articles is shown in Table 2.7. In this study, the estimate for explosive for blasting one tonne of rocks is uniform distribution range from 0.15 to 0.30 kg/tonne iron ore.

Table 2.7 Explosive used for per tonne of crude iron ore.

Unit: kg/tonne iron ore	Data source
0.15~0.30	Calculated by Equation (6)
0.2	Norgate[46]
0.20~0.22	New Millennium Capital Corp [67]

To get the value on a per tonne of iron ore produced basis, the explosive used = PF× (1+stripping

ratio). Stripping ratio defined as the ratio of waste rock and ore. The study model the stripping ratio as a triangular distribution with the ranges from 2 to 5, and the most likely value of 3[59, 60, 64, 82, 86, 87].

The emissions associated with explosive use is then calculated as the GHG emissions factor of explosive multiply by the volume of explosive used. The GHG emissions factor of explosive include the emissions from the following processes: obtaining row materials, on-site transport, production, and transport to the user, loading, and detonation of explosives. According to Kukfisz and Maranda[88], the overall GHG emissions associated with explosive use is 0.2 tonne CO_2 e/tonne explosive.

I also calculated the volume of drilled rock for blasting one tonne of rocks:

$$V = \frac{\frac{\pi}{4} \times (H + K_J \times K_B \times D)}{K_S \times K_B^2 \times H \times d_{rock}} \quad [8]$$

Then I calculated the drilling length and working hours (when using one drill) for per tonne of iron ore using the Equation (8) and (9):

$$L = \frac{V}{\frac{\pi}{4} \times D^2} \quad [9]$$

Working hours:

$$H = \frac{L}{P} \quad [10]$$

Where, P is the penetration rate, assuming 40m/hr in this model.

A diesel generator (1000kw) is used to provide electricity to the drill. The diesel use per hour changes with load and ranges from 21.6 gal/hr to 71.1 gal/hr. Diesel use for drilling holes for blasting one tonne of rock ranges from 0.3 to 1.0 MJ. With Equation 11, drilling diesel use for extracting one tonne of iron ore can be calculated.

$$E = D \times (1 + R) \quad [11]$$

Where D is the diesel use in drilling holes for blasting one tonne of rocks, R is the stripping ratio.

Dewatering. For majority of mines under the water table, it is necessary to prevent mining site flooding.

Domingues et al. summarized and compared the ratio of infiltrated water flows (in cubic meter) and ore extracted (in tonnes) for several mining sites[67]. The ratio varied with local geological characteristics (e.g. sandy vs karstic aquifers), and mining depth. According to *Domingues et al.*, the ratio for open pit mines with sandy aquifers ranged from 1:1 to 10:1, while for the underground mines in karstic aquifers, the ratio ranged from 10:1 to 100:1[67].The following model is used to estimate electricity power for dewatering in mining operations:

$$P = \frac{QH}{374\eta} \qquad [12]$$

In Equation 12, P is the pump power, kilowatt; Q is flow rate, cubic meter per hour; H is the total dynamic head, meter-water; η is the pump efficiency, which can range from 50% to over 85% in different situation[89].

Therefore, the electricity used for dewatering in in unit time, equals to pump power multiply by working hours of the pump. The following equation depicts the calculation of electricity use for pumping for per tonne of iron ore.

$$\text{Pumping electricity use per ton iron ore} = \frac{\text{annual electricity}}{\text{annual ore production}}$$

$$= \frac{\text{Pump power} \times \text{yearly working hour}}{\text{annual ore production}} = \frac{Q \times H \times \text{yearly working hour}}{374 \times \eta \times \text{annual ore production}}$$

$$= \frac{\frac{\text{Ratio of water and ore}(m^3:\text{ton}) \times \text{annual ore production}}{\text{yearly working hour}} \times H \times \text{yearly working hour}}{374 \times \eta \times \text{annual ore production}}$$

$$= \frac{\text{Ratio of water and ore}(m^3:\text{ton}) \times H}{374 \times \eta} \qquad [13]$$

According to Equation 13, electricity used for dewatering can be calculated with the parameters of Ratio of water and mining ores (m^3/tonne), Pumping efficiency (%) and Pumping water head

(m). Based on the mining site case reports in Australia and China, we estimate the parameters of Ratio of water and mining ores (m^3/tonne) and Pumping water head (m).

Loading and Hauling. After blasting, front-end loaders or excavators would shovel and load the broken rocks and ores into hauling trucks. In the majority of cases, a fleet of hauling trucks transport the waste rocks to dumping area and iron ores to the processing plants continually. The loading excavators or hauling trucks used in the mining site are all electric-diesel engine, and we can use the two indicators MJ/tonne and MJ/tonne-km to measure the diesel use of loading and hauling per tonne of substance in these processes. Table 2.8 and table 2.9 show the values for these two indicators, which are gathered from several case studies.

Table 2.8 Diesel Use for loading per tonne of substance (units: MJ/tonne).

	Best estimate/Average	Range	Number of cases	Data source
1	8.8	1.0~15	8	[90]
2	10	2.5~19	3	[91]

Table 2.9 Diesel Use for hauling per tonne of substance one kilometer (units: MJ/tonne-km)

	Best estimate/Average	Range	Number of cases	Data source
1	2.8	0.23~4.2	8	[90]
2	3.5	1.8~6.0	3	[91]

Then, diesel use for per tonne of iron ore produced can be calculated based on the following equations.

Diesel use for excavating per tonne of crude iron ore:

$$E_1 = U \times (1 + R) \quad [14]$$

Where U stands for diesel use for loading per tonne of substance, and R is the stripping ratio.

Diesel use for hauling per tonne of crude iron ore:

$$E_1 = N \times L_1 + N \times L_2 \times R \quad [15]$$

N is diesel use for hauling per tonne of substance of one kilometer, L_1 is the length of the hauling road for iron ore, from the loading spot to the processing plant, L_2 is the distance for damping waste rock, R is the stripping ratio.

For different mining sites, the distance from the working bench to the crushing plant or waste

dump varied from several hundred meters to a few kilometers, depending on the local geological circumstances and mining site design.

2.5.1.2 Ore processing

For the iron ore with Fe content higher than 60%, only crushing and screening are needed for ore processing. The following section presents the methods and data used to estimate the electricity consumption for crushing and screening

The Bond's formula is used to calculate the energy use for crushing [92]:

$$W_b = 10W_i\left(\frac{1}{\sqrt{P}} - \frac{1}{\sqrt{F}}\right) \quad [16]$$

Where: W_b is energy intensity measured in kilowatt hours per tonne, W_i is the Bond work index in kilowatt hours per tonne (kWh/tonne), a parameter that is derived experimentally for different materials in mining engineering handbooks, F is the passing size for 80% of the feed in microns, P is the "passing size" for 80% of the product in microns [93].

Based on the case reports of the mining project[8-12], I can calibrate the parameters in Bond's formula for each crushing steps, as reported in table 2.10:

Table 2.10 Parameters used for calculating electricity of crushing in Bond's formula.

	Bond work index (kWh/tonnne)	**F:feeding size (um)**	**P:product size (um)**	**Multiplication factor**
Hydraulic rock breaker	14.7	900,000	200,000	1.6
Primary crusher	14.7	200,000	80,000	2
Pecondary crusher	14.7	90,000	40,000	1
Tertiary crusher	14.7	40,000	10,000	1

Vibrating grizzly screens are usually used for sizing ores after crushing. After screening, the oversized ores return to the crushing step, while the undersized ores go to the next step of processing. According to literature and mining case reports, we calibrated the electricity use for crushing is 0.09~0.13 kWh/tonne[46, 59, 60, 64, 82, 86].

In China, most (94%) of the extracted crude ores are lower than 60% Fe content, and processing includes crushing, screening, milling, separation, and concentration steps.

The estimated energy use in beneficiation for the low-grade ores is based the data of 53 iron ore

beneficiation plant reported in the ferrous metal mining statistical yearbook of China. Using the Akaike Information Criterion and the Bayesian Information Criterion, the best fit distributions are determined for the parameters shown in Table 2.11.

Table 2.11 Estimations for electricity use for beneficiation

	Parameters(units)	*Estimates*
1	Electricity use (kWh/tonne crude ore)	Loglogistic (0, 26, 4.33)[a]
2	Crude ore Fe grade (%)	Triangular (20,26,45)[b]
3	Concentrated ore Fe grade (%)	Triangular (64,66,70)
4	Iron loss late (%)	Triangular (10,15,30)

[a] Loglogistic(γ,β,α) means the value input in the model is log-logistic distribution, with the scale parameter of α, the shape parameter of β, and a shift of γ. [b] Triangular(a,b,c) means the value input in the model is a triangular distribution, with the lower bound of a, upper bound of c, and most likely value of b.

2.5.2 Approach II: Estimation based on aggregate mining level observations.

Approach II uses data for electricity use, diesel use, stripping ratio and explosive use for extracting a tonne of rocks reported for 55 Chinese mines (24 underground and 31 open pit) by the Chinese government's Department of Metallurgy[72]. The Akaike Information Criterion was used to develop the most likely probability distribution for these mining plants data for each parameter of the two mining category (open pit and underground). The following figures show the fit comparison of mining plants data and the fitted cumulative distribution function curve for the parameters estimation.

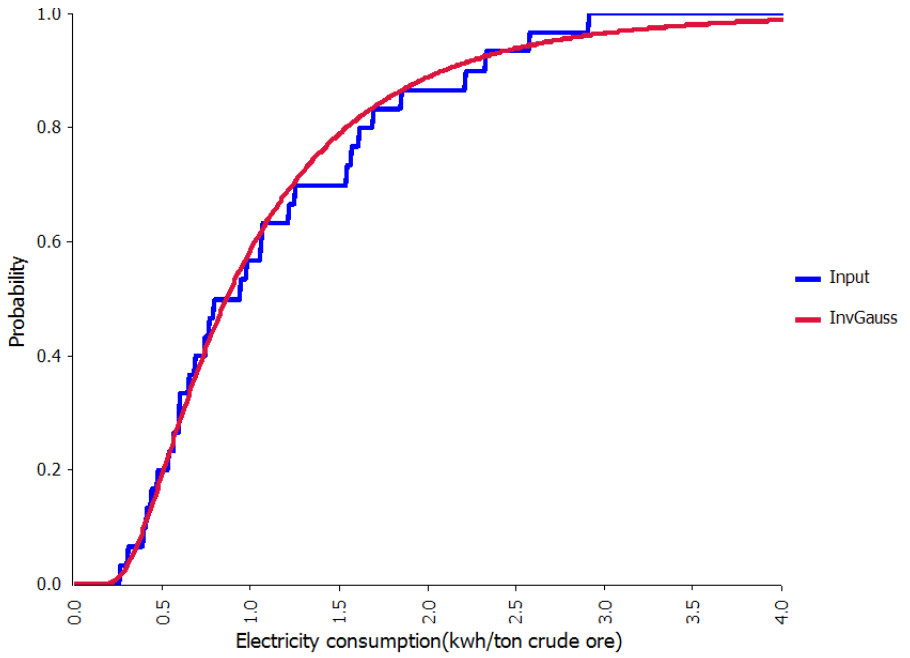

Figure 2.6 Fit comparison for the parameter electricity use of open pit mining

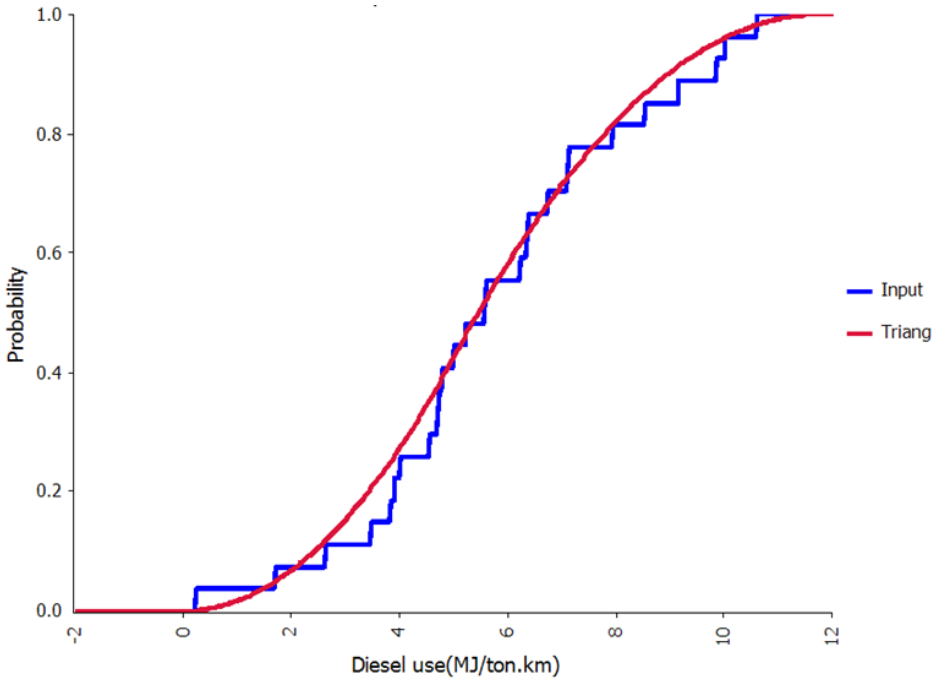

Figure 2.7 Fit comparison for the parameter diesel use of open pit mining

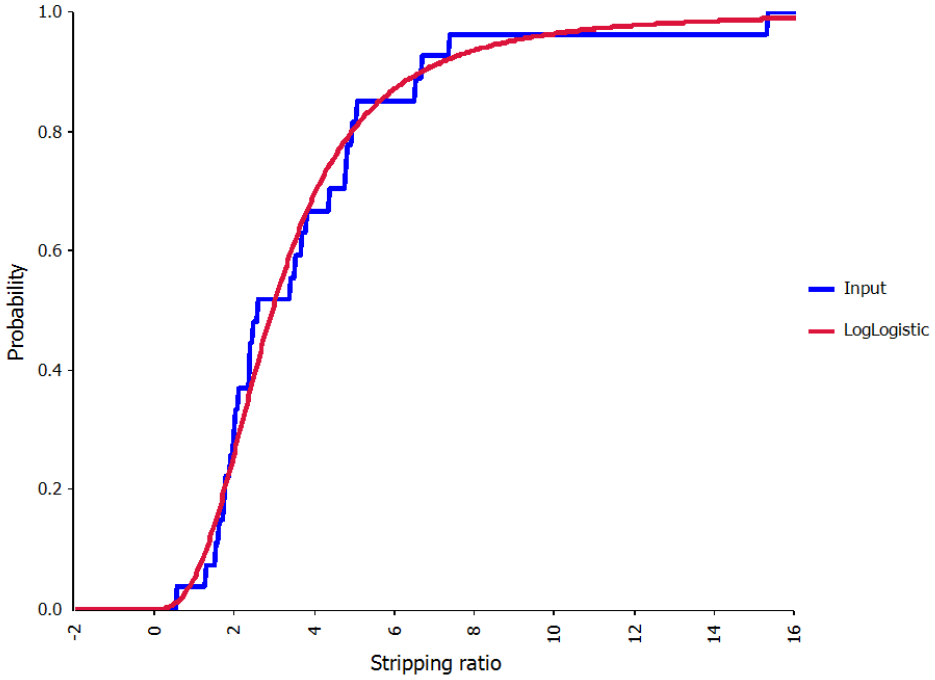

Figure 2.8 Fit comparison for the parameter stripping ratio of open pit mining

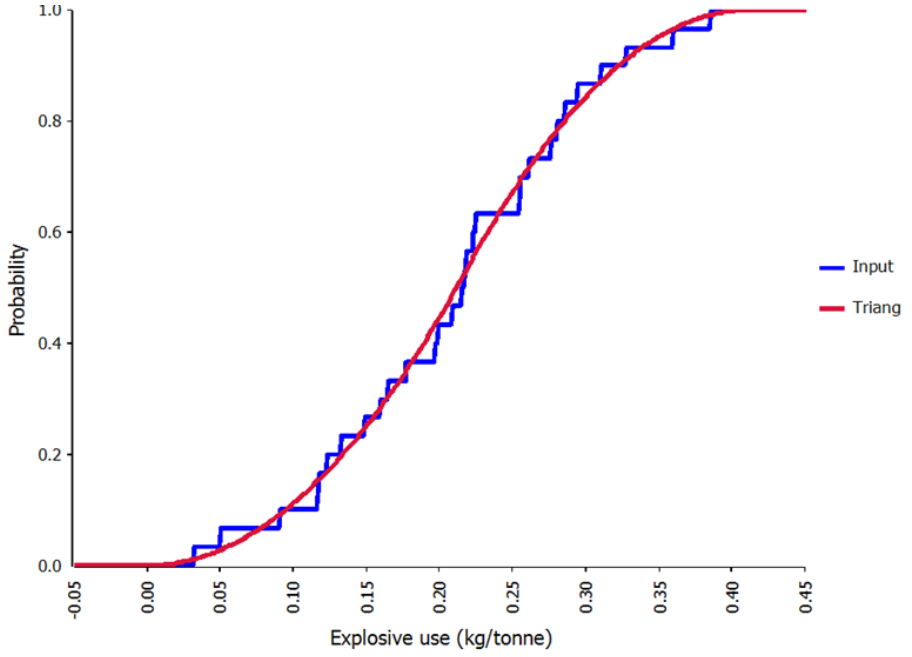

Figure 2.9 Fit comparison for the parameter explosive use of open pit mining

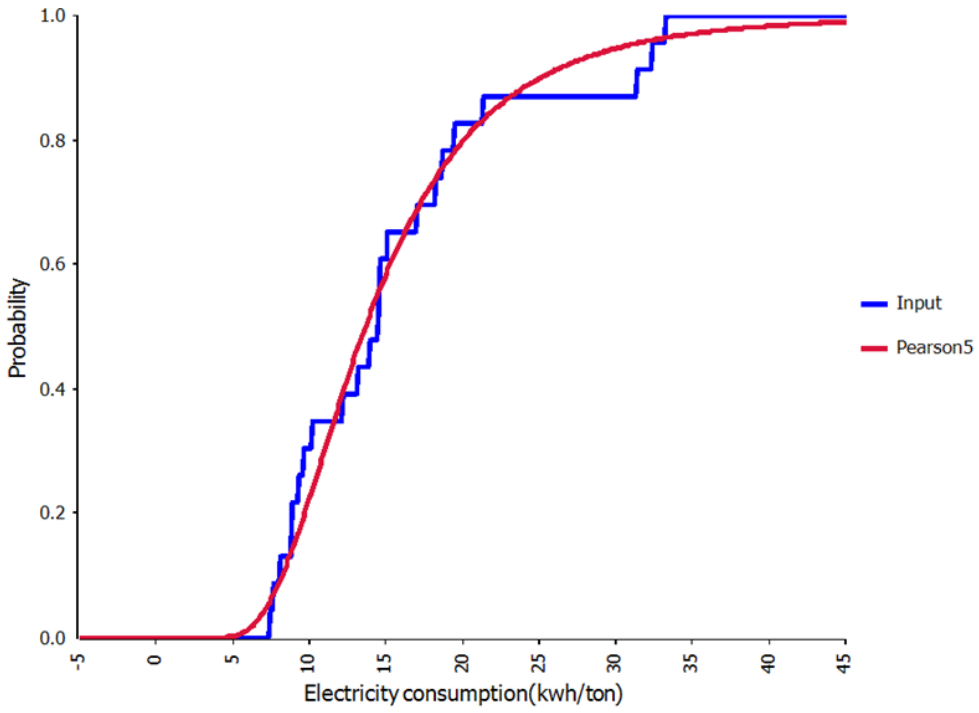

Figure 2.10 Fit comparison for the parameter electricity of underground mining

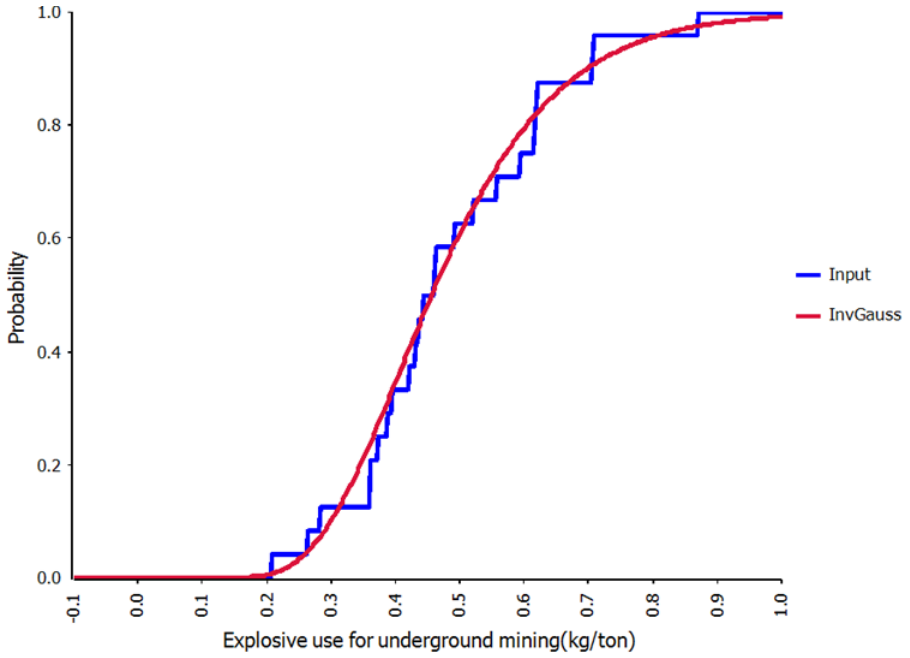

Figure 2.11 Fit comparison for the explosive use of underground mining

3. Life cycle GHG emissions of iron ore mining in China, Australia and Brazil—a comparison of different iron ore sources for China

3.1 Abstract

The large-scale urbanization and rapid infrastructure development witnessed in China are creating overwhelming iron ore and steel demand, leading to a rising greenhouse gas (GHG) emissions from the energy-intensive iron ore production processes. One path China has sought to meet increasing iron ore demand is to source iron ore from overseas. Importing iron ores from Australia or Brazil could help China meet its domestic need, but the question arises if the overall GHG emissions would increase because of the differences in resources, extraction technologies, and transportation needs.

This chapter applies the same life cycle assessment framework of Chinese iron ore in chapter 2 to Australian and Brazilian ore production and compares the LCA results of Australian and Brazilian ore to Chinese iron ore. Results show that among the three iron ore sources, Australian iron ore is the optimal choice for reducing GHG emissions. The mean life cycle GHG emissions of Australian iron ore fines is 60% less than that of Chinese iron ore fines (42 kg CO_2e/tonne compared to 110 kg CO_2e/tonne, respectively). There is no significant difference between the iron ore sourced from Brazil and delivered to China versus the China's domestic supplied iron ores, but if Chinese ore grade falls below 20% in the future, Brazilian iron ores would be preferred.

The largest source of GHG emissions for Australian and Brazilian iron ores comes from ocean shipping (accounts for 58% and 75% of the overall GHG emissions respectively). Increasing vessel capacity utilization could help reduce GHG emissions for the ocean shipping of ore.

The study suggests that importing iron ores might be viable GHG emissions reduction strategies for China.

3.2 Introduction

The large-scale urbanization and rapid infrastructure development witnessed in China are creating overwhelming iron ore and steel demands[94], leading to a rising greenhouse gas (GHG) emissions from the energy-intensive iron ore production processes. According to the result in chapter 2, total GHG emissions from Chinese iron ore mining and processing in 2020 might be three times higher than 2013 levels if the domestic and import supply ratio remains unchanged.

One path China has sought to meet increasing iron ore demand and GHG emission reduction goals is to source iron ore from overseas. In 2013, 73% of the 1.1 billion tonnes iron ore consumption in China was imported. As the top two largest net exporters of iron ores in the world, Australia and Brazil are the major suppliers for China[20]. In 2013, 57% of China's imported iron ores came from Australia, and 18% are from Brazil[19].

Importing iron ores from Australia or Brazil could help China meet its domestic need, but the question arises if the overall GHG emissions would increase because of the differences in resources, extraction technologies, and transportation needs. This paper determines the greenhouse gas emissions (GHG) associated with iron production in Australia and Brazil and subsequent importation into China.

Few studies report life cycle emissions for iron ore mining, and there are no comparisons of emissions for the world's three main production areas: Australia, Brazil and China. Life cycle GHG emissions for Australia's iron ore mining is estimated as 12 kg CO_2e/tonne by Norgate and Haque[46], and Ferreira *et al.* presented the life cycle emissions for single iron mine in Brazil as 13 kg CO_2e/tonne[54]. These studies, however, applied different system boundaries making comparisons difficult. Additionally, results from these studies are applicable to specific mine which may not represent the overall situation of that country. Finally, none of these studies for Australian and Brazilian iron ores have conducted result uncertainty analysis, and neither have include emissions of marine shipping to market overseas. The study in Chapter 2 modeled the life cycle emissions for iron ore production in China. Using Monte Carlo simulation, I estimated life cycle emissions of iron ore mining and processing in China as 110 kg CO_2e/tonne, with the 90%

confidence interval ranging from 60 to 190 kg CO_2e/tonne. The research also found that crude ore grade has a significant impact on the life cycle emissions.

Producing iron ore results in direct GHG emissions from production, and indirect emissions from upstream processes for explosives, energy production, and transportation needs. Life cycle assessment (LCA) is used to determine the direct and indirect GHG emissions for iron ore delivered to China. This study applies the same LCA modeling framework of Chinese iron ore in chapter 2 to Australian and Brazilian ore production, incorporates shipping oversea in their life cycle, and compares the LCA results of Australian and Brazilian ore to Chinese iron ore. Monte Carlo simulation will be conducted to provide the mean and uncertain estimate of the LCI results. With a further discussion of the potential impact of China's iron ore decline on the LCA comparison results, this study can inform policymakers on China's future iron ore import strategies.

3.3 Methods

3.3.1 Scope and system boundary

The life cycle of iron ore mining includes the stages of mining and ore processing. In the mining stage, iron ores are extracted through open pit mining (surface mining) in Australian and Brazil, while in China both open pit and underground mining are practiced (Figure 3.1) [19]. In general, mining obtains crude ores that require processing for sizing and increasing Fe content. Crude ores with a low Fe content (usually with Fe content lower than 60%) are crushed, screened, milled and further processed using flotation/magnetic separation, and concentration. As this point, the size is smaller than 0.1mm and is referred to as iron ore concentrate fines. For high-grade ores, such as ores from Western Australia (with 58% to 65% Fe content) and Carajas Brazil (with 65% to 67% Fe content), only a simple process of crushing and screening is conducted at this stage. Screening separates the high-grade ores into different sized products: lumps (sized from 6.3 to 31.5mm) and fines (smaller than 6.3mm). Lumps could be shipped to China and used directly in blast furnaces ready for steel making, while small-sized iron ore fines need to be sintered or pelletized to meet the size requirements of blast furnaces.

China currently imports iron ore in three forms: lumps, pellets, and sinter feed iron fines. Among the three, sinter feed iron fines account for the largest (53%) share in the total imports, and they are alternatives for China's domestic-produced iron fines to feed the sintering process in China's steel making industry. In China, 75% of domestic-produced iron ores are for sintering[19].

The functional unit used in this LCA is one metric ton of sinter feed fines. The life cycle system boundary for Australian and Brazilian iron ores includes the stages of mining, ore processing, rail transportation in each country, ocean shipping, transportation within China to the steel mill gate, and the upstream steps for producing energy and material used in ore operations. At the steel mill gate, the three sources of iron ore undergo the same processes of sintering and steel making, and this occurs outside the system boundary. Figure 3.1 shows the system boundary and process step investigated for the three iron ores compared in the study.

3.3.2 Fuel and electricity emissions factors

Iron ore life cycle GHG emissions from energy use are calculated as the amount of energy used multiplied by the appropriate emissions factor. The estimation of the fuel emissions factors includes the fuel production (emissions from all upstream processes included), transportation, and combustion. The study uses data from the literature and LCI databases[75, 78, 79] for the estimates. The emissions factor for diesel use is a uniform distribution of 90 to 100 g CO_2e/MJ, and that of heavy fuel oil ranges between 92 and 94 g CO_2e/MJ. Country grid mix electricity is assumed. The emissions factors for electricity use in Australia and Brazil were calculated based on the contribution of different primary energy sources for each country and the worldwide average GHG intensities for different sources of power generation[95-97]. The calculated grid emission factor is also compared and cross-validated with the values reported in the literature and public LCI database[75]. The emissions factor for grid mix electricity in Western Australia is a uniform distribution from 610 to 810 g CO_2e/kWh, and that for Brazil is a uniform distribution of 89 to 93 g CO_2e/kWh.

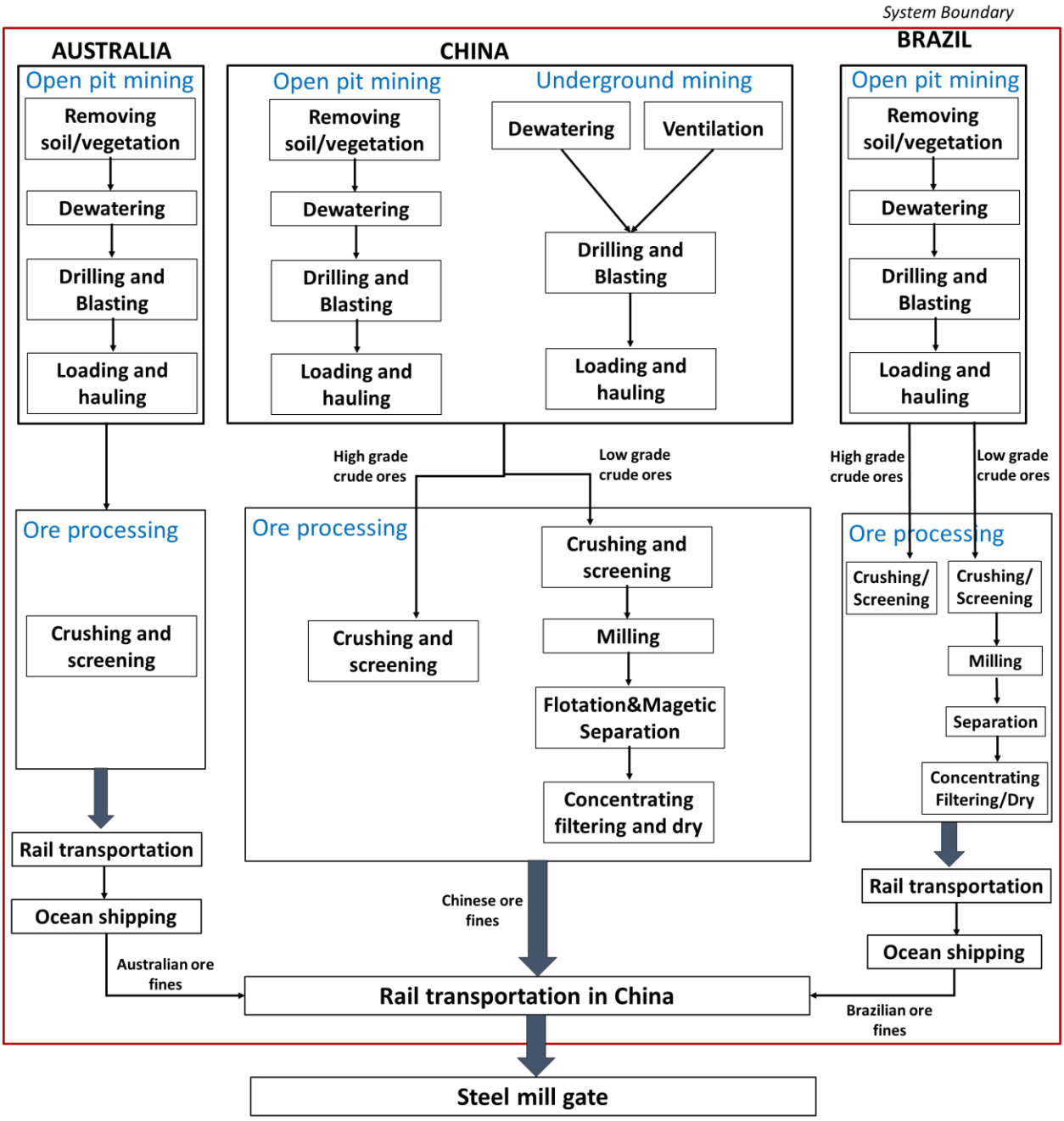

Figure 3.1 Iron ore mining, processing and shipping in Australia, Brazil, and China, and the associated life cycle assessment system boundary.

3.3.3 Mining and ore processing in Australia and Brazil

The study used methods developed in Chapter 2 to estimate emissions from mining and ore processing in Australia and Brazil, with country-specific parameters in each model. The analysis accounts GHG emissions from vegetation and soil removal, drilling and blasting, dewatering, loading, and hauling steps for mining, and crushing, screening, and concentration steps for ore processing. As primary data on material flows and emissions from mines are difficult to obtain, this study used published mining and processing technical parameters to estimate the energy use and GHG emissions. For example, the parameter of stripping ratio (tonne of waste rock/tonne of iron ore) and weight powder factor (explosive for blasting one tonne of rocks) is used to estimate the amount of explosive required and its associated GHG emissions for blasting. The values of those technical parameters and others were collected from public reports, literature, and databases. Table 3.1 summarizes the mining and ore processing steps as well as the parameters used for calculating emissions.

China imports iron ores from Western Australia, the primary iron ore producing area in Australia[2]. Australian ore from this region is produced from similar geological conditions and utilize similar production processes. Brazilian ore is produced in two areas: the Iron Ore Quadrangle area located in the southeastern state of Minas Gerais, and Carajas in the northern state of Para. The geological conditions, mineral grade, processing techniques, surrounding ecosystem, as well as the transportation distances to the ports for mining in these two areas are distinct, which leads to different GHG emissions from mining and processing. This study differentiates Brazilian iron ores from the two producing areas and estimates their associated GHG emissions separately.

3.3.4 Railway transportation

There are two distinct legs of rail transportation for iron ore shipments: shipment from the mine to the port in the producing country and shipment from the receiving Chinese port to the steel mill. Fuel consumption associated with rail transportation was calculated using the estimate of transport

[2] Iron ore from Western Australia accounts for more 97% of the total Australian iron ore production in 2011.

distance and fuel consumption factors. The fuel consumption factors are taken from public LCI database and the literature[52, 54, 55, 76].

Twenty iron ore mines in Western Australian and their corresponding shipping ports on the northwestern coast located and identified by their latitudes and longitudes. Using the Haversine Formula[72], the great-circle distance between each iron ore mine and corresponding shipping port was calculated. The direct distance is corrected for geographic deviation using a circuity factor of 1.5 for rail[73]. The rail transport distance from mines in Western Australia to export ports was represented and modeled as a uniform distribution ranging from 250 to 500 kilometers in the study.

Transportation distances vary for ores from Carajas and the Iron Ore Quadrangle in Brazil. Distances were determined using the method described for the Australian iron ore. The railway distance from Carajas to the Ponta da Madeira marine terminal was estimated as approximately 900 kilometers, while the railway distance for iron ore from the Iron Ore Quadrangle area to the nearest port on the southeastern Brazilian coast was modeled as uniform distribution ranging from 400 to 550 kilometers.

Iron ores from Australia and Brazil are shipped to ports in China. Twenty-nine iron ore receiving ports and 66 steel mills, representing 83% total pig iron production in China, were located using their latitudes and longitudes[90]. With the assumption that steel mills acquire iron ores from the nearest ports, the great-circle distance from the closest port to the identified steel mill was calculated using the Haversine Formula[72]. This distance is multiplied by a circuity factor of 1.5 for rail[73]. A discrete distribution model is then established for all 66 distances with probability value corresponding to the percentage of total pig iron production for each steel mill, as shown in Table 3.2. A discrete distribution model is used as the estimate of the uncertain railway distance from import ports to steel mills.

3.3.5 Ocean shipping

Australian and Brazilian iron ore is shipped by the bulk carrier that consumes heavy fuel oil to the various ports in China. Fuel consumption for per tonne of freight per kilometer is estimated using published data for large bulk carriers[98-101]. Port to port distances from Australia and Brazil to China

were obtained from online distance calculators[62, 102]. A discrete distribution model was then developed for the port to port distances, with probability values corresponding to the percentage of total iron ore transported through each route.

3.3.6 Monte Carlo simulation

A Monte Carlo simulation was constructed with the uncertainty ranges of the parameters discussed above to calculate the distribution of the GHG emissions associated with iron ore mining and processing in Australia and Brazil, respectively. In the sensitivity analysis section, Spearman's rank coefficient for each parameter is calculated to represent their corresponding influence on the variance of the final result.

Table 3.1 Model and parameters for iron ore mining and ore processing

Processes		Details and Assumptions	Category	Parameter (units)	Estimates			Data sources
					Australia	Brazil-iron Quadrangle	Brazil-Carajas	
Mining	Vegetation and soil removal	Soil/vegetation carbon stock loss	Soil/vegetation carbon	Soil carbon stock (kg CO_2e/m^2) [a]	Uniform (8.0, 8.8)	Uniform (11,22)	Uniform (22,37)	86, 103-106
				Vegetation carbon stock (kg CO_2e/m^2)	Uniform (7.0, 16)	Uniform (3.7,11)	Uniform (66,73)	104, 107-109
				Ground disturbance [b] (m^2/tonne)	Uniform (1.2, 1.3)	Uniform (1.2, 1.3)	Uniform (1.2, 1.3)	100, 110-115
				Mine lifetime (years)	Uniform (20, 40)	Uniform (20,40)	Uniform (20,40)	100, 110-115
		Loss of photosynthetic productivity during project life time	Net primary production (NPP)	NPP (gC/m^2/yr)	Triangular (0.23,0.24,0.27)	Uniform (0.2,0.5)	Uniform (0.6,0.9)	102, 103, 116
		Vegetation and soil clearance with bulldozer CAT D11R [c]	Diesel	Bulldozer load factor for soil clearance (%)[d];	Uniform (50,65)			117
			Diesel	Bulldozer load factor for vegetation clearance (%)	Uniform (35,50)			117
		Heavy trucks for soil transport	Diesel	Distance of dumping soil (km);	Uniform (5,10)			32-38,64
				Fuel consumption factor (MJ/tonne.km)	Uniform (1.0,1.5)			75, 78, 79, 118
	Drilling	Electric-diesel engine rotary drills are used	Diesel	Diesel use in drilling holes for blasting out one tonne of rocks (MJ/tonne)	Uniform (0.3,1.0)			65, 115, 119
				Stripping ratio (tonne of waste rock/tonne of iron ore) [e]	Triangular (1, 1.5, 1.8)	Triangular (0.4,0.8,1.4)	Uniform (0.25,0.4)	100, 110-115, 120
	Blasting	Use ammonium nitrate/fuel oil mixture explosive for blasting	Explosive	Explosive for blasting one tonne of rocks (kg/tonne)	Triangular (0.07,0.14,0.2)			115, 119
	Dewatering	Pumping out the water gushing out from underground during mining operation	Electricity	Ratio of water and mining ores (m^3/tonne)	Triangular (0, 0.4, 1)	Triangular (0, 0.4, 1)	Triangular (0, 0.4, 1)	32-38, 67
				Pumping efficiency (%)	Uniform (50, 85)			68, 69, 121
				Pumping water head (m)	Uniform	Uniform	Uniform	32-38

					(100, 300)	(100, 300)	(100, 300)	
	Loading	Front-end loader	Diesel	Diesel use for loading one tonne of rocks (MJ/tonne)	Triangular (2.5,8.5, 18.5)			91, 122, 123
	Hauling	Carrying ores from working platform to treatment plant, dumping waste rocks by heavy trucks	Diesel	Diesel use for hauling per unit (MJ/tonne-km)	Uniform (1.5, 4.8)			91, 122-124
				Hauling distance (km)	Triangular (2, 3, 5)	Uniform (2,5)	Uniform (2,5)	32-38,64, 125
		Hauling by conveyor	Electricity	Electricity use for hauling per unit (Kwh/tonne-km)	--	Uniform(0.057,0.17)		100, 115, 125
Ore processing	Crushing/Screening of high-grade crude ore	Crushing and sizing ore products	Electricity	Electricity use for crushing and screening (kwh/tonne)	Uniform (1.85, 2.5)	--	Uniform (1.85, 2.5)	46, 100, 115
	Beneficiation of low-grade crude ore	Increasing Fe content in low-grade crude ores, including processes of crushing, screening, milling, separation, and concentration	Electricity	Electricity use for beneficiation of per tonne crude ore (kWh/tonne crude ore)	--	Loglogistic (0, 26, 4.33)	--	54, 71, 126
				Fe content in crude ore (%)		Triangular (45,55,67)		20, 54, 127
				Fe content in iron ore concentrate (%)		Triangular (64,66,70)		54, 126
				Percentage of Mineral loss in beneficiation (%)		Triangular (0.1,0.15,0.3)		71, 126

a Carbon stock in top 1 meter soil is accounted. Soil carbon stock, vegetation carbon stock are correlated with net primary production, detail in the Appendix; b Ground disturbance is the quotient of the mining area and the annual iron ore production, in unit of m2/tonne; c Caterpillar D11R is a type of large bulldozer, mainly used in mining industry for push-loading scrapers; d Bulldozer load factor is the percentage of bulldozer working load compared with the full capacity; e The parameter of stripping ratio is also used in modelling the processes of blasting, loading and hauling, but is not listed repeatedly in the table. f Uniform (x, y) means the value of the parameter in the model is a uniform distribution, with a lower bound of x, and an upper bound of y; g Triangular (a, b, c) means the value of the parameter in the model is a triangular distribution, with a lower bound of a, an upper bound of c, and most likely value of b.

Table 3.2 Rail distance for different steel mills to shipping ports and percentage of iron ore shipped in the distance

	Steel mills	Distance to ports (km)	Production (% of Total)
1	Shougang Jingtang company	18	1.11
2	Shougang Changzhi Iron & Steel Group Co., Ltd	722	0.71
3	Tianjin Steel Pipe Group Co., Ltd	32	0.23
4	Tianjin Tian Gang Group Co., Ltd	62	1.29
5	Tianjin Tiantie Metallurgical Group Co., Ltd	72	1.65
6	Tianjin Rongcheng United Steel Group Co., Ltd	29	0.90
7	Handan Iron and Steel	540	2.65
8	Xuanhua Steel	434	1.42
9	Chengde Steel	290	1.80
10	Xingtai Iron and Steel Co., Ltd	502	0.66
11	Beijing Jianlong Heavy Industry Group	231	2.12
12	Tangshan Guofeng Iron & Steel Co., Ltd	89	2.02
13	De Long Steel Co., Ltd	508	0.66
14	Hebei Zongheng Steel & Iron Group Co., Ltd.	545	1.23
15	Hebei Xinwuan Steel Group Co.,Ltd	564	4.26
16	Hebei Wenfeng Iron & Steel Co., Ltd	572	0.75
17	Hebei Xinjin Iron and Steel Co., Ltd.	563	0.71
18	Wuan Wenan Iron & Steel Co., Ltd	564	0.46
19	Tangshan Ganglu Iron & Steel Co., Ltd	190	0.77
20	Hebei Qianjin Steel Group Co., Ltd	129	0.64
21	Taiyuan Iron and Steel Group Co., Ltd.	703	1.94
22	Shanxi Zhongyang Iron & Steel Co., Ltd	902	0.59
23	Shanxi Jiexiu Xintai Iron & Steel Co., Ltd	809	0.14
24	Jincheng Fusheng Iron & Steel Co., Ltd	802	0.62
25	Baotou Iron & Steel Group Co., Ltd.	1056	2.30
26	Benxi Iron and Steel Group Co., Ltd.	247	2.32
27	Beitai Iron and Steel Company	238	1.93
28	Tonghua Iron & Steel Group Co., Ltd	395	1.30
29	Baosteel Group Co., Ltd	24	9.53
30	Ningbo Iron and Steel Co., Ltd	56	1.04
31	CITIC Pacific Special Steel Group	7	1.33
32	Hubei New Metallurgical Steel Co., Ltd	501	0.37
33	Nanjing Iron and Steel Group Co., Ltd	18	1.49
34	Jiangsu Shagang Group	15	5.72
35	Jiangsu Shagang Group Huai Special Steel Co., Ltd	174	0.72
36	Jiangsu Yonggang Group Co., Ltd	19	0.97
37	Jiangsu Xixing Group Company	67	0.28
38	Jiangsu Su Steel Group Co., Ltd	87	0.14
39	Changzhou Zhongtian Iron & Steel Co., Ltd	44	1.12
40	Saint-Gobain (Xuzhou) Pipeline Co., Ltd.	271	0.16
41	Jiangsu Shente Iron & Steel Co., Ltd	109	0.27
42	Jiangyin Huaxi Iron & Steel Co., Ltd	31	0.64
43	Hangzhou Iron and Steel Group Company	241	0.70
44	Magang Group Co., Ltd	61	3.47
45	Xinyu Iron & Steel Co., Ltd.	732	2.12
46	Jiangxi Ping Steel Industry Co., Ltd	760	1.65
47	Fujian three Steel Group Co., Ltd	309	1.12
48	Laiwu Iron & Steel Group Co., Ltd	259	3.15

49	Zhangdian Iron and Steel Plant	167	0.25
50	Qingdao Iron & Steel Group Co., Ltd	24	0.81
51	Jinan Gengchen Iron and Steel Co., Ltd	277	0.20
52	Shandong Weifang Iron and Steel Group Company	97	0.60
53	Rizhao Iron & Steel Group Co., Ltd	10	3.38
54	Shandong Linyi Jiangxin Steel Co., Ltd	133	0.34
55	Anyang Iron & Steel Group Co., Ltd	606	2.15
56	Nanyang Han Ye Special Steel Co., Ltd	1015	0.49
57	Wuhan Iron and Steel Group Company	585	7.91
58	Wuhan Iron and Steel Co., Ltd	1051	1.46
59	Guangxi Iron and Steel Group Liu Steel Company	458	2.03
60	Hunan Valin Iron and Steel Group Co., Ltd	847	3.07
61	Lianyuan Iron & Steel Group Co., Ltd	797	1.45
62	Hunan Hengyang Steel Pipe Group Co., Ltd	636	0.21
63	Lengshuijiang Iron and Steel Co., Ltd	812	0.64
64	Chongqing Iron & Steel Group Co., Ltd	1334	1.09
65	Shaanxi Hanzhong Iron & Steel Group Co., Ltd	1677	0.25
66	Yingkou Medium Plate Plant	76	0.46

3.4 Results and discussion

Figure 3.2 shows the life cycle GHG emissions of Australian and Brazilian iron ore production and shipping to China. The two estimates reported for Brazilian iron fines represent the two major iron ore production areas: Brazil-Iron Quadrangle and Brazil-Carajas. Chinese iron ore production results are discussed in Chapter 2.

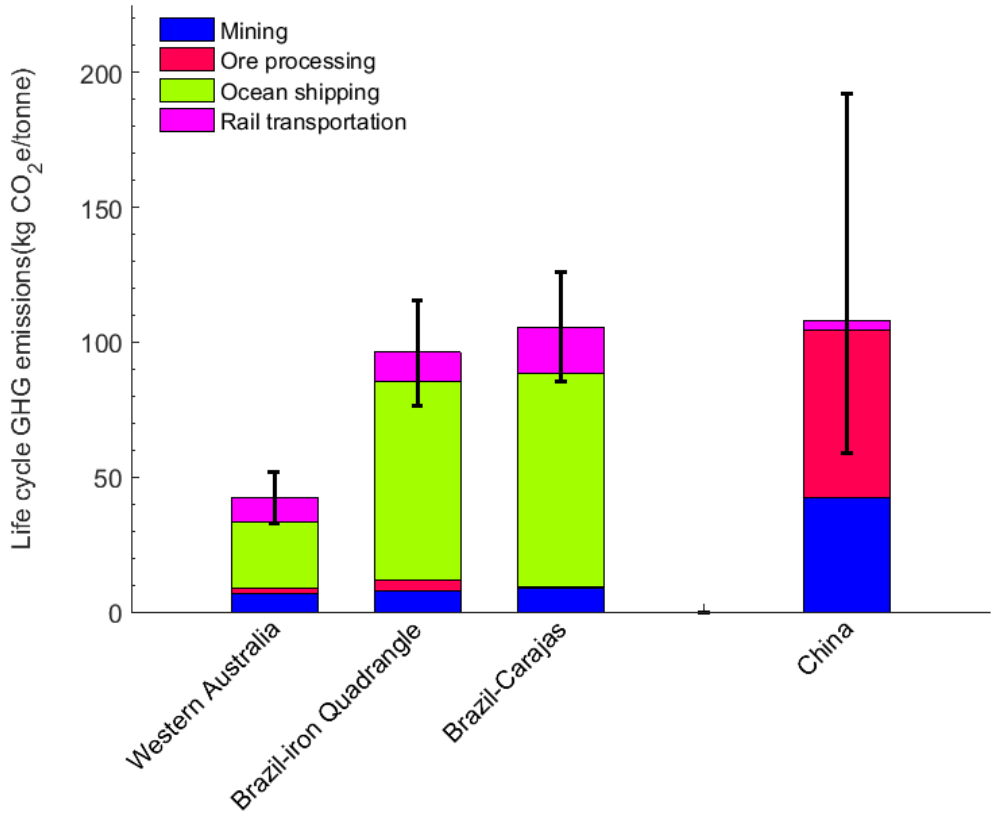

Figure 3.2 Life cycle GHG emissions for Western Australian, Brazilian and Chinese. Error bars represent 90% confidence interval from the uncertainty analysis. Life cycle emissions of Chinese iron ore are from study result in Chapter 2 (Approach II).

The mean life cycle GHG emissions of Australian iron ore fines is 60% lower than those of Chinese iron ore fines, 42 kg CO_2e/tonne compared to 110 kg CO_2e/tonne, respectively. Thus, replacing Chinese fines with Australian sourced fines could reduce overall GHG emissions. The mean estimates of emissions of Brazilian iron fines are similar to that of Chinese iron fines. Brazilian iron fines from Iron Quadrangle and Carajas are 97 kg and 107 kg CO_2e/ tonne on average, and have a 90% confidence interval range of 77 to 116 kg CO_2e/ tonne and 87 to 126 kg CO_2e/ tonne, respectively. The uncertainty range of Chinese iron ore emissions encompasses all potential values for the Brazilian iron ores. From this analysis, there is no significant difference in GHG emissions between the iron ore sourced from Brazil and delivered to China versus the China's domestic supplied iron ores.

GHG emissions for each stage of production were calculated separately. Ocean shipping accounts for 58% and 75% of the overall GHG emissions for Australian and Brazilian iron fines, respectively. Emissions for Australian/Brazilian iron fines mining and ore processing are much lower than for Chinese iron ores. GHG emissions of Australian iron fines production are 9 kg CO_2e/tonne, similar to the previous estimate of 10 kg CO_2e/tonne from Norgate and Haque[46]. GHG emissions of iron fines production from the Iron Quadrangle are 12 kg CO_2e/tonne on average, versus 13 kg CO_2e/tonne reported in Ferreira *et al*[54]. While Chinese mining and ore processing emissions are 6 to 8 times higher. Higher crude ore grade (above 50% of average iron ore grade in Australia and Brazil, 30% on average for China) is the main reason for the lower energy cost and GHG emission in iron ore mining and ore processing in Australia and Brazil. Additionally, clean grid power in Brazil (80% sourcing from hydro-power) also helps reduce GHG emissions of iron fines production in Brazil.

Although mining and ore processing emissions in Brazil are lower than those for China, the 20,000 km shipping offsets the lower emissions. Ocean shipping drives the LCA results for both Australian and Brazilian iron ores, and it should be the primary target for reducing GHG emissions in the life cycle of Australian and Brazilian iron ores. However, under current production-based GHG emissions accounting frameworks[128], countries are only responsible for the GHG emissions produced within their border and do not include the GHG emissions from international shipping. The lack of commitment from the trading countries impedes more actions to reduce GHG emissions from international shipping[129].

The second largest source of GHG emissions for Australian and Brazilian iron ores is rail transportation, which includes upstream and downstream legs: rail transport from mines to ports, and transport from Chinese ports to steel mills. Australian and Brazilian Rail transportation emissions are larger than those of Chinese iron fines because of a shorter overall distance to travel to the destination. Emissions from rail transportation account for 22% of total emissions for Australian iron fines, 11% for Brazilian Iron Quadrangle fines, 16% for Brazilian Carajas fines, yet only 3% of Chinese iron fines, as shown in Figure 3.2. Railway transportation emissions of Brazilian Carajas fines are larger than that for Brazilian Iron Quadrangle fines, again because of distance, Carajas is further away from shipping ports. The longer railway transportation for Carajas

ores makes its mean life cycle emission surpass that of ore from Iron Quadrangle, although mining and processing the average higher-grade Carajas ore emits lower emissions.

3.4.1 Potential for lowering emissions

Increasing the capacity utilization of the ocean shipping leg could reduce fuel consumption and reduce GHG emissions for the ocean shipping of ore through allocation to other products and elimination of empty backhauls. Currently, while most iron ore bulk carriers are empty for the backhaul, Japanese steel and shipping companies have adopted a triangular shipping route to improve shipping efficiency[130]. For example, a ship leaves Australia with coal for India, then moves iron ore from India to Japan, and is only empty on the leg from Japan to Australia. Triangular or multi-leg shipping routes could be exploited in this way[58].

Importing iron ore pellets instead of concentrated fines could reduce GHG emissions from the agglomeration process in China. Concentrated fines imports, with sintering in China, is the major form of iron ore imports, accounting for 53% in 2013[19], but is not the optimal choice from the aspect of lowing GHG emissions. According to the discussion of Chapter 2, sintering GHG emissions are significantly higher than pelletizing associated emissions. Importing pellets instead of sinter feed concentrates would reduce the GHG emissions from the agglomeration process by 170 to 260 kg CO_2e/tonne iron ore. In 2013, pellets accounts for only 5% in the total iron ore imports[19], implicating a large potential of growth in the future.

Australian iron ore is the best iron ore source for China among the three for reducing GHG emissions. Figure 3.3 shows the cumulative distribution functions of stochastically determined values for the emissions differences between the two Brazilian, the Australian sourced ore and the Chinese ore. Australian iron ore emissions are always less than Chinese iron ores. Replacing Chinese iron fines with Australian iron fines would reduce average GHG emissions by 71 kg CO_2e/tonne, with 90% confidence interval ranging from 16 to 150 kg CO_2e/tonne. Australian iron fines also stochastically dominate Brazilian iron fines with respect to GHG emissions under this modeling.

On average, Chinese iron ore production emits higher life cycle GHG emissions than Brazilian iron ore production, but there is still a 40% to 50% of the probability that GHG emissions of

Chinese iron ores are less than that of Brazilian iron ores. There is no clear cut "better" decision here.

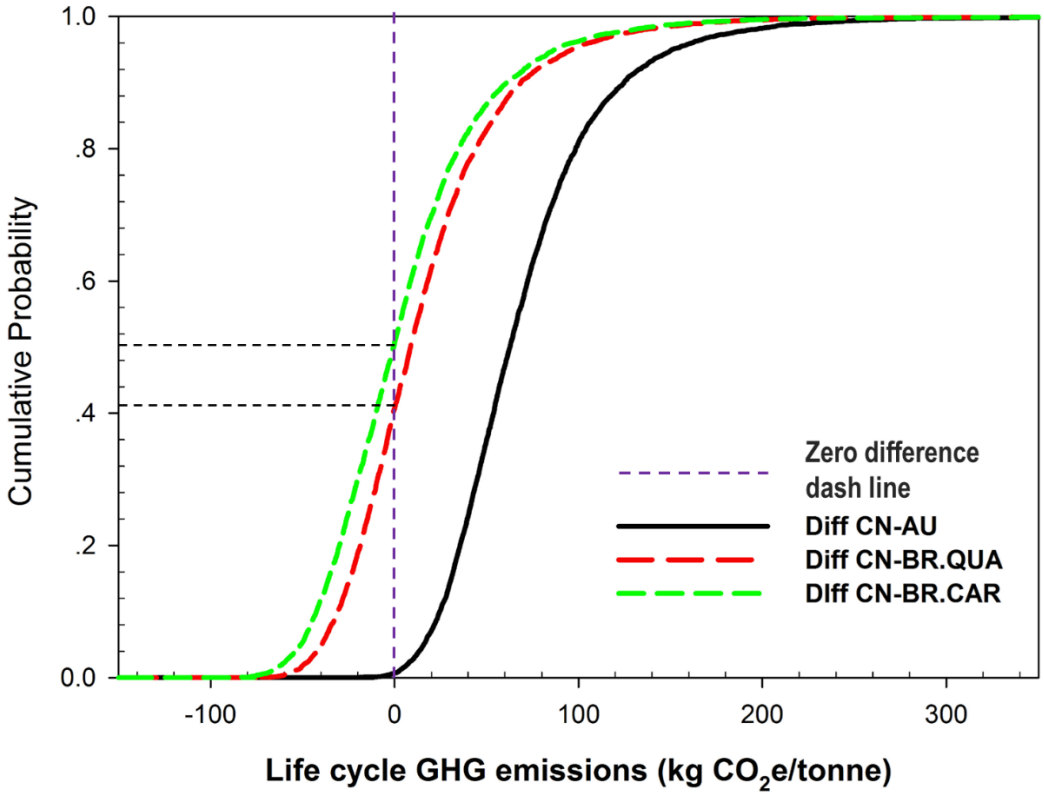

Figure 3.3 Probability distribution for the value of life cycle GHG emissions difference between different iron ore. Diff CN-AU represents the result of life cycle emissions of Chinese iron ores minus Australian iron ores emissions. Diff CN-BR.QUA represents the result of Chinese iron ores emissions minus of Brazil Iron Quadrangle ore emissions. Diff CN-BR.CAR represents the result of Chinese iron ores emissions minus emissions of iron ore from Brazil Carajas. The negative value of the difference CN-BR.QUA means the life cycle emissions of Chinese iron ores are less than that of Brazilian Iron-Quadrangle ores.

3.4.2 Importance analysis and sensitivity

Spearman's rank correlation coefficients between parameters and GHG emissions were calculated to represent the influence of each parameter on the uncertainty of the final result. Figure 3.4 and Figure 3.5 show the five parameters with the largest contribution to the variance for Australian and Brazilian iron ore analysis, respectively.

The shipping fuel consumption factor contributes the most (80%) to the uncertainty for Brazilian iron ore emissions, and second largest (36%) uncertainty for Australian iron ore emissions (detail see SI). In the study, ocean shipping fuel consumption is estimated as a uniform distribution ranging from 0.03 to 0.05 MJ heavy fuel oil per tonne-kilometer freight. If set this value to its mean and re-run the simulation, results for Iron Quadrangle and Carajas iron ores would be 97 kg and 107 kg CO_2e/ tonne on average, 88 to 106 kg CO_2e/ tonne and 98 to 116 kg CO_2e/ tonne of 90% confidence interval, respectively. Compared with the original simulation results of 77 to 116 kg CO_2e/ tonne and 87 to 126 kg CO_2e/ tonne for Iron Quadrangle and Carajas, the certain value input of shipping fuel consumption factor would significantly reduce the uncertainty.

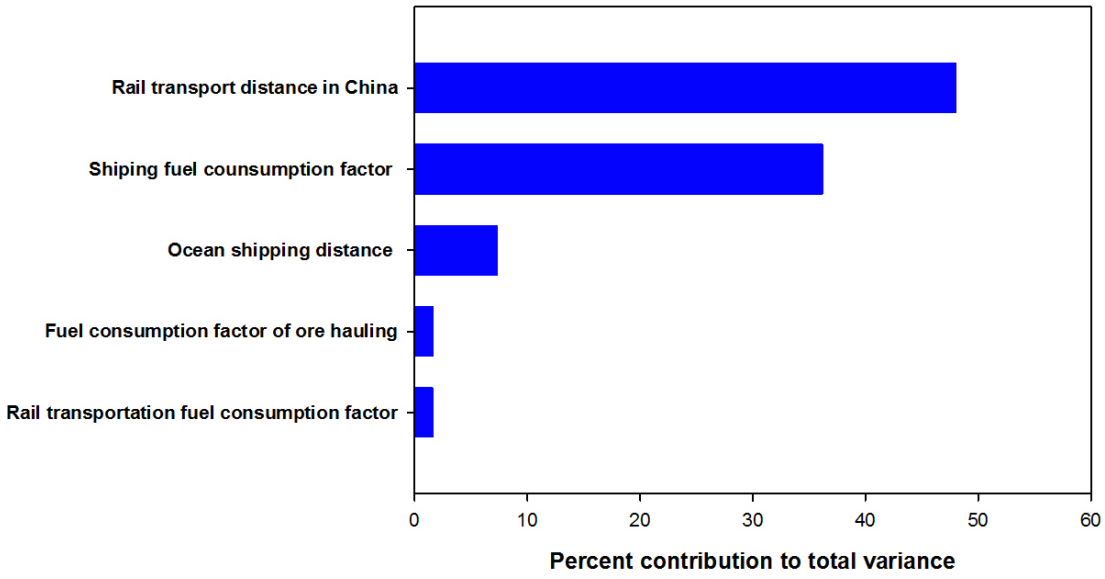

Figure 3.4 Uncertainty importance analysis for parameters in the result for Australian iron ore.

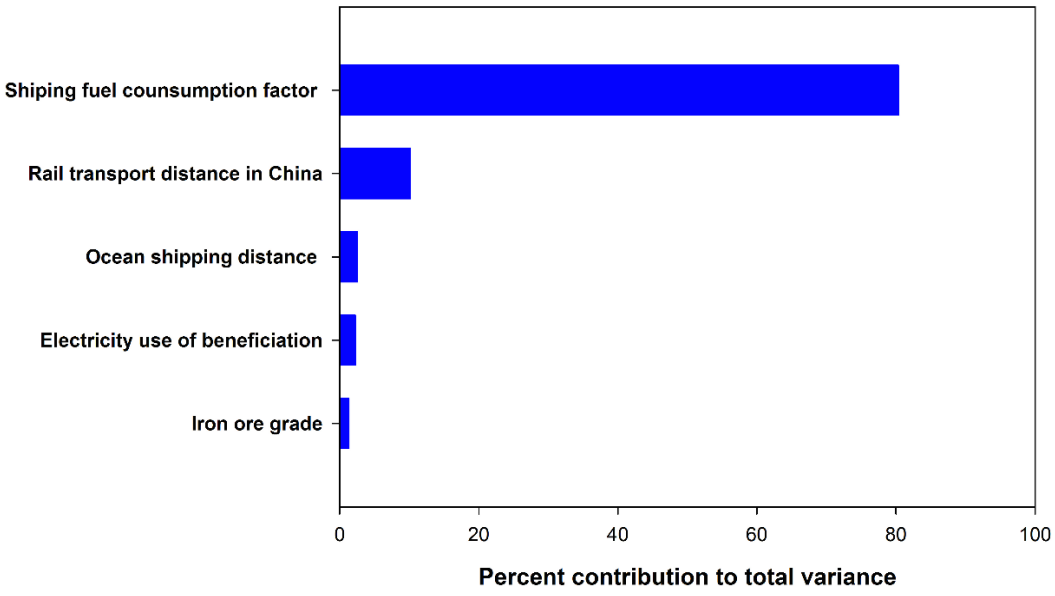

Figure 3.5 Uncertainty importance analysis for parameters in the result for Brazilian iron ore

3.4.3 Potential impacts of China's iron ore grade decline

According to results in Chapter 2, iron ore mining GHG emissions will increase significantly as crude ore grade decreases. China is now experiencing rich ore grade depletion and thus, produced ore grade is declining. From 2006 to 2012, the crude ore grade dropped from 30% Fe to 27% Fe. This section analyzes the potential impacts of China's iron ore grade decrease on the LCA comparison.

Figure 3.6 shows the change in GHG emissions of Chinese iron ores as the crude iron ore grade declines, and compares the changing Chinese iron ore emissions with Australian and Brazilian iron ore emissions. The life cycle GHG emissions for Australian and Brazilian iron ores are assumed constant in Figure 3.6. As the Chinese crude ore grade declines, emissions factor increases. Brazilian and Chinese iron ores have similar average GHG emissions when the Chinese iron ore grade is around 35%. Uncertainty estimates for Brazilian iron ores and Chinese iron ores overlapped but when Chinese ore grade falls below 20%, Brazilian iron ores would be preferred. Of note, the analysis assumes there is no change for Australian and Brazilian iron ore grade in the foreseeable future, which is reasonable considering the large quantity and high quality of the iron ore reserves in these two countries[20].

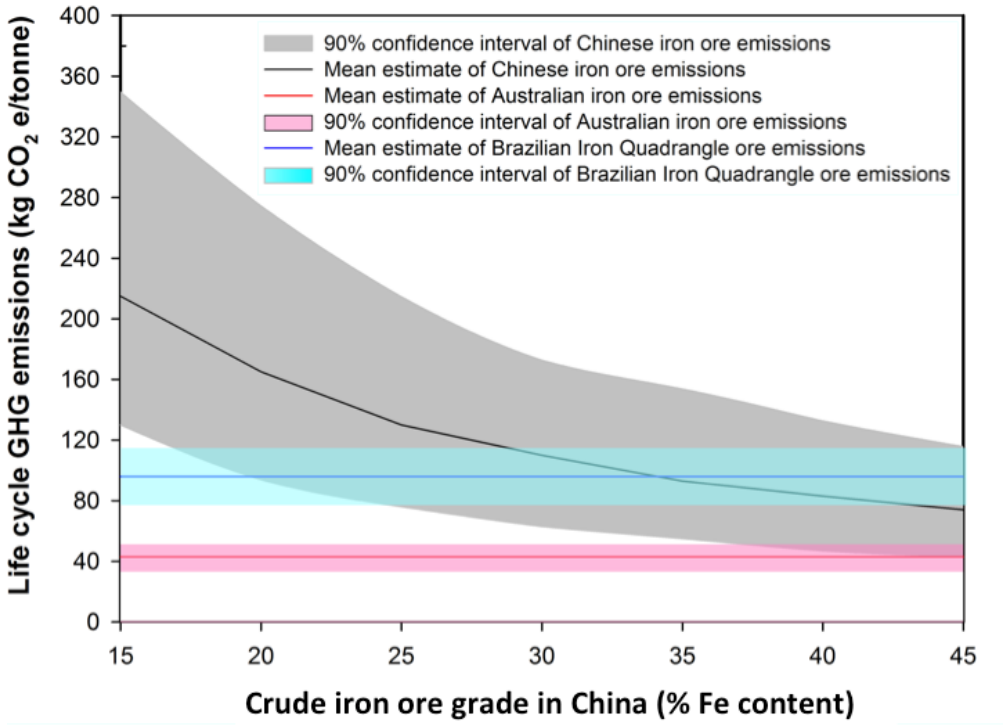

Figure 3.6 Comparison of life cycle GHG emissions of Chinese, Australian, Brazilian iron ores, as iron ore grade changes in China.

The last decade witnessed China's rising economy and unprecedented scale of urbanization, which resulted in increasing iron ore demand. From 2001 to 2013, the total iron ore demand in China grew at an average yearly rate of 15%[19]. The rising demand may not continue because of the recent slowdown of China's economic growth, but the total demand is still projected increase. According to Shen et al., China's total iron ore demand is predicted to reach 3 billion tonnes in 2050[94]. From 2006 to 2012, as the exploitation of iron resources, the China's average operating iron ore grade dropped from 30% Fe to 27% Fe[19]. The growing iron ore demand and dropping iron ore grade together makes importing iron ore a better way to meet demand and reduce GHG emissions going forward.

Assuming a drop to 20% Fe of the average Chinese iron ore grade and 3 billion tonnes of China's iron ore demand in 2050[94], China's iron ore production to meet the projected demand would result in 495 million tonne CO_2e. While importing Australian iron ore for China's demand leads to only 126 million tonne CO_2e for the mean estimate. Thus, importing Australian iron ore to replace

China's domestic low-grade iron ore would reduce 370 million tonnes CO_2e GHG emissions in 2050 as projected, which would account for 3% of China's total projected GHG emissions of 2050[85].

The study suggests that importing iron ore might be a viable GHG emissions reduction strategies for China. However, shifting toward greater reliance on iron ore imports could have socioeconomic impacts on the Chinese market. Potential impacts include decreased production in the Chinese mining sector and potential unemployment, as well as and stability and security issues for the country's economic system. More detailed analysis on these issues should be covered in the future study.

4. Integration of pre-salt natural gas into Brazilian fossil-derived feedstock

4.1 Abstract

Natural gas production and its associated downstream industries are underdeveloped in Brazil, representing a minor share of the national energy matrix currently. However, with the on-going exploitation of the deep-sea pre-salt reservoir, the increasing scale of natural gas supply might change the current situation. This study analyzes the potential impacts of increasing gas production and gas use in downstream industries. Six possible natural gas use pathways are assessed: three where natural gas is a consumed directly as an energy source (power generation, as the reducing agent for steel production, and as fuel for heavy-duty vehicles) and three were natural gas as a feedstock for product production (nitrogen fertilizer, methanol, ethylene-based polymer production). The study compares natural gas use pathways with their corresponding incumbent pathways from the impacts of global warming effects, economy and employment; and discusses the policy implications of the results.

The analysis reveal that GHG emissions associated with pre-salt gas production vary according to the stage of reservoir exploitation. At the early stage, the estimate of GHG emissions is 5.4 gCO_2e/MJ, with the 90% confidence interval of 4.5~6.4 gCO_2e/MJ; at the intermediate stage, the value becomes 7.1 gCO_2e/MJ (90% CI: 6.3~8.0 gCO2e/MJ); at the late stage, instead of being emitted, all produced gas will be reinjected back to the reservoir for advanced oil recovery.

All the six natural gas use pathways emit less GHG than the currently used process pathways on average. The mean GHG emissions reduction from natural gas use for power generation, nitrogen fertilizer production, methanol production, natural gas as the reducing agent for steel making, ethylene-based polymer production, heavy-duty vehicle fueling are 0.83, 2.3, 0.38, 35, 2.6 and 0.078 million tonne CO_2 equivalent per year, respectively. The profitability of the six pathways is affected by the price of natural gas and traditional fuel. Under current fuel prices (crude oil price= 50$/barrel, coal price=100 $/tonne, landed LNG= 5.33 $/MMBtu, Brazil natural gas= 5.04 $/MMBtu for power generation; 7.33 $/MMBtu for others), the net annual profits for the six pathways are -270, 87, 92, 1,700, 190 and -1,500 million dollars, respectively. The job creation

potential of the pathways of power generation, nitrogen fertilizer production, methanol production and as reducing agent for steel production are estimated to be 28, 17, 5 and 36 thousand, respectively.

4.2 Introduction

Natural gas production and its associated downstream industries are currently underdeveloped in Brazil, representing a minor share in the entire energy matrix[37, 38, 131]. In 2016, natural gas accounted for 12% of energy supply and 7.2% of final energy consumption[37, 38]. Moreover, 44% of the gas supply is from domestic production[37, 38], Pipeline natural gas from Bolivia and imported liquefied natural gas (LNG) are other two major sources of gas supply, comprising 35% and 21%, respectively[37, 38].

The recent discovery of petroleum reserves in the pre-salt layer, located on the Brazilian continental shelf, could potentially change the current situation. The pre-salt oil reserve is estimated to have 50 billion barrels of oil equivalent, which is four times greater than the current national oil reserves[30]. The play has an estimated gas to oil ratio (GOR) of between 200 and 350 m^3 of gas /m^3 of oil. Thus, the associated gas source can significantly increase the domestic gas supply[30]. The natural gas resources in the Lula and Cernambi reservoirs are estimated at 170 billion cubic meters, and the total gas resources in pre-salt reservoir is about 1000 billion cubic meter. If half of the total resources are recovered, it can provide the gas supply of 2015 level for more than 80 years[132]. Since reservoir production commenced in 2008, the supply of pre-salt natural gas has risen by more than 90% per year on average, and accounted for 30% of the total domestic production in 2015[37, 38]. With the on-going exploration, it is expected that pre-salt natural gas will replace imported gas as the primary source of Brazil's natural gas supply, and Brazil has the potential of gradually achieving self-sufficiency of natural gas in the future.

As the domestic natural gas supply increases, the question arises of how to integrate pre-salt natural gas into the Brazilian energy matrix. This study discusses the possible uses of natural gas, compare the economic, employment and global warming effects of different pathways of gas uses. Results of this study would inform policymakers in the plan of natural gas exploitation and associated downstream industries development.

4.2.1 Potential gas use in downstream industries

The increasing pre-salt natural gas supply, if priced competitively, could increase natural gas consumption and associated downstream industries development while reducing the use of traditional energy sources and imports of gas-derived products. The following six natural gas pathways and their corresponding incumbent pathways are analyzed to determine the possible changes in global warming effects, and economic impacts and employment impacts.

4.2.1.1 Replacing LNG with pre-salt gas for power generation

Power generation is a growing application for natural gas use in Brazil. Natural gas consumption for electricity generation grew over 350% from 2011 to 2015[37, 38]. Natural-gas-fired electricity generation is mostly used as backup for hydroelectricity. However, Natural gas is predicted to be Brazil's fastest growing source of electricity in the near future[36]. Currently, because of a deficient and unstable domestic natural gas supply, Brazil imports liquefied natural gas (LNG) from overseas to fill the gap of energy source for power generation, especially during the drought season when hydropower is inadequate[37, 38]. With the exploration of pre-salt reservoirs, increasing domestic gas supply might replace LNG imports for power generation in the future.

Gas storage facility facilitates a robust and stable natural gas power generation. Currently, Brazil has no underground gas storage, limiting the utility of domestic gas as a supplementary power source during the drought period, where storage could smooth out the price impacts of spikes in demand[131]. This study considers the underground gas storage installation as the prerequisite for replacing LNG imports with pre-salt gas. Therefore, the costs and impacts associated with the installation and operation of gas storage will be included in the analysis of pre-salt gas power generation pathway.

4.2.1.2 Nitrogen fertilizer production

Brazil is an important global producer and exporter of agricultural products and requires a large amount of fertilizer annually. In recent years, growing population, rising income and domestic consumption, as well as the swelling interest in biofuel production are accelerating the fertilizer demand growth nationwide[133]. In 2014, Brazil's consumption of nitrogen fertilizers (N) climbed by 4.7%[45].

Currently, Brazil mainly depends on increasing imports (both in absolute value and percentage) to meet its growing demand for fertilizer[45]. The potential increasing pre-salt gas supply and declining gas price could promote the nitrogen fertilizer production in the country, meeting the growing nitrogen fertilizer demand and gradually replacing imports. This study will compare the domestic production with imports, so as to analyze the net global warming effects, economic and employment impacts associated with the use of natural gas in nitrogen fertilizer production.

4.2.1.3 Methanol production

Methanol synthesis is an important application of natural gas in the chemical industry. Currently, 68% of Brazilian methanol supply comes from abroad. In 2015, Brazil spent 288 million dollars for 841 thousand tonne methanol imports[45]. These imports mainly come from Trinidad and Tobago (42%), Venezuela (18%), Chile (17%), and Argentina (11%)[45]. The study will compare domestic production versus imports, so as to analyze the potential impacts of natural gas use in methanol production.

4.2.1.4 Reducing agent for steel production

Steel represents a major component of Brazilian exports; the country is currently ranked as the fifth largest net exporter of steel worldwide. Brazil owns the second largest reservoir of iron ore globally, however, Brazil lacks coal resources as reducing agent, and currently depends greatly on importing coal for steel production. Charcoal, as an alternative to coal, that has been studied extensively given the limited domestic coal supply. However, obstacles exist here as well, as charcoal originates from native forest and the large consumption of it would potentially harm the ecosystem in the Amazon area.

Natural gas can serve as potential reducing agent in steel production. The increasing pre-salt gas supply has inspired the development and improvement of related techniques, making natural gas a more appealing and readily available option for Brazilian steel industry. The study will analyze the potential impacts of using natural gas to replace coal for the iron reduction in steel production.

4.2.2 Ethylene and Polyethylene production

The early development of petrochemical industry in Brazil began when natural gas was still in short supply in the Brazilian energy mix[134]. Brazil's petrochemical production mainly depends on the processing of naphtha(77%)[134], which is acquired from oil refineries. Due to the limited domestic oil refinery capacity, Brazil needs to import naphtha for petrochemical production. Meanwhile, the overall production capacity of Brazil's petrochemical industry is also insufficient to meet its market demand, leading to increasing demands of imports for the polymer resin and plastic[134].

The C2-C4 components in natural gas can replace naphtha for the synthesis of ethylene and propylene, which are the basic elements of petrochemical production. According to the current reservoir test results, the C2-C4 components account for 7% to 15% in the pre-salt gas[17]. The increasing pre-salt gas supply makes natural gas a viable feedstock for Brazil's future petrochemical production.

4.2.3 Transportation: CNG or LNG-powered vehicles versus diesel-powered vehicles

Diesel-powered heavy-duty vehicles are considered to be extremely environmentally hazardous. The uncontrolled diesel-powered vehicles emit high levels of particulate matters and nitrogen oxides, which are proven to be related to bronchitis, asthma, and other pulmonary diseases[135]. Diesel exhaust is classified as carcinogenic to humans by the World Health Organization[136].

Compressed Natural Gas(CNG) and LNG-powered vehicles are considered to be superior to diesel-powered heavy-duty vehicles in the aspect of reducing air pollution[137-140]. This study will analyze the potential impacts of replacing diesel-powered heavy-duty vehicles (such as trash trucks, transit buses, urban delivery vehicles, etc.) with CNG / LNG-powered vehicles in Brazil.

4.3 Methods

The following section presents data and methods used for evaluating potential impacts of growing pre-salt natural gas production and associated downstream industries development. Three categories of impacts: global warming effects, economic and social impacts are analyzed separately.

4.3.1 Global warming effect

The study applies a life-cycle approach to account the GHG emissions associated with the pre-salt gas production and consumption. The final results are presented in 100-years global warming potentials (GWPs), using GWP factors reported by the Intergovernmental Panel on Climate Change (IPCC) assessment report (IPCC 2013).

4.3.1.1 GHG emissions of pre-salt oil and gas production.

The functional unit of the life-cycle study of pre-salt gas production is 1 MJ of natural gas delivered to an onshore gas processing plant.

Pre-salt natural gas is a by-product of oil production, commonly known as associated gas. The GHG emissions associated with natural gas production are calculated by allocating the emissions of petroleum and gas production by the energy content of the two products.

GHG emissions from petroleum production vary according to the different field characteristics, production methods and the implemented controls on fugitive emissions sources[141]. The field characteristics of Brazil pre-salt reservoirs are unique: remote located over 800km off the Brazilian coast, ultra-deep 5000 to 7000 m below sea surface, buried below 2000 m thick salt layer, with unknown reservoir rock type of highly heterogeneous microbialites content, of high carbon dioxide content (over 20% in some reservoirs) in the extracted petroleum, etc.[17, 30] The above characteristics pose great technological challenges on pre-salt petroleum operations, and might result in energy and GHG emissions intensity distinct from that of conventional petroleum production.

Several previous studies have established life cycle models using field characteristics to estimate GHG emissions of petroleum production[141-146]. Oil Production Greenhouse gas Emissions Estimator (OPGEE) is one of the engineering-based life cycle assessment (LCA) tool for calculating GHG emissions of crude petroleum production. The Oil Climate Index Project[147] collected data of 30 global oilfields and applied the OPGEE model (version 1.1 E)[148] to calculate GHG emissions for the 30 oil fields. The pre-salt field “Brazil Lula” is one of the 30 oil fields[147]. However, minor discrepancy exists between the model and the real situation in “Brazil Lula”,

which might render the estimation of GHG emissions incorrect (e.g. CO_2 membrane separation is used for CO_2 removal instead of amine treater).

On the basis of previous estimates[147, 148], this study modifies some original settings in OPGEE model and derives a new estimate that reflects current pre-salt petroleum production, as shown in Table 4.1. Additionally, the OPGEE model is field-specific, and only one pre-salt field "Brazil Lula" has been analyzed in the previous Oil Climate Index Project. This study collects data from all public reported pre-salt fields, and estimates the variation of their field and technique parameters. These data are then used to calculate the energy consumption and emissions of individual processes involved in petroleum production. Monte Carlo simulation is applied to determine the result stochastic mean and uncertainty.

Table 4.1 lists the parameters and assumptions that used in this study that are different from the estimate of "Brazil Lula" in Oil Climate Index Project.

Table 4.1 Parameters and assumptions that used in this study that are different from the estimate of "Brazil Lula" in Oil Climate Index Project

Processes	Oil Climate Index-Brazil Lula[147]	Estimation in this study (pre-salt fields)
Drilling & Development	Drilling depth=field depth(6016m)	Drilling depth=true vertical depth =Uniform(5.3,6.7) km[42].
	Use the default value in OPGEE model for expected life well productivity =130,000 bbl./well	Expected life well productivity was calculated based on data from the evaluation of ten selected pre-salt production projects[42]. The estimate of expected life well productivity =triangular(1, 20, 80) million bbl./well[42]
	Soil carbon lost=0.03 g CO_2/	Soil carbon lost=0 for offshore oil field
Production& Extraction	Produced water will be reinjected back to the reservoir, and the water-oil ratio (WOR) is set to be 0.1	CO_2 removed from the produced gas and produced water will be reinjected back to the reservoir. WOR varied in different production stages. At the beginning, WOR=0. WOR keeps increasing as the production approaching the end[149].
Surface processing	Gas processing= Dehydrator + Amine Process + Demethanizer, CO_2 is removed from produced gas and vented	Gas processing= Dehydrator + Compressor + CO_2 Membrane +Dew point control + Vapor recovery, separated CO_2 is reinjected back to the reservoir instead of venting to the air.
Venting & Fugitive	Calculate emissions from each operation unit and device.	Fugitive gas is calculated as produced gas multiplied by leak rate. Leak rate = triangular(0.02,0.03,0.04)[150-152]
Transport	Crude oil carried by ocean tanker from origin field to Houston(5387mile)	Crude oil transportation is not allocated to emissions of natural gas, gas is transport via gas pipeline ashore, distance= triangular(360,400,440) km[153]

As presented in Table 4.1, the major difference between the model of this study and the Oil Climate Index lies in the gas processing, especially in the CO_2 removal technique. In the model of Oil Climate Index, CO_2 in produced gas is eliminated by ethanolamine, while in this study CO_2 is separated by CO_2 Membrane, which is the actual processing technique that is applied in the pre-salt field operation. Instead of being vented, the separated CO_2 from Membrane is reinjected back into the reservoir. The design of CO_2 separation and storage reduces the GHG emissions from the pre-salt field operation.

The field operation condition varies through its production life. With time, the proportion of CO_2 in the produced gas increases as the reinjected CO_2 accumulates in the reservoir. In practice, process parameters (e.g. amount of reinjected gas and/or water) are adjusted to the trends of key field characteristics (e.g. WOR, GOR) to optimize production throughout the field life, thus GHG emissions associated with a functional unit gas production can change.

Because of the uncertainty of petroleum production, it is impossible to accurately predict the entire trends of the field characteristics throughout production. The study uses three scenarios (the early, intermediate and late production stages) to estimate the variation of GHG emissions factors. The field characteristics and operation parameters at different production stages are taken from previous research of the pre-salt field operation[149], detailed in Table 4.2.

Table 4.2 field characteristics and operation of three production modes

Scenarios	Gas processing	Fluid rate (bbl./d)[a]	Crude oil (bbl./d)[b]	WOR	Dilution water	GOR (scf/bbl.)
Early stage	The crude oil has the maximum content of oil and gas. All gas is exported and the removed CO_2 is injected in the well.	165000	156000	0.06	4%	1300
Intermediate stage	50% of the produced gas is treated in the CO_2 removal unit in order to be exported and 50% of the produced gas is reinjected into the production wells.	175000	77000	1.30	2%	960
Late stage	Crude oil has the maximum quantity of water/CO_2. All separated gas is sent through the bypass of the CO_2 removal system and it is injected into the production wells.	165000	31000	4.40	0.8%	2600

Data sources: *Sánchez, 2015*[149]

[a,b] The fluid rate and crude oil production rate presented in the table is for one floating production storage and offloading unit

4.3.1.2 GHG emissions associated with natural gas production

4.3.1.3 Natural gas use in downstream industry

The development of downstream industries using natural gas will lead to new sources of GHG emissions within Brazil, but could reduce emissions from incumbent pathways that are replaced. For example, the growth of ammonia manufacturing in Brazil would increase GHG emissions from domestic production but reduce imports and those embedded emissions.

This study compares the life cycle GHG emissions of natural gas pathways versus the replaced traditional pathways. The life cycle GHG emissions of natural gas pathways are calculated as the combination of emissions associated with upstream pre-salt gas production, and the specific downstream manufacturing process. The life cycle GHG emissions from replaced pathways were obtained from publically available life cycle databases or literature, as detailed in Table 4.3. In cases where oversea import is involved, emissions associated with shipping process is treated as a discrete distribution model, where the probability value for each potential shipping route equals to the proportion of overall import though that route. Emissions of each shipping route are calculated as its emission factor multiplied by the shipping route distances.

Table 4.3 Data sources for estimating GHG emissions of different pathways

	Comparison pathways	Main phases included	Functional unit	Data sources
1	Pre-salt gas for power generation	Upstream gas production, Transmission, Storage	1 MJ natural gas at power plant	APCD[53] Jaramillo[154], Venkatesh[150], Abrahams[151], NETL[79], Jiang[152], Denholm[155]
	Importing LNG for power generation	Upstream gas production, Transmission, Storage Liquefaction, shipping, Regasification		
2	Nitrogen fertilizer manufacture	Upstream gas production, Transmission, Ammonia manufacturing	1 tonne of Ammonia	APCD[53] Wood[156], NRC[157] NETL[79]
	Importing Nitrogen fertilizers	Upstream gas production, Transmission, Ammonia manufacturing, shipping		
3	Methanol manufacture	Upstream gas production, Transmission, methanol manufacturing	1 tonne of Methanol	GREET[158], Matzen[159] Luiz[160]
	Importing Methanol	Upstream gas production, Transmission, methanol manufacturing, shipping		
4	Gas as reducer for steel making	Upstream gas production, Transmission, steel production	1 tonne of Steel	Price[161], NETL[79]
	Importing coal as reducer for steel making	Upstream coal production, shipping, steel production		
5	Ethane cracking for Ethylene and Polyethylene production	Upstream gas production, Transmission, ethylene manufacturing	1 tonne of Ethylene	Benchaita[162], Ghanta[163] NETL[79]
	Naphtha cracking for Ethylene and Polyethylene production	Oil production, oil refinery, transportation, ethylene manufacturing		
6	CNG/ LNG vehicles	Upstream, tailpipe	1 vehicle mile of travel	Cai[164], Fan[165], GREET[158]
	Diesel power vehicles	Upstream, tailpipe		

4.3.2 Economic Impacts

This study estimates the annual economic benefits of different natural gas use pathways if they completely replace their corresponding traditional options. The amounts of current incumbent pathways are obtained from industry reports and statistic databases[17, 45, 166], as detailed in Table 4.4.

Table 4.4 Current amounts of incumbent pathways

Potential pre-salt gas pathways	Incumbent pathways	Current amounts of incumbent pathways [a]	Economic value (Billion Brazilian Real)
Domestic natural gas for power generation	Importing LNG for power generation	7 billion cubic meters per year gas for power generation	8.3
Nitrogen fertilizer manufacture	Importing Nitrogen fertilizers	350 thousand tonnes of Ammonia, 2.8 million tonnes of Urea	3.5
Methanol manufacture	Importing Methanol	840 thousand tonnes of methanol	0.96
Gas as reducer for steel making	Importing coal as reducer for steel making	25 million tonnes of coking coal, equivalent to 9 billion cubic meter gas as iron reducer	11
Ethane cracking for Ethylene and Polyethylene production	Naphtha cracking for Ethylene and Polyethylene production	3 million tonnes of polyethylene	12
CNG/ LNG vehicles	Diesel light-duty vehicles	145 thousand units, including bus 5 thousand units, LHDT 53 thousand units, MHDT 57 thousand units, HHDT 30 thousand units [b]	0.056

Data sources: UN Statistics Division Energy Statistic Database[167]; FAO Resource Statistics-Fertilizes[168]; UN Comtrade Database[45]; Oil, natural gas and biofuels statistical yearbook[17], Brazilian automotive industry yearbook[166].
a: Current scales referred as the scale in the year 2015. b: LHDT: light heavy-duty truck, MHDT: medium heavy-duty truck, HHDT: heavy heavy-duty truck. Detailed definition and classification of the heavy-duty truck can be found in Brazilian automotive industry yearbook[166]

The annual profit of each incumbent pathway replaced by natural gas is then calculated as annual revenue minus annual cost, where annual revenue equals to product market price (obtained from statistics reports[17, 45, 166-168]) multiplied by its production scale. The annual cost includes the annual equivalent of the capital cost, annual operational cost, and the opportunity cost, which is the profit of corresponding incumbent pathway.

The annual equivalent of capital cost is calculated using the following equations:

$$A = P \times CRF \quad [1]$$

$$CRF = \frac{i(1+i)^n}{[(1+i)^n - 1] \times (1+i)^{m-1}} \quad [2]$$

In equations [1] and [2], A is the annual equivalent of capital cost; P is the capital investment; CRF is the capital recovery factor, which converts the capital investment into a stream of equal annual payments; i is discount rate, assumed to be 10%; n is expected life expense of a production plant; m is the plant construction years.

The operational cost includes feedstock cost and none-feed stock operational cost. For several natural gas use pathways, the feedstock cost mainly comes from the expense of natural gas, thus is solely related to natural gas price. The none-feedstock operational cost includes the cost of labor, maintenance, etc. The profit of incumbent pathway is calculated as annual revenue minus annual equivalent of the capital cost and operational cost. Table 4.5 presented the capital cost, operational cost and other parameters used to estimate the annual profit of different pathways. These data are obtained from statistic reports[17, 45, 166-168], research articles[169-176] and industry case studies[177].

Table 4.5 Parameters for estimating annual profits of different pathways

1. Power generation	
working capacity of required gas storage (billion cubic meters per year)	5
Investment cost of underground gas storage ($/per cubic meter)	0.5
annual service cost($/cubic meter per year)	0.1
Expected life expense of storage facility(years)	25
Plant construction years	2
Annual LNG imports (billion cubic meters per year))	7
2. Nitrogen fertilizer manufacture	
Annual imports of ammonia (kt)	354
Expected life expense of ammonia/Urea plants(years)	20
Ammonia/Urea plants construction years	3
non-feedstock operational cost per tonne ammonia ($)	26
Cost of ammonia imports($/tonne)	440
Capital investment of ammonia plant (capacity=1050kt/yr, unit: billion $)	0.85
non-feedstock operational cost per tonne Urea($)	22
Urea import price ($/tonne)	315
Annual imports of urea (kt)	2800
Capital investment of urea plant (capacity=1500kt/yr, unit: billion $)	1.18
3. Methanol manufacture	
Methanol import price ($/tonne)	342
Annual imports of methanol (kt)	840
Expected life expense of methanol plants(years)	20
Methanol plants construction years	3
Capital investment of methanol plant(capacity=50kt/yr; billion $)	0.032
4. Steel making	
Expected life expense of steel mill(years)	30
Plant construction years	3
Total steel production (million tonnes/yr)	33
Direct reduced iron route with natural gas as reducer	
Capital investment of DRI plant (capacity=2500 kt/yr, billion $)	0.75
Iron ore feed (tonne iron/ tonne steel)	1.5

Other cost (pellet premium, freight, etc. Unit: $/tonne)	70
Blast Furnace with coal as reducer	
Iron ore feed (tonne iron/ tonne steel)	1.6
5.Ethylene and Polyethylene production	
Plant expected life expense (years)	20
Plant construction years	3
Ethane cracking	
By-product credit(for 500kt/yr plant; million)	34
fuel cost (for 500kt/yr plant; million)	18
Capital investment of polyethylene plant (capacity=500kt/yr; billion)	0.96
None-feedstock operational cost ($/tonne)	200
Naphtha cracking	
By-product credit(for 1000kt/yr plant; million)	1040
Fuel cost (for 1000kt/yr plant; million)	8
Capital investment of polyethylene plants (capacity=1000kt/yr; billion)	2.5
None-feedstock operational cost ($/tonne)	276
6. Heavy-duty vehicles	
Diesel power vehicle	
Investment cost ($/billion vmt per year)	10500
Fixed O&M cost ($/billion vmt per year)	550
CNG vehicle	
Investment cost ($/billion vmt per year)	12000
Fixed O&M cost ($/billion vmt per year)	640

Data in the table are sourced from literature[17, 45, 166-177]

4.3.3 Employment Impacts

The pre-salt gas production and associated downstream industry development will generate new job positions, both in the directly involved sectors and their upstream sectors. This study uses input-output modeling to quantitatively determine the employment impacts throughout the Brazilian economic system as detailed below.

Input-output analysis

Input-output model is a quantitative model developed by Wassily Leontief in 1930s to depict the supply and demand relationships between different sectors in the economic system[178]. Equation 3 demonstrates the basic math of an input-output model.

$$X = (I - A)^{-1}Y \quad [3]$$

In Equation 3, X is the vector representing total economic output of each sector, Y is the vector of monetary final demand, I is the identity matrix, A is the matrix of intersectoral technical coefficients, $(I-A)^{-1}$ is defined as the Leontief Inverse Matrix, used as the multiplier to calculate the total output required for 1 unit final demand.

The original economic input-output model can be extended by a non-economic matrix to estimate additional inputs (e.g. energy, materials, capital, labor) and outputs (e.g. emissions) for 1 unit of final demand. In this study, an employment intensity vector is added to the economic input-output model. The element in the employment intensity vector is obtained from:

$$IE_i = \frac{E_i}{X_i} \quad [4]$$

Where IE_i represents employment intensity of sector i, E_i is the number of employees of sector i, X_i is the total economic output of sector i.

The total (direct and indirect) employment impact for economic change in sector i can be calculated using the following equation:

$$\Delta E = IE_i \times \Delta X = IE_i \times (I - A)^{-1} \times \Delta Y \quad [5]$$

The economic change (ΔY) is caused by developing natural gas pathways to replace incumbent pathways, which equal to the scale of pre-existing incumbent pathways as detailed in Table 4.3.

The study obtained the most recent version (year 2010) of economic input-output model from Brazilian Institute of Geography and Statistics[121]. The employment data of different sectors are obtained from Brazil's Annual Relation of Social Information (RAIS) database[179]. Of note, sector divisions of the input-output model and RAIS database are different. Brazil's input-output model has 67 sectors, while the RAIS database recorded the employment data by 670 National Classification of Economic Activities (CNAE). The method for corresponding the classification of input-output model activities and CNAE were adopted from the annex of the publication of Brazil's input and output model[121].

4.4 Results and discussion

The exploitation of pre-salt reservoirs and increasing natural gas supply in Brazil will prompt the use of natural gas in associated downstream industry, replacing the existing incumbent pathways. This study analyzed the global warming, economic and employment effects of the six natural gas use pathways in comparison with the corresponding incumbent pathways. Results of this study will inform policymakers in Brazil on the potential of natural gas exploitation and strategies for developing an associated downstream industry development.

4.4.1 Global warming effects

4.4.1.1 GHG emissions of pre-salt natural gas production.

The GHG emissions associated with natural gas are calculated as allocating the overall emissions of petroleum production by the energy content of natural gas, which is a by-product of pre-salt oil production.

Table 4.6 shows the estimates of average GHG emissions from petroleum production at three different stages (early, intermediate and late stages of production life), and compare them with the estimate of the pre-salt Lula Field from Oil Climate Index project.

GHG emissions per barrel crude oil production increase as the reservoir operation continues. The estimates of the early and intermediate stages are less than that from Oil Climate Index Project, while the emissions of the late stage are greater than that of Oil Climate Index.

Table 4.6 presents the GHG emissions associated with each production process. Emissions associated with drilling and development of per barrel oil are calculated by dividing the drilling emissions by the lifetime oil production. Therefore, for different production stages, the quantity of GHG emissions assigned to drilling remains constant at 0.1 kg CO_2e per barrel. This estimate is significantly lower than that of Oil Climate Index. This difference is driven by the different estimates for ultimate recovery (ie. Expected life well productivity in OPGEE model). The present

study uses the data of estimated contingent resources and planned numbers of wells from ANP[3]'s assessment report on ten pre-salt fields[42], and treats the estimated ultimate recovery as a triangular distribution(1, 20, 80)[4] million barrels per well. While the Oil Climate Index use the default value from OPGEE model, which is 130 thousand barrels per well.

From the early to late stage, the energy required to extract a barrel of oil increases, resulting in the increase of GHG emissions from Production &Processing. The Venting & Fugitive GHG emissions come from fugitive natural gas, which is proportional to the produced gas volume. The amount of gas produced per barrel oil (GOR) declines initially as free gas remains unmovable until reaching the saturation point, after which GOR keeps increasing till the end of production life[180]. The estimates of Venting & Fugitive GHG emissions shows the same trends.

The mean and uncertainty estimate with 90% confidence intervals for pre-salt gas production emissions are presented in Table 4.7. GHG emissions of natural gas production are calculated by allocating the overall emissions of petroleum production by the energy content of natural gas. Table 4.7 also presents the percentage energy content of oil and gas in the extracted crude.

Table 4.6 GHG emissions of petroleum production in pre-salt field (kgCO_2e/barrel crude oil)

	This study			**Oil Climate Index**
	Early stage	**Intermediate stage**	**Late stage**	
Drilling & Development	0.1	0.1	0.1	8
Production & Processing	8	18	44	14
Venting & Fugitive	30	22	63	35
Miscellaneous	--	--	--	3
Total (mean)	38	40	107	60

Table 4.7 Allocation and GHG emissions of natural gas production in pre-salt field

	Allocation by energy content (%)		**GHG emissions of natural gas production (gCO2e/MJ)**	
	Oil	**Natural gas**	**Mean**	**90% confidence interval**
Early stage	83	17	5.4	4.5~6.4
Intermediate stage	95	5	7.1	6.3~8.0
Late stage	100	0	--[a]	

a: All produced gas will be reinjected back to the reservoir in this production mode.

[3] ANP: Brazil's National Agency of Petroleum, Natural Gas and Biofuels

[4] Triangular distribution (min, mode, max)

Figure 4.1 presents the estimated GHG emissions factor of Brazil's pre-salt gas production and that of different types of US natural gas production. According to figure 4.1, the GHG emissions factors of associated gas production (pre-salt gas and Bakken shale oil associated gas) are estimated to be "lower" than those of non-associated gas (US shale gas and conventional gas). However, it cannot demonstrate that exploiting associated gas would reduce GHG emissions because associated gas production is along with oil production and only a fraction of the total emissions are allocated to the associated gas. Natural gas from Brazil's pre-salt reservoir and US Bakken shale play are both associated gas, while the GHG emissions factor of the former one is higher than that of the latter one.

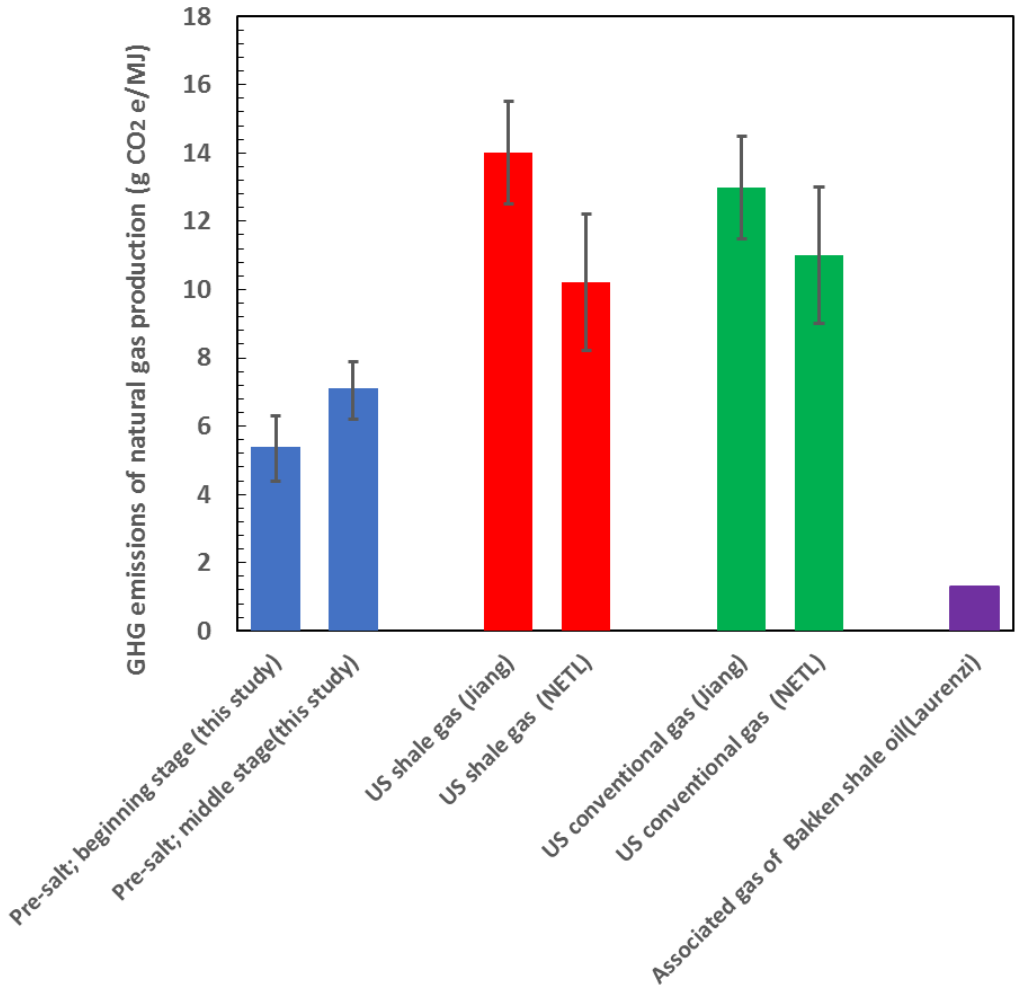

Figure 4.1 GHG emissions factor of Brazil's pre-salt gas production and that of US natural gas production (data source for U.S. gas production: NETL[79], Jiang[152], Laurenzi[181])

4.4.1.2 GHG emissions associated with gas use in downstream industry

This study estimates the GHG emissions of different natural gas use pathways, and compares them with those of traditional non-natural gas pathways. Results are summarized in Figure 4.2 to Figure 4.7.

Figure 4.2 shows that GHG emissions associated with power generation from pre-salt gas are less than that from importing LNG. Natural gas produced from pre-salt reservoirs is associated gas, thus associated with relatively lower upstream GHG emissions compared with the global average emission level, which aggregates the associated and non-associated gas. On the contrary, the imported LNG for power generation requires the additional processes of gas liquefaction, shipping and re-gasification before power generation, significantly increase the GHG emissions along this pathway.

Currently, LNG is an important backup source of power generation during the drought season when hydropower is in shortage. As the population and economy grow, the demand for natural gas power will increase. According to Electricity in the 2024 Brazilian Energy Plan (PDE 2024), natural gas installed generation capacity will increase by 10.6% from 2014 to 2024[36]. The exploitation of pre-salt gas could supply sufficient energy demand and significantly reduce GHG emissions by replacing LNG.

As demonstrated in Figure 4.3, the mean estimate for GHG emissions of domestic ammonia is lower than that of imports, though the uncertain ranges overlap. Ninety-nine percent of Brazil's ammonia imports comes from Trinidad and Tobago[45]. The limited data source and high uncertainty of ammonia production processes in those two countries may have made the current results inconclusive.

Figure 4.4 demonstrates that replacing methanol imports with production from pre-salt gas would reduce global net GHG emissions. Figure 4.5 and Figure 4.6 revealed that substituting coal and oil in steel and ethylene manufacturing with natural gas would also lead to reduced GHG emissions.

On the other hand, the life cycle GHG emissions of CNG/LNG-powered heavy-duty vehicles are not significantly different from that of diesel vehicles. Therefore, replacing diesel-powered heavy-

duty vehicles with CNG/LNG-powered vehicles have no noteworthy benefit in the aspect of global warming mitigation.

Of note, the pathways of power generation, fertilizer production and methanol production are all aimed at replacing imports with domestic production. Therefore, these three pathways will transfer GHG emissions from abroad to Brazil, but from the global aspect, the net GHG emissions will be reduced.

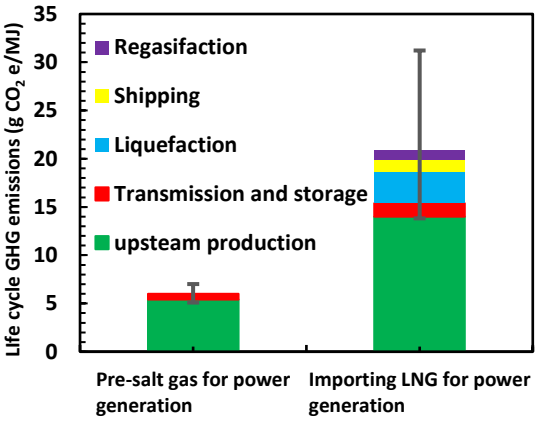

Figure 4.2 life cycle GHG emissions of pre-salt gas vs. LNG

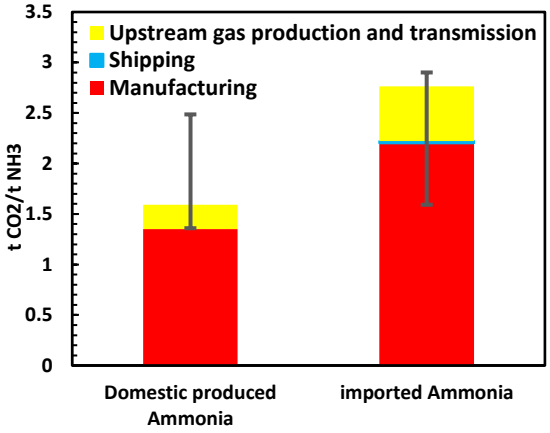

Figure 4.3 life cycle GHG emissions of Brazilian vs. imported Ammonia

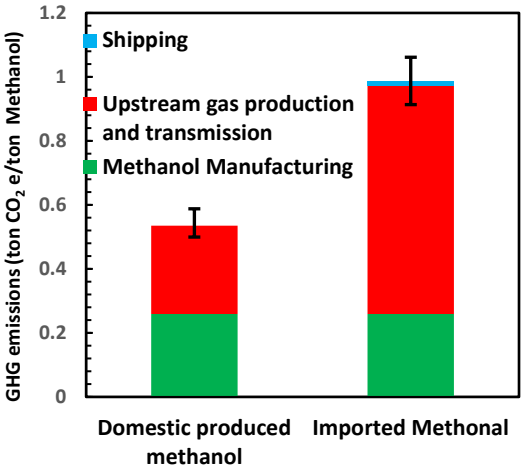

Figure 4.4 life cycle GHG emissions of Brazilian vs. imported methanol

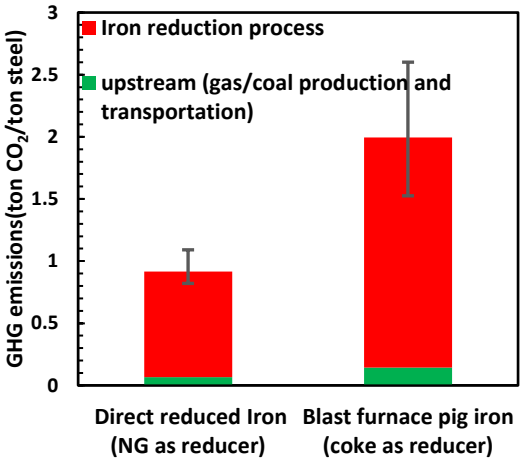

Figure 4.5 Life cycle GHG emissions of steel (Natural gas vs. coke as reducer)

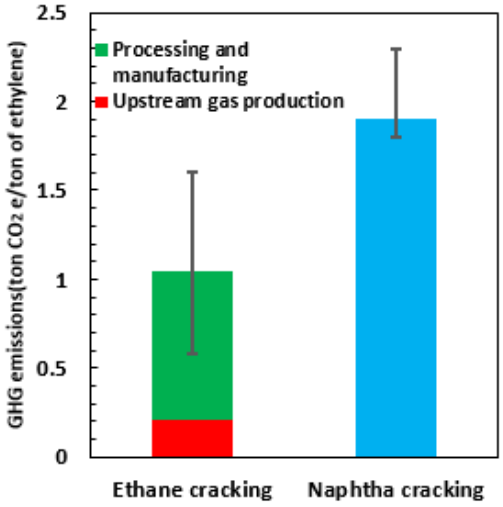

Figure 4.6 Life cycle GHG emissions of ethylene (Ethane vs. Naphtha cracking)

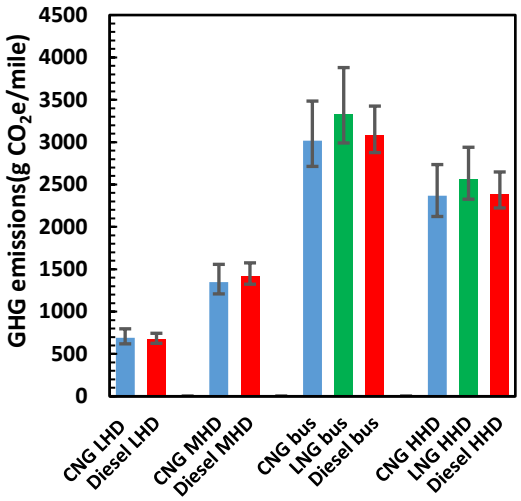

Figure 4.7 Life cycle GHG emissions vehicle travel mile (CNG vs. LNG vs. Diesel vehicle)

4.4.2 Economic impacts

The following section analyzes the economic impact, and determines the break-even price for natural gas to maintain identical cost as compared with incumbent pathways. Information of break-even prices of natural gas in different pathways will provide guidance to policymakers on natural gas pricing and marketing.

4.4.2.1 Replacing LNG with pre-salt gas for power generation

The annual profit of power generation from pre-salt gas varies with the prices of landed LNG and local natural gas. The present study offers estimates of the annual profit under different pricing conditions of LNG and local natural gas, as detailed in Table 4.8.

Table 4.8 Annual profit for replacing LNG with pre-salt gas for power generation

		LNG landed price ($/MMBtu)										
		5	6	7	8	9	10	11	12	13	14	15
Brazil natural gas price($/MMBtu)	3.0	0.12	0.35	0.58	0.81	1.04	1.26	1.49	1.72	1.95	2.18	2.41
	4.0	-0.11	0.12	0.35	0.58	0.81	1.04	1.26	1.49	1.72	1.95	2.18
	5.0	-0.34	-0.11	0.12	0.35	0.58	0.81	1.04	1.26	1.49	1.72	1.95
	6.0	-0.57	-0.34	-0.11	0.12	0.35	0.58	0.81	1.04	1.26	1.49	1.72
	7.0	-0.80	-0.57	-0.34	-0.11	0.12	0.35	0.58	0.81	1.04	1.26	1.49
	8.0	-1.03	-0.80	-0.57	-0.34	-0.11	0.12	0.35	0.58	0.81	1.04	1.26
	9.0	-1.26	-1.03	-0.80	-0.57	-0.34	-0.11	0.12	0.35	0.58	0.81	1.04
	10.0	-1.49	-1.26	-1.03	-0.80	-0.57	-0.34	-0.11	0.12	0.35	0.58	0.81
	11.0	-1.72	-1.49	-1.26	-1.03	-0.80	-0.57	-0.34	-0.11	0.12	0.35	0.58

The negative value indicates that economic profit of alternative path is higher than the domestic pre-salt gas path. In this table, the negative profit means importing LNG for power generation achieves higher benefit than using local natural gas.

As mentioned above, installation of underground natural gas storage facilities is the premise of stable power generation with pre-salt gas in Brazil, which is insufficient currently. Thus when the additional investment of such facilities is taken into consideration, the net profit of pre-salt power generation will be negative when the LNG landed price is lower than 5$/MMBtu.

The past two years have witnessed the rapid decline of LNG price. Brazil's land LNG price was 18 $/MMBtu in 2014, while the LNG price had fallen to 5.33$/MMBtu by January 2017[182]. Major driving forces of the downtrend of price include the increasing supply of low-priced shale gas, as well as incremental LNG exports from U.S. The declining LNG price might hinder the utilization of pre-salt gas in power generation sector in Brazil.

Table 4.9 Break-even natural gas price[a] under different LNG price.

LNG landed price ($/MMBtu)	5	6	7	8	9	10	11	12
Break-even price ($/MMBtu)	3.5	4.5	5.5	6.5	7.5	8.5	9.5	10.5

Break-even natural gas price: the Brazil's natural gas price when the pre-salt gas power generation path and LNG path achieve equal economic profit

4.4.2.2 Nitrogen fertilizer manufacturing

The annual profit of using pre-salt gas to produce ammonia and urea to replace imports varies with the price of natural gas, as detailed in Table 4.10.

The break-even price of natural gas for ammonia and urea production is calculated to be 8.3 and 8.6 $/MMBtu, respectively. Therefore, in the situation that price of natural gas in Brazil exceeds 9$/MMBtu, imports of ammonia and urea would be economically superior to domestic production.

Table 4.10 The variation of annual profit of ammonia and urea domestic production

Natural gas price ($/MMBtu)	Annual profit (Ammonia, unit: billion $)	Annual profit (Urea, billion $)
3	0.07	0.33
4	0.05	0.27
5	0.04	0.21
6	0.03	0.15
7	0.02	0.09
8	0.00	0.04
9	-0.01	-0.02
10	-0.02	-0.08
11	-0.03	-0.14
12	-0.05	-0.20
13	-0.06	-0.26
14	-0.07	-0.32
15	-0.09	-0.38
16	-0.10	-0.44

The negative value indicates that importing pathway achieves a higher profit than domestic production.

4.4.2.3 Methanol manufacturing

Table 4.11 presents the annual profits of substituting methanol imports with domestic production from natural gas under different pricing conditions. The break-even price of natural gas to maintain current annual profit achieved with import is calculated to be 9.5 $/MMBtu.

Table 4.11 The variation of annual profit of methanol domestic production

Natural gas price ($/MMBtu)	Annual profit (billion $)
3	0.28
4	0.24
5	0.19
6	0.15
7	0.11
8	0.06
9	0.02
10	-0.03
11	-0.07
12	-0.11
13	-0.16
14	-0.20
15	-0.25
16	-0.29

The negative value indicates that importing pathway achieves a higher profit than domestic production.

4.4.2.4 Reducing agent for steel production

Table 4.12 presents the calculated annual profits of substituting coking coal with natural gas as reducing agent in steel production, which varies with the price of coal and natural gas. The break-even price of ranges from 9.7 to 14 $/MMBtu, depending on coal price which ranges from 70 to 130 $/tonne, as detailed in Table 4.13. With the price of imported coal being 100 $/tonne in 2016, this substitution would result in favorable economic outcome if the natural gas price is lower than 11.9$/MMBtu.

Table 4.12 Annual profit for replacing coal with natural gas for steel making reductant

		Coal price												
		70	75	80	85	90	95	100	105	110	115	120	125	130
Natural gas price($/ MMBtu)	3	2.44	2.57	2.71	2.84	2.97	3.10	3.23	3.37	3.50	3.63	3.76	3.89	4.03
	4	2.08	2.21	2.34	2.48	2.61	2.74	2.87	3.00	3.14	3.27	3.40	3.53	3.66
	5	1.72	1.85	1.98	2.11	2.24	2.38	2.51	2.64	2.77	2.90	3.04	3.17	3.30
	6	1.35	1.49	1.62	1.75	1.88	2.01	2.15	2.28	2.41	2.54	2.67	2.81	2.94
	7	0.99	1.12	1.25	1.39	1.52	1.65	1.78	1.91	2.05	2.18	2.31	2.44	2.57
	8	0.63	0.76	0.89	1.02	1.16	1.29	1.42	1.55	1.68	1.82	1.95	2.08	2.21
	9	0.26	0.40	0.53	0.66	0.79	0.92	1.06	1.19	1.32	1.45	1.58	1.72	1.85
	10	-0.10	0.03	0.17	0.30	0.43	0.56	0.69	0.83	0.96	1.09	1.22	1.35	1.49
	11	-0.46	-0.33	-0.20	-0.07	0.07	0.20	0.33	0.46	0.59	0.73	0.86	0.99	1.12
	12	-0.82	-0.69	-0.56	-0.43	-0.30	-0.16	-0.03	0.10	0.23	0.36	0.50	0.63	0.76
	13	-1.19	-1.06	-0.92	-0.79	-0.66	-0.53	-0.40	-0.26	-0.13	0.00	0.13	0.26	0.40
	14	-1.55	-1.42	-1.29	-1.15	-1.02	-0.89	-0.76	-0.63	-0.49	-0.36	-0.23	-0.10	0.03
	15	-1.91	-1.78	-1.65	-1.52	-1.39	-1.25	-1.12	-0.99	-0.86	-0.73	-0.59	-0.46	-0.33
	16	-2.28	-2.14	-2.01	-1.88	-1.75	-1.62	-1.48	-1.35	-1.22	-1.09	-0.96	-0.82	-0.69

The negative value indicates that economic profit of alternative path is higher than the domestic pre-salt gas pathway.

Table 4.13 Break-even natural gas price under different coal imported price.

Coal imported price ($/tonne)	70	75	80	85	90	95	100	105	110	115	120	125	130
Break-even natural gas price($/MMBtu)	9.7	10.1	10.5	10.8	11.2	11.5	11.9	12.3	12.6	13.0	13.4	13.7	14.1

4.4.2.5 Ethylene and ethylene-based polymers manufacturing

Ethane and naphtha are produced from natural gas and oil refinery, respectively. Therefore, the economic benefits of substituting naphtha with ethane as feedstock to produce ethylene and ethylene-based polymers are influenced by the fluctuations of natural gas price and crude oil price.

Table 4.14 presents the calculated annual profits for polyethylene production from ethane cracking under different pricing conditions of natural gas and crude oil. The break-even price of natural gas to maintain current profits is presented in Table 4.15: with the current crude oil price at 50$/bbl.,

substituting naphtha cracking with ethane cracking is economically favorable if natural gas is cheaper than 8.1$/MMBtu.

Table 4.14 Annual profit for substituting naphtha with ethane to produce polyethylene

		Crude oil price ($/barrel)												
		40	45	50	55	60	65	70	75	80	85	90	95	100
Natural gas price($/MMBtu)	3	0.97	1.10	1.23	1.35	1.48	1.61	1.73	1.86	1.99	2.11	2.24	2.37	2.49
	4	0.73	0.86	0.99	1.11	1.24	1.37	1.49	1.62	1.75	1.87	2.00	2.13	2.25
	5	0.49	0.62	0.75	0.87	1.00	1.13	1.25	1.38	1.51	1.63	1.76	1.89	2.01
	6	0.25	0.38	0.51	0.63	0.76	0.89	1.01	1.14	1.27	1.39	1.52	1.65	1.77
	7	0.01	0.14	0.27	0.39	0.52	0.65	0.77	0.90	1.03	1.15	1.28	1.41	1.53
	8	-0.23	-0.10	0.03	0.15	0.28	0.41	0.53	0.66	0.79	0.91	1.04	1.17	1.29
	9	-0.47	-0.34	-0.21	-0.09	0.04	0.17	0.29	0.42	0.55	0.67	0.80	0.93	1.05
	10	-0.71	-0.58	-0.45	-0.33	-0.20	-0.07	0.05	0.18	0.31	0.43	0.56	0.69	0.81
	11	-0.95	-0.82	-0.69	-0.57	-0.44	-0.31	-0.19	-0.06	0.07	0.19	0.32	0.45	0.57
	12	-1.19	-1.06	-0.93	-0.81	-0.68	-0.55	-0.43	-0.30	-0.17	-0.05	0.08	0.21	0.33
	13	-1.43	-1.30	-1.17	-1.05	-0.92	-0.79	-0.67	-0.54	-0.41	-0.29	-0.16	-0.03	0.09
	14	-1.67	-1.54	-1.41	-1.29	-1.16	-1.03	-0.91	-0.78	-0.65	-0.53	-0.40	-0.27	-0.15
	15	-1.91	-1.78	-1.65	-1.53	-1.40	-1.27	-1.15	-1.02	-0.89	-0.77	-0.64	-0.51	-0.39
	16	-2.15	-2.02	-1.89	-1.77	-1.64	-1.51	-1.39	-1.26	-1.13	-1.01	-0.88	-0.75	-0.63

The negative value indicates that economic profit of alternative path is higher than the domestic pre-salt gas pathway.

Table 4.15 Break-even natural gas price under different crude oil price

Crude oil price($/barrel)	Break-even natural gas price($/MMBtu)
50	8.1
55	8.8
60	9.3
65	9.7
70	10.2
75	10.9
80	11.3
85	11.9

4.4.2.6 CNG/LNG to replace diesel as fuel for heavy-duty vehicles

Table 4.16 presents the calculated annual profits of substituting diesel-powered heavy-duty vehicles with CNG-powered vehicles under difference pricing conditions. As demonstrated in the

table, this substitution could not maintain current annual profits when the price of natural gas exceeds 7$/MMBtu. With the crude oil price of 50$/bbl. at present (Second quarter of 2017)[183], the substitution could only be profitable with natural gas cheaper than 3$/MMBtu. Table 4.17 presents the break-even price of natural gas for CNG-powered vehicles to be economically equivalent to diesel-powered heavy-duty vehicles.

Table 4.16 Annual profit for replacing diesel heavy-duty vehicles with CNG vehicles

		Crude oil price												
		40	45	50	55	60	65	70	75	80	85	90	95	100
Natural gas price($/MMBtu)	3	-0.18	-0.06	0.05	0.17	0.28	0.40	0.52	0.63	0.75	0.86	0.98	1.09	1.21
	4	-0.55	-0.43	-0.32	-0.20	-0.08	0.03	0.15	0.26	0.38	0.49	0.61	0.73	0.84
	5	-0.91	-0.80	-0.68	-0.57	-0.45	-0.34	-0.22	-0.10	0.01	0.13	0.24	0.36	0.47
	6	-1.28	-1.17	-1.05	-0.94	-0.82	-0.70	-0.59	-0.47	-0.36	-0.24	-0.13	-0.01	0.11
	7	-1.65	-1.54	-1.42	-1.30	-1.19	-1.07	-0.96	-0.84	-0.73	-0.61	-0.49	-0.38	-0.26
	8	-2.02	-1.90	-1.79	-1.67	-1.56	-1.44	-1.32	-1.21	-1.09	-0.98	-0.86	-0.75	-0.63
	9	-2.39	-2.27	-2.16	-2.04	-1.92	-1.81	-1.69	-1.58	-1.46	-1.35	-1.23	-1.11	-1.00
	10	-2.76	-2.64	-2.52	-2.41	-2.29	-2.18	-2.06	-1.95	-1.83	-1.71	-1.60	-1.48	-1.37
	11	-3.12	-3.01	-2.89	-2.78	-2.66	-2.54	-2.43	-2.31	-2.20	-2.08	-1.97	-1.85	-1.73
	12	-3.49	-3.38	-3.26	-3.14	-3.03	-2.91	-2.80	-2.68	-2.57	-2.45	-2.33	-2.22	-2.10
	13	-3.86	-3.74	-3.63	-3.51	-3.40	-3.28	-3.17	-3.05	-2.93	-2.82	-2.70	-2.59	-2.47
	14	-4.23	-4.11	-4.00	-3.88	-3.76	-3.65	-3.53	-3.42	-3.30	-3.19	-3.07	-2.95	-2.84
	15	-4.60	-4.48	-4.36	-4.25	-4.13	-4.02	-3.90	-3.79	-3.67	-3.55	-3.44	-3.32	-3.21
	16	-4.96	-4.85	-4.73	-4.62	-4.50	-4.39	-4.27	-4.15	-4.04	-3.92	-3.81	-3.69	-3.58

The negative value indicates that economic profit of alternative path is higher than the domestic pre-salt gas pathway.

Table 4.17 Break-even natural gas price under different crude oil price

Crude oil price($/barrel)	Break-even natural gas price($/MMBtu)
50	3.2
55	3.4
60	3.8
65	4.2
70	4.6
75	4.9
80	5.4
85	5.9

4.4.2.7 Comparing economic profits of the above natural gas use pathways

This section discusses and compares the economic benefits and calculated break-even price of natural gas under current pricing conditions (crude oil price= 50$/barrel, coal price=100 $/tonne, landed LNG= 5.33 $/MMBtu) in the pathways discussed above.

Figure 4.8 demonstrates the association between fluctuating natural gas price and the annual profits of various natural gas pathways. Apparently, under the current relatively low landed LNG price, the replacement with pre-salt gas for power generation could barely achieve positive economic outcomes. Similarly, substituting diesel-powered vehicles with CNG-powered vehicles is economically unfavorable as the fuel cost of CNG vehicles is significantly higher than current crude oil price. On the other hand, the rest four pathways could all increase annual profits as long as the Brazil's natural gas price is below 8$/MMBtu.

The break-even price is the price of natural gas where the economic gains of natural gas pathway and non-natural-gas incumbent pathway are equal. When the real natural gas price in Brazil is lower than the break-even price, a pathway can achieve positive economic profits compared with imports. The higher the break-even natural gas price implies the pathway indicates it can achieve profits at a higher cost of natural gas feedstock.

Crude oil price has a strong economic influence on both heavy-duty vehicle fueling and polyethylene production pathways. As demonstrated in Figure 4.9, the calculated break-even price of natural gas in polyethylene production pathways remain higher than that in heavy-duty vehicle fueling pathway. Thus, the former pathway proves economically superior to the latter regardless of crude oil price, implicating a potential stimulus for faster development in associated downstream industries.

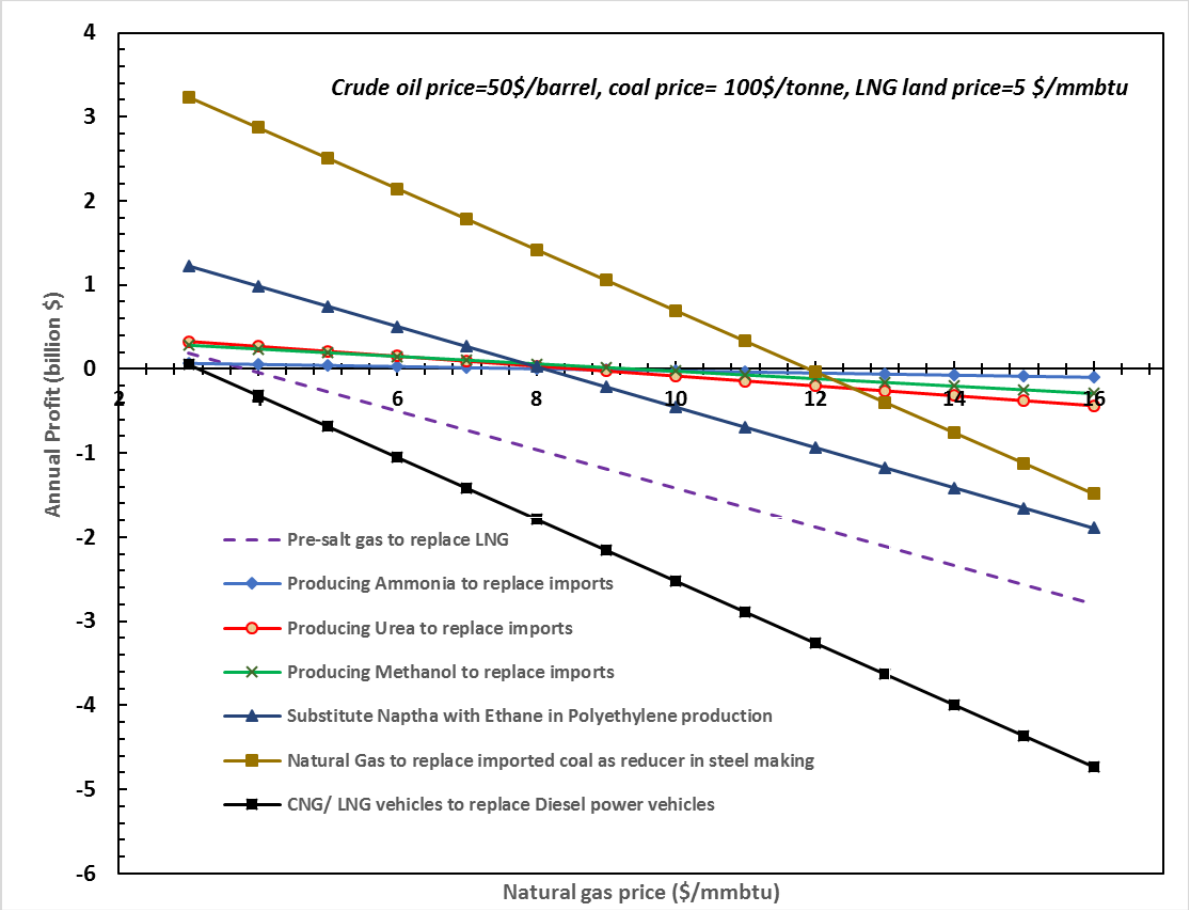

Figure 4.8 Annual profits of different natural gas use pathways change as the natural gas sale price varies

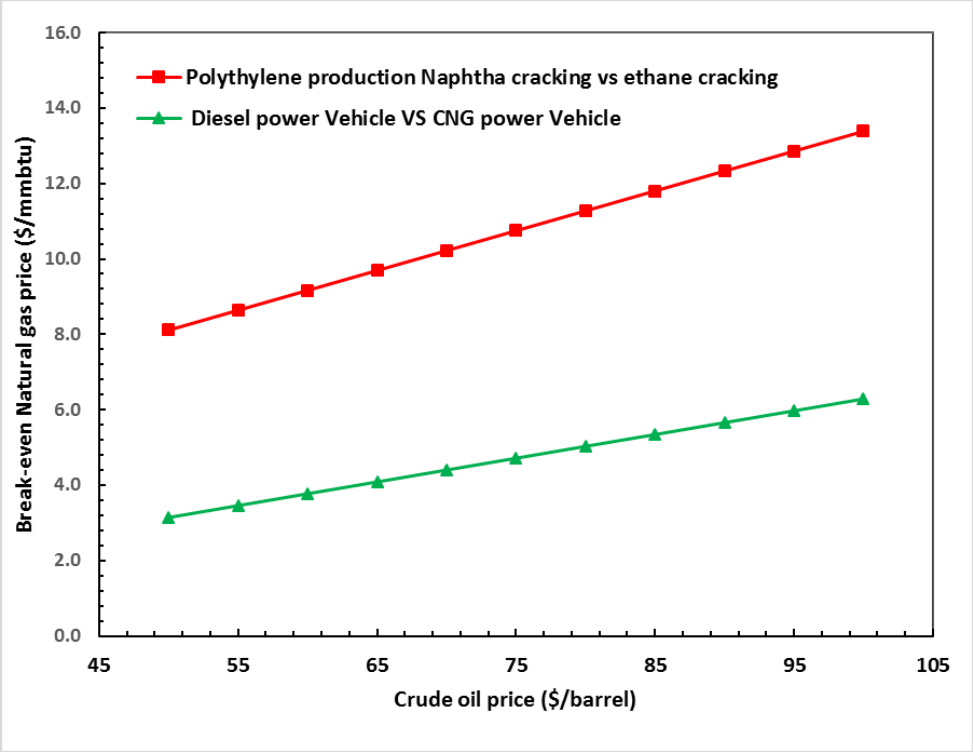

Figure 4.9 The break-even price of vehicle fueling and polyethylene production paths considering the change of crude oil price

Under current pricing conditions(crude oil price= 50$/barrel, coal price=100 $/tonne, landed LNG= 5.33 $/MMBtu), the pathway of steel production has the highest calculated break-even price for natural gas at 12 $/MMBtu, while the break-even price for the heavy-duty vehicle fueling pathway is lowest, as detailed in Table 4.18.

Table 4.18 Current break-even natural gas price for different pathway

Pathways	**Break-even natural gas price (unit:$/MMBtu)**
Pre-salt gas to replace LNG for power generation	3.8
Producing Ammonia to replace imports	8.3
Producing Urea to replace imports	8.6
Producing methanol to replace imports	9.5
Natural Gas to replace imported coal as reducer in steel making	11.9
Ethane to replace Naphtha in Ethylene and Polyethylene production	8.1
CNG/ LNG vehicles to replace Diesel power heavy-duty vehicles	3.1

Brazil's natural gas pricing is tightly regulated by the state-owned enterprise Petrobras, who has strong control over the supply and sale of natural gas nationwide, as well as considerable shares in various downstream industries (e.g. natural gas power plants, fertilizer manufacturers, petrochemical plants). According to a report by Petrobras, the prices for natural gas sold to thermoelectric plants and household in May 2017 are 5.04 $/MMBtu and 7.33 $/MMBtu, respectively[184]. Petrobras did not disclose information about the production cost of pre-salt gas. It can be inferred that the production cost of natural gas should be lower than the price sale to thermoelectric plants, thus lower than 5.04 $/mmbtu. The LNG landed price of Brazil 2017 is 5.33 $/mmbtu, a bit higher than the sale price for thermoelectric plants[182]. Previous literature revealed that the industrial sale price was lower than the household sale price for natural gas[131], thus lower than the calculated break-even price for pathways of ammonia production, methanol production, steel production and polyethylene manufacturing. Therefore under current pricing condition, the replacement of traditional production pathways with pre-salt gas would be economically beneficial in the above pathways. On the other hand, the economic benefit of using pre-salt gas for power generation and fueling CNG-powered vehicles could not be proven. Of note, the economic analysis and comparison is based on the assumption that different natural gas downstream industries (except of electricity sector) accept the same natural gas market price, and Petrobras does not subsidies any of the industries.

4.4.3 Employment Impacts

This study applied an extended input-output model to analyze employment impacts of the natural gas use pathways discussed above. Figure 4.10 presents the estimation of new job positions created from four natural gas use pathways.

Among the four, the pathway of steel production has the largest number of jobs created, at 36 thousand. The five most affected sectors in this pathway are wholesale and retail trade; extraction of oil and gas, including support activities; ground transportation; other administrative activities and complementary services; and legal, accounting, consulting and corporate headquarters activities. Altogether, these five sectors contribute 52% of the created job opportunities in this pathway. The number of jobs created from the pathway of power generation, fertilizer production

and methanol production is 28 thousand, 17 thousand and 5 thousand respectively, as detailed in Figure 4.10.

Apparently, the sector of wholesale and retail trade offers the highest job opportunities in all four pathways, though it is not directly affected by any of the pathways. The job opportunities offered by the sector of wholesale and retail trade are relatively low-paid jobs with the average monthly wage of 862 Brazilian Real (comparing with the average monthly wage of 1190 Brazilian Real for all sectors).

Due to the limitation of the input-output analysis, estimates of employment effects from the pathways of polyethylene production and CNG-powered vehicles could not be calculated. In these two pathways, natural gas substituted oil as feedstock without a change in the economic scales the manufacturing industry, thus no employment implications could be quantified. This limitation should be addressed in future studies.

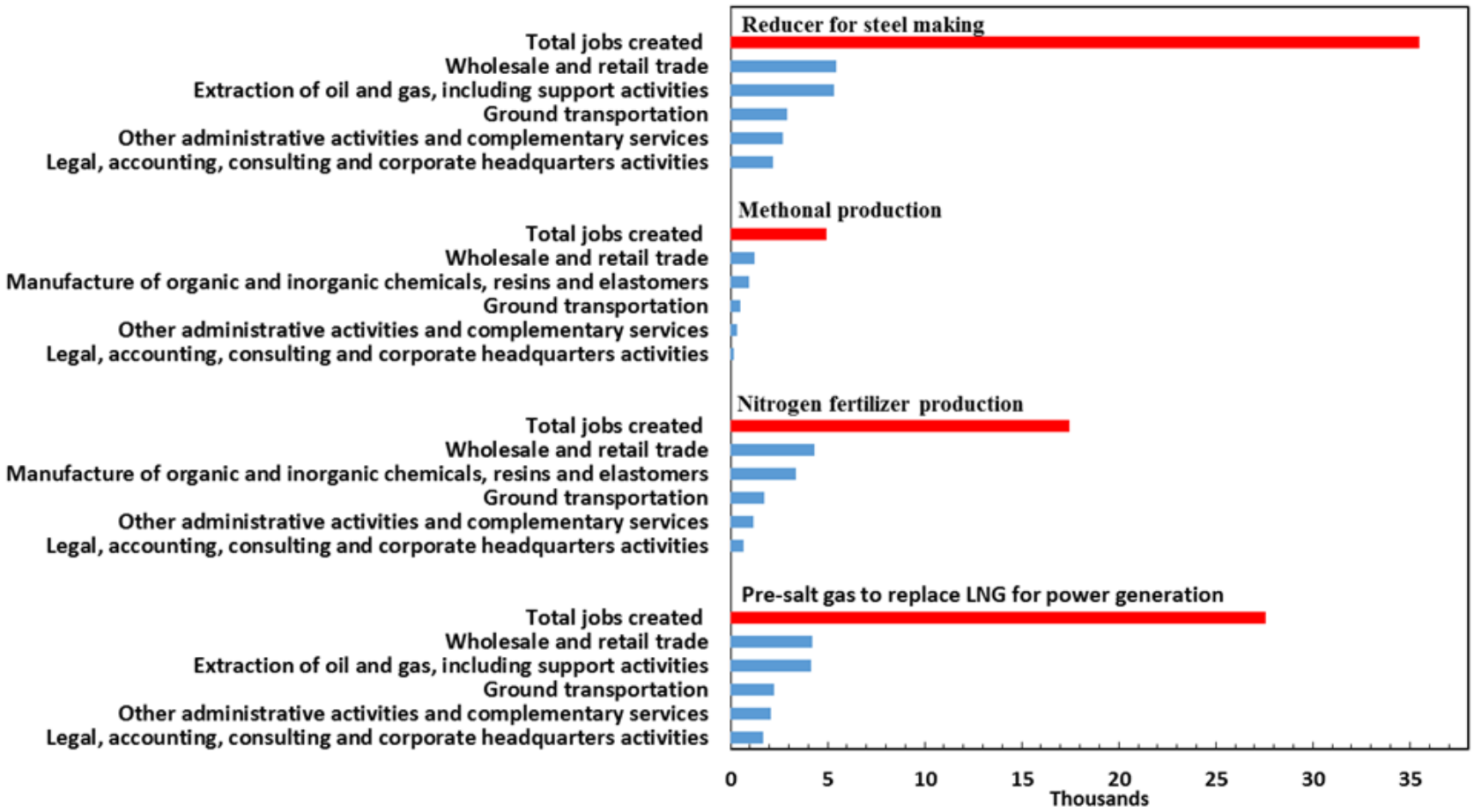

Figure 4.10 Number of total jobs and jobs in top 5 affected sectors for different natural gas pathways

4.5 Final remarks

This study analyzes the impacts of six possible natural gas pathways on global warming effects, economy and employment. This section summarizes the main findings and discusses the policy implications on Brazil's natural gas exploitation and downstream industry development.

Table 4.19 summarizes the GHG emissions reduction effects, annual profits (under current fuel pricing condition), break-even prices of natural gas, and potential jobs created of the six natural gas use pathways. As shown in the table, among the six pathways, substituting coal as reducing agent for steel production is associated with the largest scale of GHG emission reduction, economic benefit and employment increase. Similarly, nitrogen fertilizer production pathway and methanol production pathways also showed benefits in all three aspects analyzed.

Table 4.19 GHG emissions reduction, annual profits, break-even natural gas price, and job-creating potential of the six natural gas use pathways

	GHG emissions reduction (thousand tonnes CO_2 equivalent)	**Annual profit (billion $)**	**Break-even natural gas price ($/MMBtu)**	**Potential jobs created (thousand)**
Pre-salt gas to replace LNG for power generation	825	-0.27	3.8	28
Producing Nitrogen fertilizer to replace imports	2280	0.087	8.6	17
Producing methanol to replace imports	378	0.092	9.5	5
Natural Gas to replace imported coal as reducer in steel making	35300	1.66	11.9	36
Ethane to replace Naphtha in Ethylene and Polyethylene production	2550	0.19	8.1	--
CNG heavy-duty vehicles to replace Diesel power heavy-duty vehicles	78	-1.54	3.1	--

Brazil has committed under Paris Agreement to reduce GHG emissions by 37 percent by 2025 relative to 2005 levels. Thus, GHG emissions reduction is one of the important factor that should be considered for different pathways comparisons and policy making strategies. All six natural gas use pathways emit less GHG than the currently used process pathways on average. The pathway of using natural gas to replace imported coal for a steel making reducing agent leads to the largest GHG emissions reduction. While the GHG emissions reduction associated with CNG replacing diesel for heavy-duty vehicle fueling are not significant. Under current fuel prices, fertilizer production, methanol production, polymer production, and as use as a reducing agent in steel making will achieve positive annul profits, while using natural gas for power generation and heavy vehicle fueling will not.

Table 4.19 presents the job creation potential of the different natural gas pathways. The pathway of using natural gas to replace imported coal as reducer in steel making has the largest job created potentials, while the pathway of methanol production has the smallest number of job created.

The employment effects of the different pathways were estimated using an Input-output model, and it should be noticed that there are several limitations of the analysis. First, the Input-output model is based on the assumption of linear relationship between different sectors, which is unrealistic. Secondly, the analysis used a model year of 2010 for projections, however, the economic structure could change and the model might not be applicable for the future. Finally, the input-output modelling assumes products of each sector are homogeneous, which might lead to the inaccuracy and uncertainty of results.

Of note, besides the three impacts analyzed in the present study, additional factors should be taken into consideration while evaluating the potential benefits of natural gas use pathways. For example, as more than 40% of the steel produced in Brazil is for exports, the industry is facing unprecedented challenge currently with a shrinking Europe market and competition from low-priced steel of China. Despite that the results

of present study advocates for using natural gas in place of coal as reducing agents, it is difficult to motivate the industry for technology upgrades and initial investment on additional natural gas route installation. Similarly, for vehicle fueling pathway, despite that economic profit is negative under current fuel pricing, and GHG emissions reduction is insignificant, the substitution still has potential practical value in the aspect of reducing particulate matter and other pollutants potentially hazardous to human health. Also, despite that replacement of LNG with pre-salt gas for power generation might barely create positive economic outcomes with the declining LNG price, the substitution has significance for the nation's power supply stability, national security and the improvement of gas transmission and storage infrastructure in the long-term. These above aspects are beyond the quantitative analysis of the present study and could be the focus of future studies.

5. Conclusions and Future Work

The study discussed the impacts of exploitation of mineral and hydrocarbon resources in emerging countries on global warming effect, economy and society. Specifically, three sub-projects have been conducted:

Project 1 focused on the issue of the growing GHG emissions from iron ore production with the rapid economic development in China. The growing demand for iron ore drives increased production. On the other hand, fast consumption leads to the depletion of iron-ore resources and increased exploitation of lower quality ores, resulting in accelerating energy consumption and increased GHG emissions associated with every tonne of iron ore extracted and processed. Results of Project 1 shows that the total GHG emissions for the iron ore mining/processing sector will increase by three times by 2020 from the level in 2013, assuming that the fraction of ore provided by the domestic supply remains unchanged.

Project 2 was an extension of the first project, exploring the alternatives of outsourcing iron ore overseas. Previous literature criticized the practice of outsourcing as it transfers of environmental problems abroad and increases the environmental burdens in developing countries. However, results of Project 2 showed that importing iron ore from Australia and Brazil, where there were better operating conditions and technologies, lead to a lower net global GHG emissions comparing with domestic production. This project also raised the issue of GHG emissions from marine transportation. Results showed that ocean shipping contributed the largest proportion of the overall GHG emissions, accounting for 58% and 75% for Australian and Brazilian iron ore, respectively. However, under current production-based GHG emissions accounting framework, a country is only responsible for the GHG emissions produced within the country boundary, not including the GHG emissions from international shipping. The lack of commitment impedes more actions to reduce GHG emissions from international shipping.

Contrary to the first two projects which focused on challenges of development with deficient resources, Project 3 discussed the issue of how to optimally use abundant newly discovered resources for future development. Results of Project 3 demonstrated that under current pricing conditions, using pre-salt gas for nitrogen fertilizer production, methanol production and substituting coal as the reducing agent for steel production can achieve benefits in all three aspects of global warming effects, economic and employment impacts.

5.1 Research Questions Revisited

The following section will summarize the main findings of the current study and present brief answers to the research questions raised in each project.

5.1.1 Topic 1: Analysis of life cycle GHG emissions of iron ore mining and processing in China —uncertainty and trends.

1. *What is the life cycle GHG emissions of iron ore mining and processing in China? How certain are the estimates?*

Three approaches were applied to calculate the GHG emissions for iron ore mining and processing. Approach I (bottom up model) estimated the GHG emissions from open pit mining and iron processing to be 270 kg CO2e/tonne of ore, with the 90% confidence interval (CI) ranging from 220 to 370 kg CO2e/tonne of ore. Approach II used mining plants data reported by Department of Metallurgy of China, and estimated the GHG emissions from overall iron ore mining (both open pit and underground are included) and processing to be 270 kg CO2e/tonne of ore, with the 90% CI of 210 to 370 kg CO2e/tonne of ore. Approach III used statistical energy data of iron mining and processing sector. The mean estimate based on Approach III was 280 kg CO2e/tonne of ore, and the 90% CI estimate was 260 to 310 kg CO2e/tonne of ore. Thus, all three approaches applied in the current study resulted in similar estimates.

2. *What parameters/factors contribute most to the uncertainty of the LCA results?*

The top 5 parameters that contributed most to the uncertainty of the LCA results were iron ore grade, electricity use of beneficiation, emission related to sintering, stripping ratio, diesel consumption factor for iron ore hauling, contributing 42%, 28%, 12%, 8%, 4% to the total variance of the result uncertainty, respectively.

3. *What are the emissions from different iron ore mining and processing steps? Which stage contributes most to the overall life cycle emissions?*

The GHG emissions associated with agglomeration were 165 kg CO2e/tonne of ore, contributing most (62%) to the overall life cycle emissions of iron ore production. Emissions associated with mining, ore processing, and rail transportation were calculated to be 35, 62, 3.7 kg CO2e/tonne of ore, representing 13%, 23%, 1.4% of the overall life cycle GHG emissions, respectively.

The bottom up approach also provided estimates of the GHG emissions associated with the four steps for iron ore mining: vegetation and soil removal, drilling and blasting, dewatering, loading and hauling. The GHG emissions associated with the four mining steps were 9.2, 0.8, 2.5, 26 kg CO2e/tonne of ore, respectively. Among the four, iron ore loading and hauling contributed the largest (67%) portion to the emissions associated with mining process.

4. *What is the future trend of GHG emissions of iron ore mining and processing as the iron ore grade decreases?*

The rapid increasing scale of iron mining and depletion of high-grade ore in China necessitate the use of lower grade ore in the future. From 2006 to 2012, average iron ore grade decreased from 30% to 27%[17]. Assuming the rate of grade change remains stable, by the year 2020, the average iron ore grade would be 23%, leading to 9% increase in life-cycle mean GHG emissions, from 285 kg CO_2e/tonne in 2012 to 310 kg

CO_2e/tonne in 2020. Figure 5.1 shows the increasing GHG emissions as the iron ore grade declines.

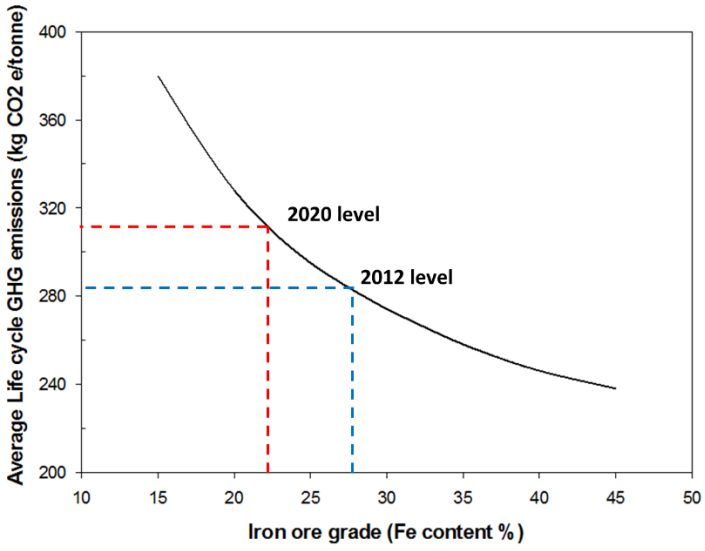

Figure 5.1 Mean life-cycle GHG emissions per tonne of iron ore as iron ore grade declines

5. *What are viable ways to reduce GHG emissions associated with China's increasing iron ore consumption?*

Increasing the fraction of pelletized iron ore used in the blast furnaces can reduce overall GHG emissions. Clean grid power can help reduce emissions from iron ore processing.

It is possible that importing high-grade iron ores from abroad might be a viable way for GHG emissions reduction. However, detailed analysis of GHG emissions from long distance shipping would be necessary to make final conclusions.

5.1.2 Topic 2: Life cycle GHG emissions of iron ore mining in China, Australia and Brazil—a comparison of different iron ore sources for China.

1. *What are the life cycle GHG emissions of iron ore mining and processing in Brazil and Australia? How certain are the estimates? How do the GHG emissions for iron ore production from the two countries compare to iron ore produced in China? Which iron ore source leads to the lowest GHG emissions?*

The life cycle GHG emissions of Australian iron ore fines was calculated to be 42 kg CO_2e/tonne, with the 90% CI ranging from 33 to 52 kg CO_2e/tonne. The life cycle GHG emissions of Brazilian iron ore fines from Iron Quadrangle and Carajas were calculated to be 97 (90% CI 77~116) kg CO_2e/ tonne, and 107 (90% CI 87 ~126) kg CO_2e/ tonne, respectively. While t life cycle GHG emissions of Chinese iron ore fines was calculated to be 110 kg CO_2e/tonne, with a 90% CI of 60 to 190 kg CO_2e/ tonne.

Thus, the GHG emissions of one functional unit of imported Australian iron ore were significantly lower than that of Chinese ore, while there was no significant difference between the average GHG emissions from imported Brazilian iron ore versus China's domestic iron ores. Therefore, sourcing iron ore from Australia could potentially lead to the lowest GHG emissions.

Of note, the comparison LCA study used one metric ton of sinter feed fines as the functional unit, excluding the agglomeration process in the system boundary.

2. *What are the emissions associated with different iron ore mining and processing stages for Australia and Brazil? Which stage contributes most to the overall life cycle emissions?*

GHG emissions associated with mining, ore processing, ocean shipping, rail transportation for Australian iron ore were calculated to be 6.8, 1.9, 25, 9.4 kg CO_2e/tonne, respectively. For Brazilian iron fines from Iron Quadrangle, emissions of these four processes were calculated to be 7.8, 3.9, 74, 11 kg CO_2e/tonne, respectively.

For Brazilian ores from Carajas, emissions of these four processes were calculated to be 9.0, 0.2, 79, 17 kg CO_2e/tonne, respectively. Ocean shipping contributed the largest portion for imported Australian and Brazilian iron ores, accounting for 58% and 75% of the overall emissions respectively.

3. *What are viable ways to reduce the embedded GHG emissions of Brazilian and Australian iron ores?*

Increasing vessel capacity utilization (e.g. through adopting a triangular shipping route) could reduce GHG emissions for the ocean shipping. Another viable way was to build steel mills near shipping ports in China to reduce GHG emissions from rail transportation.

4. *Considering the future trends of iron ore grade, how will the comparison LCA results of Chinese, Brazilian and Australian iron ore change over time?*

Chinese iron ore grade was projected to decline in the near future, leading to an increase in the emissions factor. GHG emissions factor of Australian iron ore was estimated to be lower than that of Chinese ore. Uncertainty estimates of emission factor for Brazilian iron ores and Chinese iron ores overlapped most of the time, however, when Chinese ore grade falls below 20%, Brazilian iron ores would become superior with lower GHG emissions.

5. *What parameters/factors contribute most to the uncertainty of the LCA results?*

The top 5 parameters that contributed most to the uncertainty of the LCA results of imported Australian iron ore were rail transport distance in China (48%), shipping fuel consumption factor (36%), ocean shipping distance (7%), fuel consumption factor of ore hauling (2%), rail transportation fuel consumption factor (2%).

The top 5 parameters that contributed most to the uncertainty of the LCA results of imported Brazilian iron ore were shipping fuel consumption factor (80%), rail transport

distance in China (10%), ocean shipping distance (3%), electricity use of beneficiation (2%), iron ore grade (1%).

5.1.3 Topic 3: Integration of pre-salt natural gas into Brazilian Fossil-derived feedstock.

1. *What are the global warming effects of pre-salt natural gas exploration and downstream industry developments? How certain are the estimates?*

GHG emissions associated with a functional unit gas production is changing throughout the entire production life. At the early stage, GHG emissions of pre-salt gas production were estimated to be 5.4 gCO2e/MJ, with the 90% CI ranging from 4.5 to 6.4 gCO2e/MJ. At the intermediate stage, the emissions were estimated as 7.1 gCO2e/MJ, the 90% CI ranging from 6.3 to 8.0 gCO2e/MJ. At the late stage, all produced gas would be reinjected back to the reservoir.

Life cycle GHG emissions associated with natural gas use pathways of power generation, nitrogen fertilizer production, methanol production, as the reducing agent for steel production, ethylene-based polymer production were 6.0 (90%CI: 5.2~7.2) g CO_2e/MJ, 1.6 (90%CI: 1.4~2.5) tonne CO_2e/tonne NH_3, 0.54 (90%CI: 0.50~0.58) tonne CO_2e/tonne CH_3OH, 0.92 (90%CI: 0.77~0.97) tonne CO_2e/tonne steel, 1.1 (90%CI: 0.58~1.6) tonne CO_2e/tonne ethylene, respectively. GHG emissions of CNG-powered light heavy-duty vehicle, CNG-powered median heavy-duty vehicle, CNG-powered bus, LNG-powered bus, CNG-powered heavy heavy-duty vehicle, LNG-powered heavy heavy-duty vehicle were calculated to be 690(90%CI: 620~800), 1300(90%CI: 1200~1600), 3000(90%CI: 2700~3500), 3300(90%CI: 3000~3900), 2400 (90%CI: 2100~2700), 2600(90%CI: 2300~2900) g CO_2e/mile, respectively.

Comparing with the non-natural-gas traditional pathways, the use of natural gas for power generation, nitrogen fertilizer production, methanol production, as the reducing agent for steel making, ethylene-based polymer production, heavy-duty vehicle fueling

would reduced mean GHG emissions by 0.83, 2.3, 0.38, 35, 2.6 and 0.078 million tonne CO_2 equivalent per year, respectively.

2. *With the exploration of pre-salt natural gas resources, what are the possible use of the increasing gas supply in Brazil?*

The possible use of the increasing gas supply in Brazil included: power generation, nitrogen fertilizer production, methanol production, as the reducing agent for steel production, ethylene-based polymer production, and as fuel for heavy-duty vehicles.

3. *What are the break-even gas prices for alternative natural gas uses? What are the economic profits of these uses under different gas price?*

The break-even gas price for natural gas use pathways to achieve equivalent profits of the corresponding traditional pathways varied with the change of traditional fuel price. Under current pricing conditions (crude oil price= 50$/barrel, coal price=100 $/tonne, landed LNG= 5.33$/MMBtu), the break-even prices for the pathways of power generation, nitrogen fertilizer production, methanol production, as the reducing agent for steel making, ethylene-based polymer production, heavy-duty vehicle fueling were calculated to be 3.2, 3.4, 3.8, 4.2, 4.6, 4.9, 5.4, 5.9 $/MMBtu, respectively.

Figure 5.2 presents the annual profits of different natural gas pathways change as the variation of natural gas price.

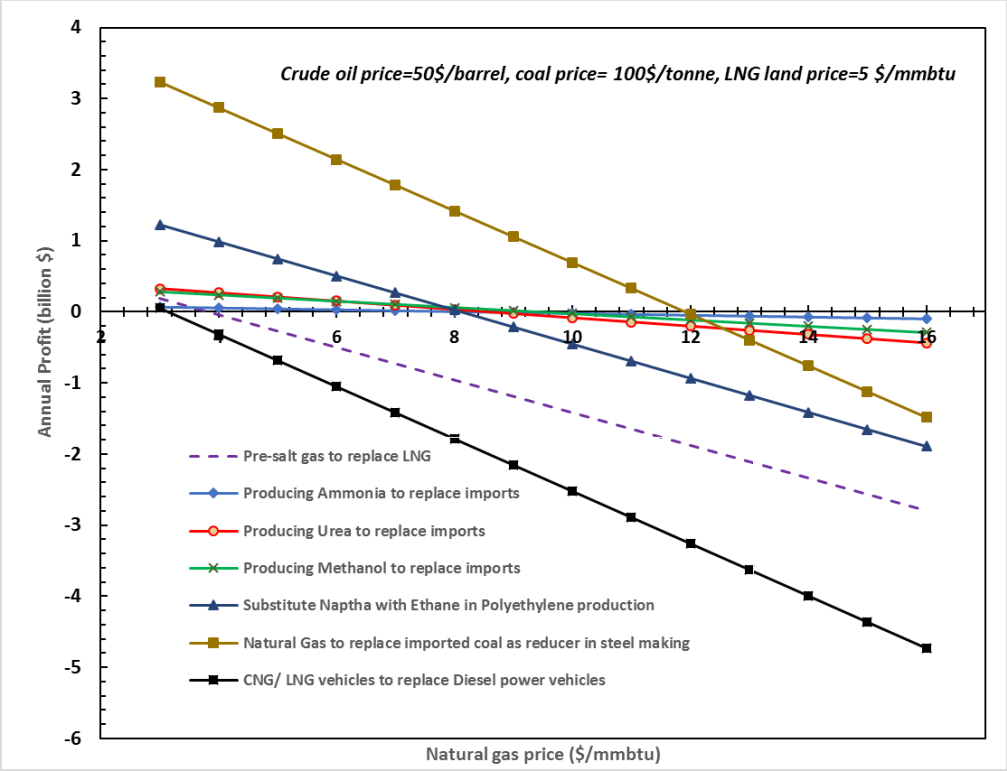

Figure 5.2 Annual profits of different natural gas use pathways change as the natural gas sale price varies

4. *What are the social impacts in terms of jobs of natural gas exploration and associated downstream industry development? How many jobs will be created by the different gas uses?*

The potential to create jobs from the pathways of power generation, nitrogen fertilizer production, methanol production and as reducing agent for steel production were estimated to be 28, 17, 5 and 36 thousand, respectively.

5. What are the policy implications for the future development of the natural gas sector and associated downstream industry?

Under current fuel price, substituting coal with natural gas as reducing agent for steel production leads to largest scale of GHG emission reduction, economic and

employment benefits. Also, using natural gas for nitrogen fertilizer production and methanol production can also obtain positive benefits in all three aspects.

As long as the Brazil's natural gas price is below 8$/MMBtu, the natural gas pathways of nitrogen fertilizer production, methanol production, as reducing agent for steel production, ethylene-based polymer production could all create beneficial economic outcomes.

The sector of wholesale and retail trade offers the highest job opportunities in all natural gas use scenarios, which are mainly relatively low-paid jobs.

As the international LNG price is declining, replacing LNG with pre-salt gas for power generation could barely create positive economic outcomes. While, the substitution still has significance for the nation's power supply stability, national security and the improvement of gas transmission and storage infrastructure in the long-term.

5.2 Deliverables

The deliverables from this thesis work are research papers to be submitted to journal publications. A research paper of Project 1 is planned to be submitted to the journal of *Resources Policy*. The research paper of Project 2 is planned to be submitted to the journal of *Environmental Science & Technology*. A research paper of Project 3 is planned to be submitted to the journal of *Energy Policy*.

5.3 Research Contributions

Data deficiency has been the primary reason for the limited life cycle analysis on mineral mining[185]. Project 1 established an engineering-based life-cycle model, which estimated iron ore life associated GHG emissions based on characteristics of iron ore deposit and parameters of production techniques. The data required by the life-cycle model were available from public sources, overcoming the difficulty of obtaining data

from mining companies. The bottom-up model from the project is a white-box model, which can provide break-down results of GHG emissions associated with each individual mining and processing step.

Project 2 used the life cycle model developed in Project 1 in iron ore mining of Australia and Brazil, proving the applicability of the model in different scenarios. Project 2 represented the first attempt to compare the GHG emissions embedded in the iron ores from Australia, Brazil and China, the three largest iron ore production countries.

Project 3 was the first to estimate GHG emissions associated with natural gas production in Brazil pre-salt reservoir, and provided detailed analysis according to the changes of reservoir characteristics and technical parameters of different stages of the production life (the early, intermediate and late stage). The project was also the first to discuss and compare the different natural gas use pathways in Brazil from the aspects of global warming effects, economic and employment impacts. Results of the project provided information for future policies regarding the development of the natural gas sector and associated downstream industries.

5.4 Future Work

On the basis of current researches, the proposed future work include:

1. *More in-depth discussion on iron ore mining and processing in China*

- Exploring the possibility, associated economic and social impacts of replacing sintering with pelletizing for iron ore agglomeration in China.

Project 1 suggested that increasing the fraction of iron ores that are pelletized could potentially reduce overall GHG emissions associated with iron ore processing in China. Replacing the current sintering with pelletizing would also lead to profound economic and social impacts, including front-end costs of new pelletizing facilities, demolition of existing sintering plants, and increased unemployment of previous sintering operators.

The economic and social impacts and implications should be analyzed in the future work to provide recommendations for related policies regarding replacing sintering with pelletizing.

- Analysis of other potential environmental impacts of iron ore mining.

Project 1 focused on the analysis of the GHG emissions of iron ore mining and processing, which is only one aspect of the environmental impacts. Other potential environmental impacts of iron ore mining include: water and resource depletion, soil erosion and degradation, acidification, trace metal contamination in soil and terrestrial plants, and food chain contamination, which should be discussed in the future work.

2. *Potential economic and social impacts of replacing domestic production with imports of iron ore.*

Project 2 suggested that importing iron ores might be viable GHG emissions reduction strategies for China. However, shifting towards greater reliance on iron ore imports could have socioeconomic impacts on the Chinese market. Potential impacts include decreased production in the Chinese mining sector, unemployment, vulnerability to the fluctuating price of imported iron ore, as well as the security issues for the country's economic system. More detailed analysis on these issues should be covered in the future work.

3. *Exploitation of pre-salt oil and its impacts on Brazil's environment, economy and society.*

Project 3 discussed the extraction and use of pre-salt natural gas, while the future work will focus on the exploitation of pre-salt oil and its potential on Brazil's environment, economy and society. Currently, the primary use of oil is for vehicle fueling, which accounts for about 60% of the total consumption [37, 38]. The potential increasing oil supply from pre-salt reservoirs would promote the use of oil in other sectors, such as petrochemicals manufacture, power generation, etc. Some of the uses of oil overlap

with that of natural gas, for example, both oil and natural gas can be used as feedstock for polymers manufacturing. Therefore, the competitive and supplementary relationships of pre-salt oil and natural gas should be discussed in the future work. Additionally, most of Brazil's current produced crude oil is of heavy grade[29, 31], while the crude oil from pre-salt reservoirs is lighter with an intermediate API of 28~32[30, 41, 175]. The change of crude oil grade would affect the structure and products of Brazil's oil refinery industry, which should also be one of the focuses in the future work.

6. References

1. U.S. Energy Information Administration: History of energy consumption in the United States; https://www.eia.gov/todayinenergy/detail.php?id=10.

2. Bergstrom, J. C.; Randall, A., *Resource economics: an economic approach to natural resource and environmental policy*. Edward Elgar Publishing: 2016.

3. Gan, Y.; Zhang, T.; Liang, S.; Zhao, Z.; Li, N., How to deal with resource productivity. *Journal of Industrial Ecology* **2013,** *17*, (3), 440-451.

4. Gunasekaran, A.; Jabbour, C. J. C.; Jabbour, A. B. L. d. S., Managing organizations for sustainable development in emerging countries: an introduction. *International Journal of Sustainable Development & World Ecology* **2014,** *21*, (3), 195-197.

5. Behrens, A.; Giljum, S.; Kovanda, J.; Niza, S., The material basis of the global economy: Worldwide patterns of natural resource extraction and their implications for sustainable resource use policies. *Ecological Economics* **2007,** *64*, (2), 444-453.

6. Adriaanse, A.; Bringezu, S.; Hammond, A.; Moriguchi, Y.; Rodenburg, E.; Rogich, D.; Schütz, H., Resource flows: the material basis of industrial economies. **1997**.

7. Höök, M.; Tang, X., Depletion of fossil fuels and anthropogenic climate change—A review. *Energy Policy* **2013,** *52*, 797-809.

8. Baes, C.; Goeller, H.; Olson, J.; Rotty, R., Carbon Dioxide and Climate: The Uncontrolled Experiment: Possibly severe consequences of growing CO 2 release from fossil fuels require a much better understanding of the carbon cycle, climate change, and the resulting impacts on the atmosphere. *American Scientist* **1977,** *65*, (3), 310-320.

9. Caldeira, K.; Wickett, M. E., Oceanography: anthropogenic carbon and ocean pH. *Nature* **2003,** *425*, (6956), 365-365.

10. *Sales Volume Reports Brazilian Market for Light and Commercial Vehicles for 2012~2014* Automotive Marketing Consulting 2015.

11. Chen, W.; Yin, X.; Ma, D., A bottom-up analysis of China's iron and steel industrial energy consumption and CO 2 emissions. *Applied Energy* **2014,** *136*, 1174-1183.

12. National Bureau of Statistics of China: China statistical yearbook 2011. *Pekin ISBN* **2011,** *9787*, 5037-6351.

13. Shanghai Statistics Bureau: Shanghai Statistical Yearbook. In China Statistics Press: 2011.

14. National Bureau of Statistics of China: Chinese Statistical Yearbook, 2015. In Beijing, 2016.

15. Wu, J.; Yang, J.; Ma, L.; Li, Z.; Shen, X., A system analysis of the development strategy of iron ore in China. *Resources Policy* **2016,** *48*, 32-40.

16. *Ministry of Land and Resources of the People's Republic of China: Prospecting breakthrough strategy action plan (2011−2020); www.gov.cn/zwgk/2012−06/22/content_2166982.htm*.

17. *Oil, natural gas and biofuels statistical yearbook 2014*; National Agency of Petroleum, Natural gas and Biofuels: Rio de Janeiro, 2016.

18. Investing.com website: Iron ore fines 62% Fe CFR Futures; https://www.investing.com/. (Sep. 12),

19. *China Steel Yearbook 2013;* China Steel Development and Research Institute: Beijing, 2014.

20. *U.S. Geological Survey website*. http://www.usgs.gov/ (Feb. 03),

21. *Geoscience Australia-Iron ore;* Australian Government: 2010; http://www.australianminesatlas.gov.au/aimr/commodity/iron_ore.html#Industry_Developments.

22. *Western Australian Mineral and Petroleum Statistic Digest 2016; Department of Mines and Petroleum.*

23. *Western Australia Iron Ore Industry Profile; Government of Western Australia, Department of State Development* 2017.

24. dos Santos, R. S. P.; Milanez, B., The Global Production Network for iron ore: materiality, corporate strategies, and social contestation in Brazil. *The Extractive Industries and Society* **2015,** *2*, (4), 756-765.

25. de Vicq, R.; Matschullat, J.; Leite, M. G. P.; Junior, H. A. N.; Mendonça, F. P. C., Iron Quadrangle stream sediments, Brazil: geochemical maps and reference values. *Environmental Earth Sciences* **2015,** *74*, (5), 4407-4417.

26. Ditzel, J. In *Carajas Iron Ore Project*, Metal Bulletin's Third International Iron Ore Symposium, 1983; 1983.

27. *Carajás S11D Iron Project;* Vale. **2013**.

28. *Vale production in 1Q17;* Vale; www.vale.com.

29. *Brazil;* U.S. Energy Information Administration. (Sep. 20),

30. Estrella, G., Pre-salt production development in Brazil. *Energy solutions for all–Promoting Cooperation, Innovation and Investment* **2011**, 96-99.

31. Bacha, E. L.; Bonelli, R., Accounting for Brazil's Growth Experience–1940-2002. **2015**.

32. de Oliveira, J. P., The policymaking process for creating competitive assets for the use of biomass energy: the Brazilian alcohol programme. *Renewable and Sustainable Energy Reviews* **2002,** *6*, (1), 129-140.

33. Belincanta, J.; Alchorne, J.; Teixeira da Silva, M., The Brazilian Experience With Ethanol Fuel: Aspects Of Production, Use, Quality Distribution Logistics. *Brazilian Journal of Chemical Engineering* **2016,** *33*, (4), 1091-1102.

34. Guo, M.; Song, W.; Buhain, J., Bioenergy and biofuels: History, status, and perspective. *Renewable and Sustainable Energy Reviews* **2015,** *42*, 712-725.

35. NEVES, M. M., Difficulties in Expanding Hydropower Generation in Brazil. *The George Washington University, Washington* **2009**.

36. *Ministry of Mines and Energy: Electricity in the 2024 Brazilian Energy Plan*; 2014.

37. Oil, Natural Gas and Biofuels Statistical Yearbook 2015; National Agency of Petroleum, Natural Gas and Biofuels: Rio de Janeiro. In 2016.

38. BP Statistical Review of World Energy 2015; BP. In 2016.

39. *U.S. Natural Gas Exports and Re-Exports by Country;* U.S. Energy Information Administration. https://www.eia.gov/. (Sep. 14),

40. Tewalt, S. J.; Willett, J. C.; Finkelman, R. B., The world coal quality inventory: a status report. *International journal of coal geology* **2005,** *63*, (1), 190-194.

41. Formigli, J. M.; Pinto, C.; Carlos, A.; Almeida, A. S. In *SS: Santos Basin's Pre-Salt Reservoirs Development: The Way Ahead*, Offshore Technology Conference, 2009; Offshore Technology Conference: 2009.

42. Gaffney, C., Review and evaluation of ten selected discoveries and prospects in the

pre-salt play of the deepwater Santos basin, Brazil. In Rio de Janeiro: Agencia Nacional de Petroleo, Gas Natural e Biocombustiveis-ANP: 2010.

43. Campos, A.; Baumgartner, W.; Pena, M.; Halls, M.; Paiva, M.; Plank, C. C. In *CO2 reduction at the FPSO Fluminense: Case study*, SPE International Conference on Health, Safety and Environment in Oil and Gas Exploration and Production, 2010; Society of Petroleum Engineers: 2010.

44. Costa Fraga, C. T.; Lara, A. Q.; Pinto, C.; Carlos, A.; Moreira Branco, C. C. In *Challenges and Solutions to Develop Brazilian Pre-salt Deepwater Fields*, 21st World Petroleum Congress, 2014; World Petroleum Congress: 2014.

45. UN Comtrade Database. https://comtrade.un.org

46. Norgate, T.; Haque, N., Energy and greenhouse gas impacts of mining and mineral processing operations. *Journal of Cleaner Production.* **2010,** *18*, (3), 266-274.

47. Friedlingstein, P.; Andrew, R. M.; Rogelj, J.; Peters, G. P.; Canadell, J. G.; Knutti, R.; Luderer, G.; Raupach, M. R.; Schaeffer, M.; Van Vuuren, D. P., Persistent growth of CO2 emissions and implications for reaching climate targets. *Nature Geoscience* **2014,** *7*, (10), 709-715.

48. Karali, N.; Xu, T.; Sathaye, J., Developing long-term strategies to reduce energy use and CO2 emissions—analysis of three mitigation scenarios for iron and steel production in China. *Mitigation and Adaptation Strategies for Global Change* **2014**, 1-21.

49. Li, L.; Lei, Y.; Pan, D., Study of CO2 emissions in China's iron and steel industry based on economic input–output life cycle assessment. *Natural Hazards* **2016,** *81*, (2), 957-970.

50. Hasanbeigi, A.; Morrow, W.; Sathaye, J.; Masanet, E.; Xu, T., A bottom-up model to estimate the energy efficiency improvement and CO 2 emission reduction potentials in the Chinese iron and steel industry. *Energy* **2013,** *50*, 315-325.

51. Li, G.; Nie, Z.; Zhou, H.; Di, X.; Liu, Y.; Zuo, T., An accumulative model for the comparative life cycle assessment case study: iron and steel process. *The International Journal of Life Cycle Assessment.* **2002,** *7*, (4), 225-229.

52. Iosif, M.; Hanrot, F.; Ablitzer, D., Process integrated modelling for steelmaking life cycle inventory analysis. *Environmental Impact Assessment Review.* **2008,** *28*, (7), 429-438.

53. San Joaquin Valley Unified Air Pollution Control District, Emission Inventory

Methodology-Natural gas transmission losses. **2007**.

54. Ferreira, H.; Leite, M. G. P., A Life Cycle Assessment study of iron ore mining. *Journal of Cleaner Production* **2015,** *108*, 1081-1091.

55. Kogel, J. E., *Industrial minerals & rocks: commodities, markets, and uses*. SME: 2006.

56. Yu, D.; Shi, X.; Wang, H.; Sun, W.; Chen, J.; Liu, Q.; Zhao, Y., Regional patterns of soil organic carbon stocks in China. *Journal of Environmental Management.* **2007,** *85*, (3), 680-689.

57. Fang, J.; Guo, Z.; Piao, S.; Chen, A., Terrestrial vegetation carbon sinks in China, 1981–2000. *Science in China Series D: Earth Sciences* **2007,** *50*, (9), 1341-1350.

58. *Mines overview;* Baotou Steel Group Barun Mining Co., Ltd.; http://www.byebbr.com/services.html.

59. *Anshan Iron and Steel Group Mining Company Qidashan mining rights assessment report*; Liaoning Huanyu Mining Consulting Ltd.: Liaoning, 2013; http://www.mlr.gov.cn/kqsc/kqpg/pgbg/201409/P020140905367899539205.pdf.

60. Chang, S., Exploitation of Resources and Transformation of Mining Technology in Baiyunebo Iron Mine. *Science and Technology of Baotou Steel.* **2010,** *6*, (3).

61. Haberl, H.; Erb, K. H.; Krausmann, F.; Gaube, V.; Bondeau, A.; Plutzar, C.; Gingrich, S.; Lucht, W.; Fischer-Kowalski, M., Quantifying and mapping the human appropriation of net primary production in earth's terrestrial ecosystems. *Proceedings of the National Academy of Sciences.* **2007,** *104*, (31), 12942-12947.

62. Imhoff, M. L.; Bounoua, L., Exploring Global Patterns of Net Primary Production Carbon Supply and Demand Using Satellite Observations and Statistical Data. *Journal of Geophysical Research.* **2006,** *111*.

63. Kecojevic, V.; Komljenovic, D., Impact of Bulldozer's Engine Load Factor on Fuel Consumption, CO_2 Emission and Cost. *American Journal of Environmental Sciences.* **2011,** *7*, (2), 125.

64. Tannant, D. D.; Regensburg, B., *Guidelines for mine haul road design*. School of Mining and Petroleum Engineering, Department of Civil and Environmental Engineering, University of Alberta: 2001.

65. Teale, R. In *The concept of specific energy in rock drilling*, International Journal of Rock Mechanics and Mining Sciences & Geomechanics Abstracts, 1965; Elsevier: 1965;

pp 57-73.

66. A Technical Report on the Feasibility study of the Direct Shipping Iron Ore (DSO) Project; New Millennium Capital Corp: 2010.

67. Domingues, A. F.; Boson, P. H. G.; Alípaz, S. *Water Resource Management and The Mining Industry*; National Water Agency: Brasília, 2013.

68. Jones, G. M.; Bosserman, B. E.; Sanks, R. L.; Tchobanoglous, G., *Pumping station design*. Gulf Professional Publishing: 2006.

69. Volk, M., *Pump characteristics and applications*. CRC Press: 2013.

70. *Analysis of Diesel Use for Mine Haul and Transport Operations;* Department of Resource, Energy and Tourism, Australian Gorernment: 2010.

71. *Ferro Metallurgy and Mining Statistical Yearbook 2011*; Department of Metallurgy, Chinese Government: 2012.

72. Robusto, C., The cosine-haversine formula. *American Mathematical Monthly.* **1957**, 38-40.

73. Akaike, H., A new look at the statistical model identification. *Automatic Control, IEEE Transactions on* **1974,** *19*, (6), 716-723.

74. Kumar, S.; Srinivasan, T. M. *Sintering and pelletisation of Indian iron ores*; Mineral Enterprise Limited: Bangalore 2010.

75. AusLCA datasets; Australian life cycle assessment society, 2011; http://alcas.asn.au/AusLCI/index.php/Datasets.

76. Venkatesh, A.; Jaramillo, P.; Griffin, W. M.; Matthews, H. S., Uncertainty analysis of life cycle greenhouse gas emissions from petroleum-based fuels and impacts on low carbon fuel policies. *Environmental science & technology.* **2010,** *45*, (1), 125-131.

77. Lixue, J.; Xunmin, O.; Linwei, M.; Zheng, L.; Weidou, N., Life-cycle GHG emission factors of final energy in China. *Energy Procedia* **2013,** *37*, 2848-2855.

78. *SimaPro LCA software*. Product Ecology Consultants: Amersfoort, Netherlands, 2008; http://www.pre.nl/.

79. *Life Cycle Inventory Database; National Renewable Energy Laboratory; https://www.lcacommons.gov/nrel/search.*

80. Emissions & Generation Resource Integrated Database. United States Environmental Protection Agency; https://www.epa.gov/energy/emissions-generation-resource-integrated-database-egrid.

81. *The Chinese energy statistics year book;* Energy Statistics Division of National Bureau of Statistics: In China Statistics Press: Beijing, 2012.

82. Ferson, S., What Monte Carlo methods cannot do. *Human and Ecological Risk Assessment* **1996,** *2*, (4), 990-1007.

83. H. Scott Matthews, Chris T. Hendrickson, and Deanna Matthews, Life Cycle Assessment: Quantitative Approaches for Decisions that Matter, 2014. Publicly available via http://www.lcatextbook.com/.

84. Manxing, X., IMPROVEMENT AND DEVELOPMENT OF BLAST FURNACE BURDEN DESIGN IN CHINA [J]. *Sintering and Pelletizing* **2001,** *2*, 001.

85. Zhou, N.; Fridley, D.; McNeil, M.; Zheng, N.; Ke, J.; Levine, M. *China's energy and carbon emissions outlook to 2050*; Ernest Orlando Lawrence Berkeley National Laboratory, Berkeley, CA (US): 2011.

86. Robert I Ellison, a. C. H. Soil carbon: permanent pasture as an approach to CO2 sequestration. http://judithcurry.com/2013/06/07/soil-carbon-permanent-pasture-as-an-approach-to-co2-sequestration/ (Jul. 21),

87. *China Steel Development and Research Institute:China Steel Yearbook 2013*. China Steel Development and Research Institute: Beijing, 2014.

88. SEA DISTANCES / PORT DISTANCES http://www.sea-distances.org/ (Jul. 16),

89. Gossett, B., Base Mounted Centrifugal Pump Performance Curves.

90. Department of Metallurgy, Chinese Government: Ferro Metallurgy and Mining Statistical Yearbook 2011. In 2012.

91. Department of Resource, Energy and Tourism, Australian Gorernment: Analysis of Diesel Use for Mine Haul and Transport Operations. **2010**.

92. Tanaka, T.; Yoshimoto, K., Application of Bond Theory to Large Grinding Mill. *Kobe Res. Dev.* **1985,** *35*, (1), 34-37.

93. Tanaka, T., Comminution Laws. Several Probabilities. *Industrial & Engineering Chemistry Process Design and Development* **1966,** *5*, (4), 353-358.

94. Shen, L.; Cheng, S.; Gunson, A. J.; Wan, H., Urbanization, sustainability and the utilization of energy and mineral resources in China. *Cities* **2005,** *22*, (4), 287-302.

95. International Energy Agency: CO2 emissions from fuel combustion, 2012 ed. https://www.iea.org/co2highlights/co2highlights.pdf (Accessed 22 April, 2014),

96. Moomaw, W., P. Burgherr, G. Heath, M. Lenzen, J. Nyboer, A. Verbruggen Table A.II.4: Aggregated results of literature review of LCAs of GHG emissions from electricity generation technologies as displayed in Figure 9.8 (g CO2 eq/kWh).

97. Dimaggio, P. J.; Powell, W. W., The iron cage revisited: Institutional isomorphism and collective rationality in organizational fields. *American sociological review* **1983**, 147-160.

98. *Ecological Transport Information Tool for Worldwide Transports*; Heidelberg, 2011.

99. *International Maritime Organization: Updated 2000 Study on Greenhouse Gas Emissions from Ships* 2008.

100. Rio Tinto Iron Ore: Yandicoogina Junction South West and Oxbow Iron Ore Project --Public Environmental Review. **2012**.

101. Danish Shipowners' Association: *Calculation tool for determining ship's energy consumption and flue gas emissions*. https://www.shipowners.dk/services/beregningsvaerktoejer/ (Jul. 15),

102. Pidwirny, M., *Primary Productivity Table*; http://www.world-builders.org/lessons/less/biomes/primaryP.html.

103. Grace, P. R.; Post, W. M.; Hennessy, K., The potential impact of climate change on Australia's soil organic carbon resources. *Carbon Balance and Management* **2006,** *1*, (1), 14.

104. Mark Alchin, E. T., Chris Chilcott *An evaluation of the opportunity and risks of carbon offset based enterprises in the Kimberley-Pilbara region of Western Australia* Mar., 2010.

105. Spain AV, I. R., Probert ME, Soil organic matter. In soils: Australian Viewpoint Melbourne/London, Division of Soil CSIRO/Academic Press. **1983**, 551-563.

106. Yu, D.; Shi, X.; Wang, H.; Sun, W.; Chen, J.; Liu, Q.; Zhao, Y., Regional patterns of soil organic carbon stocks in China. *Journal of Environmental Management* **2007,** *85*, (3), 680-689.

107. Grace, J.; José, J. S.; Meir, P.; Miranda, H. S.; Montes, R. A., Productivity and carbon fluxes of tropical savannas. *Journal of Biogeography* **2006,** *33*, (3), 387-400.

108. Chen, X.; Hutley, L. B.; Eamus, D., Carbon balance of a tropical savanna of northern Australia. *Oecologia* **2003,** *137*, (3), 405-416.

109. Ruesch, A.; Gibbs, H. K., New IPCC Tier-1 global biomass carbon map for the year 2000. **2008**.

110. *Benxi Iron & Steel (group) CO., LTD Website;*

http://www.bxsteel.com/bxsteel/homepage.html.

111. BHP Iron Ore Pty Ltd: Duplication of iron ore mining operation, Yandi mine ML 270SA, Hamersley Range, 90 km north-west of Newman--report and recommendationsof the environmental Protection Authority. **1995**.

112. New Millennium Capital Corp. :A Technical Report on the Feasibility study of the Direct Shipping Iron Ore (DSO) Project. **2010**.

113. *China Steel Yearbook 2013; China Steel Development and Research Institute: Beijing, 2014.* China Steel Development and Research Institute: Beijing.

114. Flinders Mines Ltd: Pilbara Iron Ore Project (PIOP). http://www.flindersmines.com/projects/Pilbara.aspx (Accessed 23 May, 2014),

115. *Hamersley Iron Pty. Ltd: Brockman Syncline 4 Iron Ore Project: Public Environmental Review*. Hamersley Iron Pty. Limited: 2005.

116. Haberl, H.; Erb, K. H.; Krausmann, F.; Gaube, V.; Bondeau, A.; Plutzar, C.; Gingrich, S.; Lucht, W.; Fischer-Kowalski, M., Quantifying and mapping the human appropriation of net primary production in earth's terrestrial ecosystems. *Proceedings of the National Academy of Sciences* **2007,** *104*, (31), 12942-12947.

117. Kecojevic, V.; Komljenovic, D., Impact of Bulldozer's Engine Load Factor on Fuel Consumption, CO2 Emission and Cost. *American Journal of Environmental Sciences* **2011,** *7*, (2), 125.

118. Wang, M., The Greenhouse Gases, Regulated Emissions, and Energy Use in Transportation (GREET) Model: Version 1.5. *Center for Transportation Research, Argonne National Laboratory* **2008**.

119. Norgate, T.; Haque, N., Energy and greenhouse gas impacts of mining and mineral processing operations. *Journal of Cleaner Production* **2010,** *18*, (3), 266-274.

120. Land and Resource Economic Research Institution of China: Conservation and Utilization Mineral Resources in China (in Mardarin). In 2011.

121. Tutterow, V., Energy Efficiency in Pumping Systems: Experience and Trends in the Pulp and Paper Industry. *American Council for an Energy Efficient Economy (ACEEE)* **1999**.

122. Department of Resource, Energy and Tourism, Australian Gorernment: Energy Efficiency Opportunities-Energy mass balance: mining. In 2010.

123. Pero, L., The Downer Energy and Emissions Measure. In Energy Efficiency Opportunities Workshop 2011: 2011.

124. *Australia Government : Australian iron ore freight transport*; 2012.

125. Lucio, J.; Senra, C.; Souza, A. In *Paving the future–a case study replacing truck-andshovels by shovel-and-conveyor continuous mining at Carajas open pit mines*, Proceedings of iron ore conference, 2009; 2009; pp 269-76.

126. Filippov, L.; Severov, V.; Filippova, I., An overview of the beneficiation of iron ores via reverse cationic flotation. *International journal of mineral processing* **2014,** *127*, 62-69.

127. Derby, O. A., The iron ores of Brazil. *Rem: Revista Escola de Minas* **2010,** *63*, (3), 473-479.

128. Afionis, S.; Sakai, M.; Scott, K.; Barrett, J.; Gouldson, A., Consumption-based carbon accounting: does it have a future? *Wiley Interdisciplinary Reviews: Climate Change* **2017,** *8*, (1).

129. Hackmann, B., Analysis of the governance architecture to regulate GHG emissions from international shipping. *International Environmental Agreements: Politics, Law and Economics* **2012,** *12*, (1), 85-103.

130. Bunker, S. G.; Ciccantell, P. S., *East Asia and the global economy: Japan's ascent, with implications for China's future*. JHU Press: 2007.

131. Gomes, I., Brazil: Country of the future or has its time come for natural gas? **2014**.

132. *The Oil, Natural Gas and Biofuels Statistical Yearbook 2015;* Brazil's National Agency of Petroleum, Natural Gas and Biofuels (ANP). **2016**.

133. Heffer, P.; Prud'homme, M. In *Fertilizer outlook 2010–2014*, 78th IFA annual

conference, Paris, 2010; 2010.

134. Cezário, W. R.; de Souza Antunes, A. M.; Leite, L. F.; de Menezes, R. P. B., The energy revolution in the USA and the pre-salt reserves in Brazil: risks and opportunities for the Brazilian petrochemical industry. *Futures* **2015,** *73*, 1-11.

135. Kagawa, J., Health effects of diesel exhaust emissions—a mixture of air pollutants of worldwide concern. *Toxicology* **2002,** *181*, 349-353.

136. Siemiatycki, J.; Richardson, L.; Straif, K.; Latreille, B.; Lakhani, R.; Campbell, S.; Rousseau, M.-C.; Boffetta, P., Listing occupational carcinogens. *Environmental health perspectives* **2004,** *112*, (15), 1447.

137. Zhang, S.; Wu, Y.; Hu, J.; Huang, R.; Zhou, Y.; Bao, X.; Fu, L.; Hao, J., Can Euro V heavy-duty diesel engines, diesel hybrid and alternative fuel technologies mitigate NOX emissions? New evidence from on-road tests of buses in China. *Applied Energy* **2014,** *132*, 118-126.

138. Wang, W. G.; Clark, N.; Lyons, D.; Yang, R.; Gautam, M.; Bata, R.; Loth, J., Emissions comparisons from alternative fuel buses and diesel buses with a chassis dynamometer testing facility. *Environmental Science & Technology* **1997,** *31*, (11), 3132-3137.

139. Goyal, P., Present scenario of air quality in Delhi: a case study of CNG implementation. *Atmospheric Environment* **2003,** *37*, (38), 5423-5431.

140. Fontaras, G.; Martini, G.; Manfredi, U.; Marotta, A.; Krasenbrink, A.; Maffioletti, F.; Terenghi, R.; Colombo, M., Assessment of on-road emissions of four Euro V diesel and CNG waste collection trucks for supporting air-quality improvement initiatives in the city of Milan. *Science of the total environment* **2012,** *426*, 65-72.

141. El-Houjeiri, H. M.; Brandt, A. R.; Duffy, J. E., Open-source LCA tool for estimating greenhouse gas emissions from crude oil production using field characteristics. *Environmental science & technology* **2013,** *47*, (11), 5998-6006.

142. Keesom, W.; Unnasch, S.; Moretta, J., *Life cycle assessment comparison of North American and imported crudes*. Alberta Energy Research Institute: 2009.

143. Rosenfeld, J.; Pont, J.; Law, K.; Hirshfeld, D.; Kolb, J., Comparison of North American and imported crude oil life cycle GHG emissions. *Final Report Prepared for: Alberta Energy Research Institute, TIAX LLC (Case No. D5595)* **2009**.

144. Energy-Redefined, L., Carbon intensity of crude oil in Europe crude. *Energy-Redefined LLC, for International Council on Clean Transportation* **2010**.

145. Gerdes, K.; Skone, T., An evaluation of the extraction, transport and refining of imported crude oils and the impact on life cycle greenhouse gas emissions. *National Energy Technology Laboratory* **2009**.

146. Brandt, A. R., Variability and uncertainty in life cycle assessment models for greenhouse gas emissions from Canadian oil sands production. *Environmental science & technology* **2012,** *46*, (2), 1253-1261.

147. Gordon, D.; Brandt, A. R.; Bergerson, J.; Koomey, J., *Know your oil: Creating a global oil-climate index*. Carnegie Endowment for International Peace Washington, DC: 2015.

148. Hassan, M.; Vafi, K.; Duffy, J.; McNally, S.; Brandta, A. R., Oil Production Greenhouse Gas Emissions Estimator OPGEE v1. 1 Draft E. **2014**.

149. Sánchez, Y. A. C.; de Oliveira Junior, S.; da Silva, J. A. M.; Nguyen, T.-V. In *Energy and Exergy Performance of three FPSO Operational Modes*, ABCM International Congress of Mechanical Engineering (COBEM 2015), 2015; 2015.

150. Venkatesh, A.; Jaramillo, P.; Griffin, W. M.; Matthews, H. S., Uncertainty in life cycle greenhouse gas emissions from United States natural gas end-uses and its effects on policy. *Environmental science & technology* **2011,** *45*, (19), 8182-8189.

151. Abrahams, L. S.; Samaras, C.; Griffin, W. M.; Matthews, H. S., Life cycle greenhouse gas emissions from US liquefied natural gas exports: implications for end uses. *Environmental science & technology* **2015,** *49*, (5), 3237-3245.

152. Jiang, M.; Griffin, W. M.; Hendrickson, C.; Jaramillo, P.; VanBriesen, J.; Venkatesh, A., Life cycle greenhouse gas emissions of Marcellus shale gas. *Environmental Research Letters* **2011,** *6*, (3), 034014.

153. Solano, R. F.; de Azevedo, F. B.; Oazen, E. In *Design Challenges of Gas Export Pipelines for Pre-salt Area Offshore Brazil*, International Conference On Offshore Mechanics and Arctic Engineering, 2013; 2013.

154. Jaramillo, P.; Griffin, W. M.; Matthews, H. S., Comparative life-cycle air emissions of coal, domestic natural gas, LNG, and SNG for electricity generation. *Environmental Science & Technology* **2007,** *41*, (17), 6290-6296.

155. Denholm, P.; Kulcinski, G. L., Life cycle energy requirements and greenhouse gas emissions from large scale energy storage systems. *Energy Conversion and Management* **2004,** *45*, (13), 2153-2172.

156. Wood, S.; Cowie, A., A review of greenhouse gas emission factors for fertiliser

production. **2004**.

157. Natural Resources Canada, Canadian Ammonia Producers: Benchmarking Energy Efficiency and Carbon Dioxide Emissions. In Natural Resources Canada, Ottawa, Canada: 2008.

158. Wang, M., GREET Model 1 2016. *Computer program, Argonne National Laboratory* **2016**.

159. Matzen, M.; Demirel, Y., Methanol and dimethyl ether from renewable hydrogen and carbon dioxide: Alternative fuels production and life-cycle assessment. *Journal of Cleaner Production* **2016,** *139*, 1068-1077.

160. Luiz Alexander Kulay, E. T. S., Gil Anderi da Silva *Life cycle inventory of Brazilian Methonal: Contribution for National Database.*; 2008.

161. Price, L.; Phylipsen, D.; Worrell, E., Energy use and carbon dioxide emissions in the steel sector in key developing countries. *Lawrence Berkeley National Laboratory* **2001**.

162. Benchaita, T., Greenhouse gas emissions from new petrochemical plants. *Inter-American Development Bank* **2013**.

163. Ghanta, M.; Fahey, D.; Subramaniam, B., Environmental impacts of ethylene production from diverse feedstocks and energy sources. *Applied Petrochemical Research* **2014,** *4*, (2), 167-179.

164. Cai, H.; Burnham, A.; Wang, M.; Hang, W.; Vyas, A. *The GREET Model Expansion for Well-to-Wheels Analysis of Heavy-Duty Vehicles*; Argonne National Lab.(ANL), Argonne, IL (United States): 2015.

165. Tong, F.; Jaramillo, P.; Azevedo, I. s. M., Comparison of life cycle greenhouse gases from natural gas pathways for medium and heavy-duty vehicles. *Environmental science & technology* **2015,** *49*, (12), 7123-7133.

166. Associação Nacional dos Fabricantes de Veículos Automotores; Brazilian automotive industry yearbook; http://www.anfavea.com.br.

167. United Nations Energy Statistics Database; https://unstats.un.org/unsd/energy/edbase.htm. (Aug 18),

168. Food and Agriculture Organization of the United Nations statistics website; http://www.fao.org/faostat/en/#home. (Aug, 18),

169. Seddon, D., *Petrochemical economics: Technology selection in a carbon constrained world*. World Scientific: 2010; Vol. 8.

170. Engelman, R.; Fracasso, E.; Pinheiro, I., Competitive Strategy and Sustainable Product: Braskem's Green Polyethylene. In 2010.

171. Ejarque, J. M., Evaluating the economic cost of natural gas strategic storage restrictions. *Energy Economics* **2011,** *33*, (1), 44-55.

172. Rubio, R.; Ojeda-Esteybar, D.; Ano, O.; Vargas, A. In *Integrated natural gas and electricity market: A survey of the state of the art in operation planning and market issues*, Transmission and Distribution Conference and Exposition: Latin America, 2008 IEEE/PES, 2008; IEEE: 2008; pp 1-8.

173. Schlömer, S.; Bruckner, T.; Fulton, L.; Hertwich, E.; McKinnon, A.; Perczyk, D.; Roy, J.; Schaeffer, R.; Sims, R.; Smith, P., Annex III: Technology-specific cost and performance parameters. *Climate Change* **2014**, 1329-1356.

174. da Costa, A.; Amaral, C.; Poiate, E.; Pereira, A.; Martha, L.; Gattass, M.; Roehl, D. In *Underground storage of natural gas and CO 2 in salt caverns in deep and ultra-deep water offshore Brazil*, 12th ISRM Congress, 2011; International Society for Rock Mechanics: 2011.

175. Žlender, B.; Kravanja, S., Cost optimization of the underground gas storage. *Engineering Structures* **2011,** *33*, (9), 2554-2562.

176. Nian, C. W.; You, F., Design of methanol plant. In 2013.

177. *Agrium Fact Book 2015-2016*; 2016.

178. Leontief, W. W.; Leontief, W., *Input-output economics*. Oxford University Press on Demand: 1986.

179. Annual Report of Social Information database; Ministry of Labor and Employment. In 2016.

180. Wang, Y.; Lu, B. In *A coupled reservoir-geomechanics model and applications to wellbore stability and sand prediction*, SPE International Thermal Operations and Heavy Oil Symposium, 2001; Society of Petroleum Engineers: 2001.

181. Laurenzi, I. J.; Bergerson, J. A.; Motazedi, K., Life cycle greenhouse gas emissions and freshwater consumption associated with Bakken tight oil. *Proceedings of the National Academy of Sciences* **2016,** *113*, (48), E7672-E7680.

182. *Federal Energy Regulatory Commission,* National Natural Gas Market Overview: World LNG Landed Prices. In.

183. Nasdaq crude oil price; http://www.nasdaq.com/markets/crude-oil.aspx. (Aug, 18),

184. Petrobras website: Prices and Costs http://www.investidorpetrobras.com.br/en/operational-highlights/prices-and-costs (Aug. 22),

185. Stewart, M., *Report of life cycle assessment workshop: the application of LCA to mining, minerals and metals;* International Institute for Environment and Development: London, UK, 2001; http://pubs.iied.org/pdfs/G00942.pdf.